Fundamental Heterogeneous Reaction Chemistry Related to Secondary Organic Aerosols (SOA) in the Atmosphere

Hajime Akimoto

Center for Global Environmental Research, National Institute for Environmental Studies (NIES), 16-2 Onogawa, Tsukuba, Ibaraki 305-8506, Japan*
*Asia Center for Air Pollution Research (ACAP)**, 1182 Sowa, Nishi-ku, Niigata 950-2144, Japan*
**Present affiliation as Visiting Scientist.*
***A part of the work was carried out here until March 31, 2015.*
e-mail: akimoto.hajime@nies.go.jp

Received July 7, 2015; **Revised** April 8, 2016; **Accepted** April 8, 2016; **Online published** November 11, 2016.

Citation: Akimoto, H. (2016), Fundamental heterogeneous reaction chemistry related to secondary organic aerosols (SOA) in the atmosphere, *Monogr. Environ. Earth Planets*, *4*, 1–45, doi:10.5047/meep.2016.00401.0001.

Abstract Typical reaction pathways of formation of dicarboxylic acids, larger multifunctional compounds, oligomers, and organosulfur and organonitrogen compounds in secondary organic aerosols (SOA), revealed by laboratory experimental studies are reviewed with a short introduction to field observations. In most of the reactions forming these compounds, glyoxal, methyl glyoxal and related difunctional carbonyl compounds play an important role as precursors, and so their formation pathways in the gas phase are discussed first. A substantial discussion is then presented for the OH-initiated aqueous phase radical oxidation reactions of glyoxal and other carbonyls which form dicarboxylic acids, larger multifunctional compounds and oligomers, and aqueous-phase non-radical reactions which form oligomers, organosulfates and organonitrogen compounds. Finally, the heterogeneous oxidation reaction of gaseous O_3, OH and NO_3 with liquid and solid organic aerosols at the air-particle interface is discussed relating to the aging of SOA in the atmosphere.

Keywords: Secondary organic aerosols, Heterogeneous reactions, Multiphase reactions, Aqueous phase organic reactions, Dicarboxylic acids, Oligomers, Organic sulfur, Organic nitrogen.

1. Introduction

Studies of the gas phase kinetics related to atmospheric chemistry has a long history going back the 1960s, and a tremendous amount of data on reaction rate constants and reaction mechanisms concerning the photochemical oxidation of atmospheric inorganic and organic compounds has been accumulated (Calvert *et al*., 2000, 2002, 2008, 2011; Atkinson *et al*., 2004, 2006, 2007, 2008; Sander *et al*., 2011; Akimoto, 2016). Through these extensive efforts in laboratory experimental studies, as well as quantum chemical computational investigations, the OH-initiated radical chain reaction system in tropospheric chemistry has been well established, which provides a solid scientific basis for the formation of ozone/oxidants in clean and polluted atmospheres, the oxidative degradation of volatile organic compounds to form a variety of secondary organics, and the atmospheric lifetime of most of the trace species including the reactive greenhouse gases (methane, hydrofluorocarbons, etc.) (Finlayson-Pitts and Pitts, 2000; Akimoto, 2016). The heterogeneous kinetics of inorganic ionic chemistry related to the oxidation of SO_2 in cloud and fog droplets to form acid rain has also been well established (Seinfeld and Pandis, 2006).

In stratospheric chemistry, HO_x, NO_x and ClO_x radical chain cycles in the gas phase, as well as the heterogeneous kinetics of polar stratospheric clouds (PSCs), have been studied extensively and have provided a solid scientific basis for stratospheric ozone formation in the natural atmosphere of the earth, and the destruction of ozone by anthropogenic chlorofluorocarbons (CFCs) etc. (Brasseur and Solomon, 2005; Akimoto, 2016).

In contrast to these history on atmospheric chemistry, the fundamental kinetics related to the formation and transformation of secondary organic aerosol (SOA) in $PM_{2.5}$ (particulate matter with a diameter less than 2.5 μm) have been poorly established, even though extensive efforts have been made in recent years. This is the main reason why underestimates of SOA prediction by atmospheric models as compared with observations have been noted frequently, both in the free troposphere and the polluted boundary layer (e.g. Heald *et al*., 2005; Volkamer *et al*., 2006b). There is definitely a gap in our understanding of the formation and aging pathways of oxygenated organic aerosols (OOA) in SOA.

doi:10.5047/meep.2016.00401.0001 ISSN: 2186-4853

In order to establish a fundamental understanding of SOA, more basic studies on the chemistry and physics of multiphase and heterogeneous atmospheric processes, including reaction kinetics and thermochemistry, by laboratory experiments and quantum chemical computational studies, are necessary as has been the case in homogeneous atmospheric reaction chemistry.

For example, the formation of dicarboxylic acids, one of the major species in SOA (Kawamura and Sakaguchi, 1999) cannot be explained by homogeneous gas phase reactions. Also, the oligomers, which have been found to be abundant in SOA (Kalberer *et al*., 2004), are thought to form from dicarbonyl compounds in droplets by aqueous-phase reactions. However, efforts to reproduce the observed SOA concentrations by models have been hampered by the lack of kinetic data for product pathways in the atmospheric aqueous phase. Another reaction process related to SOA is the heterogeneous oxidation of SOA on the surface of solid particles by OH, O_3, and NO_3, which is related to the aging of SOA in the atmosphere (e.g. Kroll and Seinfeld, 2008; George and Abbatt, 2010). These features provide a new aspect of atmospheric chemistry.

It is very interesting to note that such aqueous phase organic chemistry, as well as heterogeneous kinetics, results in a new reaction chemistry that differs from previously known chemistry in gas phase and bulk aqueous phase reactions. For example, oleic acid, which has C=C double bond in the molecule reacts with OH and O_3 on a solid surface, but the reaction pathways and reaction rates are very much different from the gas phase (Moise and Rudich, 2002; Thornberry and Abbatt, 2004; Vieceli *et al*., 2004).

In this review, the following selected topics on the reaction kinetics and mechanisms of SOA formation and transformation are discussed including the gas-phase reaction mechanisms of the formation of precursors. The selected topics are: (1) how the formation of small dicarboxylic compounds are formed; (2) how dicarboxylic acids, oligomers, organosulfates and organonitrogen compounds are formed in the liquid phase reaction of dialdehydes; and (3) how SOA aging can be explained by the surface reactions of solid organic aerosols with OH and O_3. Since this review focuses only on reaction chemistry, readers may want to refer to other reviews on more general chemistry and other specific topics of secondary organic aerosols (Kroll and Seinfeld, 2008; Jimenez *et al*., 2009; Hallquist *et al*., 2009; Herrmann *et al*., 2010; Ervens *et al*., 2011; Donahue *et al*., 2012). Very recently, *Chemical Reviews* published a special issue, "Roles of Chemistry in the Earth's Climate", which includes several articles related to the present review (Ravishankara *et al*., 2015, and following papers).

2. Formation of Dicarboxylic Acids in SOA

2.1 Field observation of dicarboxylic acids

Dicarboxylic acids and related compounds are ubiquitously observed in atmospheric aerosols in a variety of environments such as remote marine ones (Kawamura and Sakaguchi, 1999; Rinaldi *et al*., 2011; Fu *et al*., 2013), the Arctic circle (Kawamura *et al*., 2010), and rural and urban areas (Kerminen *et al*., 2000; Limbeck *et al*., 2001; Yao *et al*., 2002; Huang *et al*., 2006; Sorooshian *et al*., 2006; Wang *et al*., 2012). Figure 1 lists the typical dicarboxylic acids, ketoacids, and dicarbonyls detected in marine aerosols (Sempéré and Kawamura, 2003). Among these compounds, small carbon number diacids, oxalic (C2), malonic (C3), and succinic (C4) acids shown in Fig. 1, are usually more abundant than higher carbon number compounds (e.g. Mkoma and Kawamura, 2013). In particular, the amount of C2 always predominates (Rinaldi *et al*., 2011; Mkoma and Kawamura, 2013), as exemplified in Fig. 2 for marine aerosols. The ubiquitous existence of dicarboxylic acids and the predominance of C2, followed by other low carbon number diacids, are a peculiar feature of organic aerosols. It can also be noted in Fig. 2 that higher carbon number diacids, such as glutaric acid (C5), adipic acid (C6), and azelaic acid (C9), are also present. Although the abundances of these higher molecular weight diacids are much less than the lower molecular weight diacids, they are also observed widely in atmospheric aerosols in a variety of environments, particularly in terrestrial sites influenced by biogenic hydrocarbon sources. It can be noted also that, in addition to dicarboxylic acids, ketoacids such as glyoxylic acid (ωC2) and pyruvic acid (Pyr), and dicarbonyl compounds such as glyoxal (Gly) and methylglyoxal (MGly) are also detected in aerosols, as shown in Fig. 2.

The presence of oxalic acid (C2, HOOC-COOH) as a major species in organic aerosols has long been a big puzzle since this cannot be explained by the gas phase reactions in the atmosphere. Glyoxal (Gly, OHC-CHO) may be conceived as a precursor of oxalic acid, but the production of oxalic acid in the gas phase oxidation of glyoxal has never been observed. The photolysis and OH-initiated reaction of glyoxal in the gas phase proceeds as indicated in the following pathways (Calvert *et al*., 2011),

$$\text{OHC-CHO} + h\nu \rightarrow \text{OHC-CO} + \text{H} \quad (1)$$

$$\text{OHC-CHO} + \text{OH} \rightarrow \text{OHC-CO} + \text{H}_2\text{O} \quad (2)$$

$$\text{OHC-CO} \rightarrow \text{HCO} + \text{CO} \quad (3)$$

$$\text{OHC-CO} + \text{O}_2(+\text{M}) \rightarrow \text{OHC-C(O)O}_2(+\text{M})$$
$$\text{M: third body of reaction} \quad (4)$$

$$\text{OHC-C(O)O}_2 \rightarrow \text{OC-C(O)O}_2\text{H} \rightarrow \text{CO} + \text{CO}_2 + \text{OH} \quad (5)$$

$$\text{OHC-C(O)O}_2 + \text{NO} \rightarrow \text{OHC-C(O)O} + \text{NO}_2 \quad (6)$$

$$\text{OHC-C(O)O} \rightarrow \text{HCO} + \text{CO}_2. \quad (7)$$

In remote areas with low NO_x, ketohydroperoxide, OHC-C(O)O_2H, may be produced by the reaction,

$$\text{OHC-C(O)O}_2 + \text{HO}_2 \rightarrow \text{OHC-C(O)O}_2\text{H} + \text{O}_2, \quad (8)$$

but the production of oxalic acid cannot be conceived in the gas phase oxidation of glyoxal.

From observed atmospheric concentration dynamics, Chebbi and Carlier (1996) have suggested that glyoxal is an in-cloud precursor for carboxylic acids in the troposphere. The possible formation of secondary organic aerosols in cloud and fog was suggested by Blando and Turpin (2000),

doi:10.5047/meep.2016.00401.0001

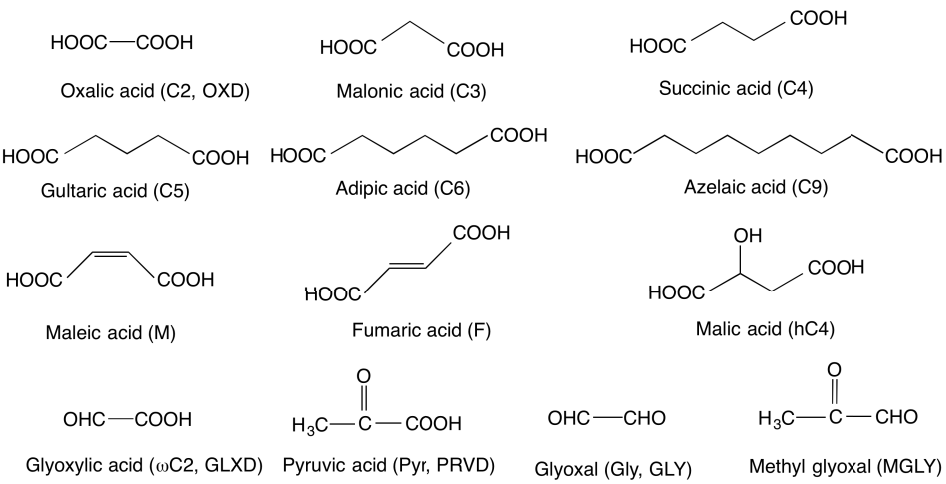

Fig. 1. Typical dicarboxylic acids and dicarbonyls detected in marine aerosols (extracted from Sempéré and Kawamura, 2003). The first abbreviations in the parentheses are with reference to Fig. 2, and the second abbreviations appear in the text in later sections.

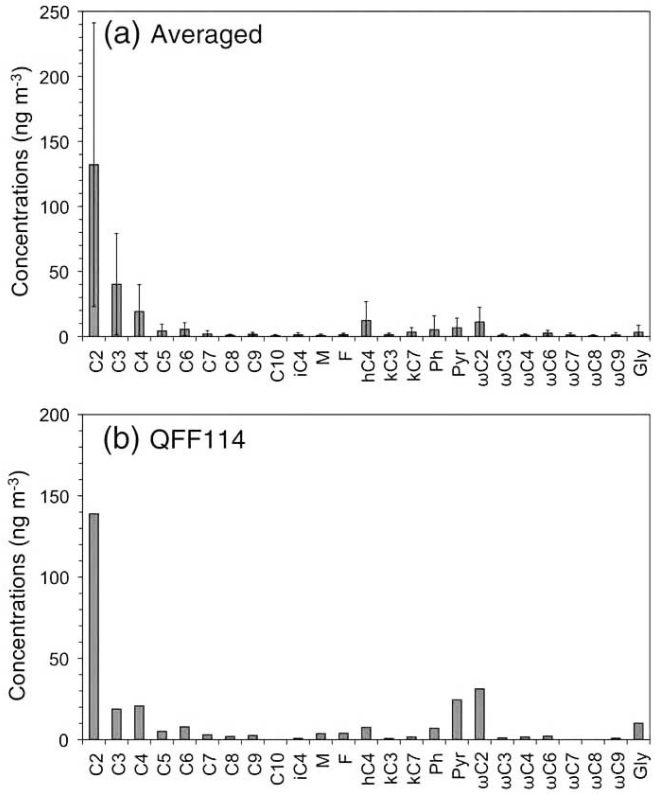

Fig. 2. Molecular distributions of diacids and related compounds in marine aerosols. Concentrations are given for: (a) polar samples, and (b) in a western North Pacific sample influenced by biomass burning. Molecular specifications are given in Fig. 1. (Reprinted from *Marine Chem.*, *148*, Fu, P., K. Kawamura, K. Usukura, and K. Miura, Dicarboxylic acids, ketocarboxylic acids and glyoxal in the marine aerosols collected during a round-the-world cruise, 22–32, Copyright 2013, with permission from Elsevier.)

and a formation mechanism of oxalic acid from glyoxal in a cloud has been proposed by Warneck (2003) based on an earlier study by Buxton *et al*. (1997) on the aqueous phase oxidation of glyoxal initiated by OH. Since then a substantial number of studies have been made regarding the liquid phase oxidation of glyoxal and related species in cloud water or aqueous aerosols. In-cloud and below cloud measurements (Crahan *et al*., 2004), in addition to other field measurements (Yu *et al*., 2005) support an in-cloud formation mechanism for oxalic acid.

The reaction mechanism of glyoxal and methylglyoxal to form dicarboxylic acids typified by oxalic acid in the aqueous phase is discussed below after identifying the gas phase production processes of glyoxal, methylglyoxal, and

doi:10.5047/meep.2016.00401.0001

Table 1. Abbreviations of carbonyl compounds appearing in this review.

Compounds	Chemical formula	Abbreviations
Formic acid	HCOOH	FMD
Acetic acid	CH_3COOH	ACD
Glyoxal	OHC-CHO	GLY
Methylglyoxal	$CH_3C(O)CHO$	MGLY
Oxalic acid	HOOC-COOH	OXD
Glycolaldehyde	$HOCH_2CHO$	GLCA
Glyoxylic acid	CHOCOOH	GLXD
Glycolic acid	$HOCH_2COOH$	GLCD
Hydroxy acetone	$CH_3C(O)CH_2OH$	HACT
Pyruvic acid	$CH_3COCOOH$	PRVD
Tartaric acid	HOOC(HO)HC-CH(OH)COOH	TTRD
Methyl vinyl ketone	CH_2=CHC(O)CH_3	MVK
Methacrolein	CH_2=C(CH_3)CHO	MACR

other precursor species in the atmosphere.

2.2 Production of glyoxal, methylglyoxal and related species in the gas phase reactions

Terrestrial sources of glyoxal and related species are the oxidation products of acetylene, ethylene, aromatic hydrocarbons such as toluene, and isoprene from both anthropogenic and natural sources. The primary source of glyoxal from marine biology has been proposed as a source of natural oxalic acid in the remote ocean (Turekian *et al*., 2003; Rinaldi *et al*., 2011). Table 1 presents a summary of abbreviations for the carbonyl compounds appearing in Section 2 of this review.

2.2.1 OH + acetylene The OH-initiated oxidation reaction of acetylene (C_2H_2) in the presence of NO has long been studied and is known to produce glyoxal (GLY) as a main product (Hatakeyama *et al*., 1986). It has recently been confirmed that glyoxal is the primary product by the use of a flow system with detection by a chemical ionization mass spectrometer (CIMS) (Yeung *et al*., 2005). Similarly, methyl glyoxal (MGLY, CH_3COCHO) and biacetyl (CH_3COCH_3CO) are formed as main products from propyne (C_3H_4), and 2-butyne (2-C_4H_6), respectively, (Hatakeyama *et al*., 1986; Yeung *et al*., 2005), although their mixing ratios are much lower than acetylene in the polluted atmosphere. As well as these dicarbonyls, the formation of formic acid has been reported but dicarboxylic acid has not been observed in the oxidation of acetylene. The main reaction processes to form glyoxal and formic acid from acetylene are shown as follows (Hatakeyama *et al*., 1986; Galano *et al*., 2008).

$$CH{\equiv}CH + OH(+M) \rightarrow HOCH{=}CH(+M) \quad (9)$$
$$HOCH{=}CH + O_2(+M) \rightarrow HOCH{=}CHO_2(+M) \quad (10)$$
$$HOCH{=}CHO_2 + NO \rightarrow HOCH{=}CHO + NO_2 \quad (11)$$
$$HOCH{=}CHO + O_2 \rightarrow \underline{\text{OHC-CHO}} + HO_2 \quad (12)$$
$$HOCH{=}CHO_2 \rightarrow HOCH(O)\text{-}CHO \rightarrow HCOOH + HCO. \quad (13)$$

2.2.2 OH + ethylene Reaction of the OH-initiated oxidation of ethylene (C_2H_4) in the presence of NO has been studied and reported to produce glycolaldehyde (GLCA, $HOCH_2CHO$) and formaldehyde (HCHO) as main products with yields of 22% and 78%, respectively (Niki *et al*., 1981). GLCA is water-soluble and is oxidized to form oxalic acid (OXD) in the aqueous phase as will be discussed later. The major pathway of the reaction to produce glycolaldehyde and formaldehyde from ethylene can be shown as:

$$CH_2{=}CH_2 + OH(+M) \rightarrow HOCH_2CH_2(+M) \quad (14)$$
$$HOCH_2CH_2 + O_2(+M) \rightarrow HOCH_2CH_2O_2(+M) \quad (15)$$
$$HOCH_2CH_2O_2 + NO \rightarrow HOCH_2CH_2O + NO_2 \quad (16)$$
$$HOCH_2CH_2O + O_2 \rightarrow \underline{HOCH_2CHO} + HO_2 \quad (17)$$
$$HOCH_2CH_2O(+M) \rightarrow HOCH_2 + \underline{HCHO}(+M) \quad (18)$$
$$HOCH_2 + O_2 \rightarrow \underline{HCHO} + HO_2. \quad (19)$$

2.2.3 OH + isoprene Glyoxal (GLY), methylglyoxal (MGLY), glycolaldehyde (GLCA), and hydroxyacetone (HACT, $CH_3C(O)CH_2OH$) are known to be formed by the OH-initiated oxidation of isoprene, partly as initial products (first generation), and mostly as secondary products from methyl vinyl ketone (MVK, CH_2=CHC(O)CH_3) and methacrolein (MACR, CH_2=C(CH_3)CHO), which are the main products of the OH-initiated oxidation reaction of isoprene (Fan and Zhang, 2004; Fu *et al*., 2008; Galloway *et al*., 2011). Experimental yields of MVK and MACR under high NO_X conditions are reported to be 30–41 and 21–26%, respectively, (Paulot *et al*., 2009a; Galloway *et al*., 2011; Liu *et al*., 2013), while they are only (4.6 ± 0.7) and (3.2 ± 0.6)% under a pristine low NO_x condition (Liu *et al*., 2013). The direct initial production of GYCA and HACT has been identified by Paulot *et al*. (2009a) with yields of 4.2 and 3.8%, respectively, while Volkamer *et al*. (2006a) reported the yield of GLY as 0.3–3.0%. Secondary oxidation reactions with OH of MVK and MACR in the presence of NO_x are known to be an important source of GLCA, HACT and MGLY in the oxidation of isoprene.

doi:10.5047/meep.2016.00401.0001

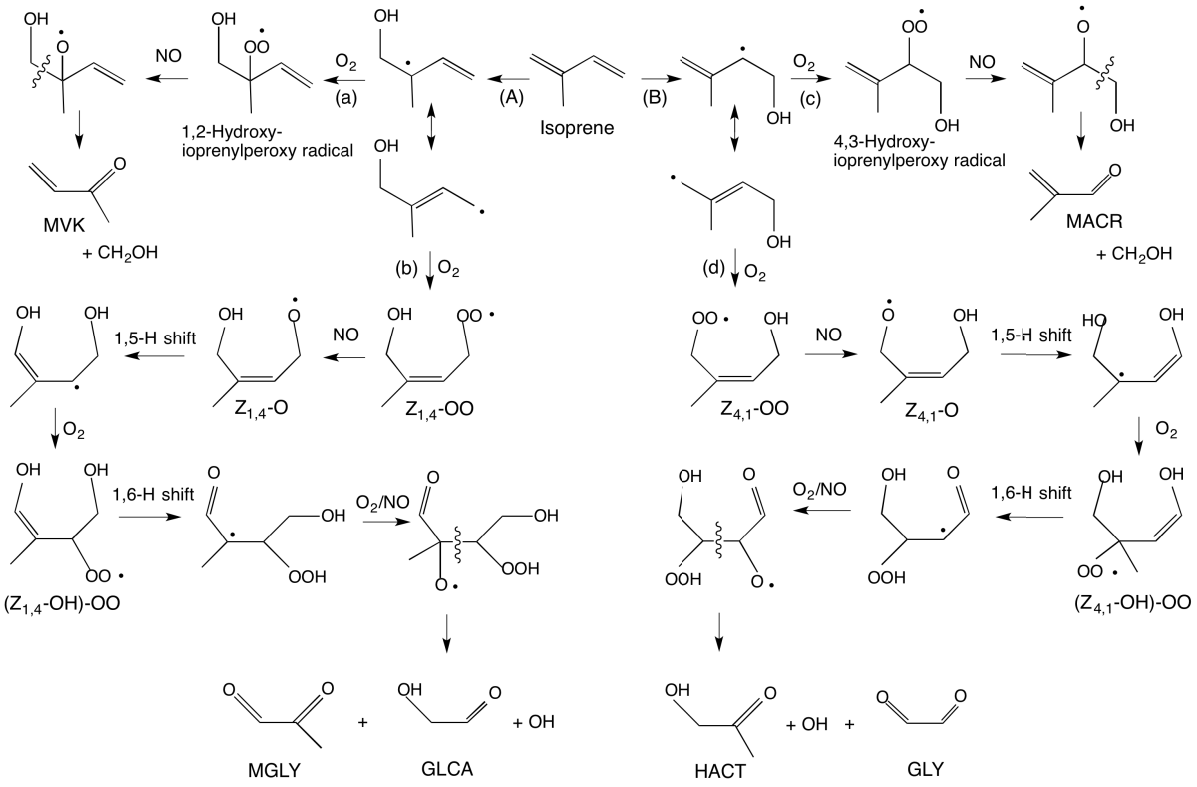

Fig. 3. The mechanisms of the formation of MVK and MACR, and the primary formation of GLY, MGLY, GLCA, and HACT from OH-initiated oxidation of isoprene in the presence of NO_x (based on Dibble, 2002; Fang and Zhang, 2004; Paulot *et al*., 2009a; Peeters and Nguyen, 2012).

The major pathways of the formation of MVK and MACR, as well as the direct formation of dicarbonyl compounds as first generation products in the reaction of the OH-initiated oxidation of isoprene in the presence of NO_x are shown in Fig. 3 based on Dibble (2002), Fan and Zhang (2004), Paulot *et al*. (2009a) and Peeters and Nguyen (2012).

Since isoprene has two double bonds which are asymmetric, there are four positions of carbon atoms to which OH can add. Among them the major pathways are the addition of OH to the edge carbons of either of the double bonds to form allyl-type radicals, (A) and (B) as follows. The allyl-type radicals are stabilized by the conjugation as shown in Eqs. (20) and (21).

$$\begin{aligned} &CH_2{=}C(CH_3)\text{-}CH{=}CH_2 + OH \\ &\quad \xrightarrow{(A)} HOCH_2\dot{C}(CH_3)\text{-}CH{=}CH_2 \\ &\qquad\qquad \updownarrow \\ &\qquad\quad HOCH_2\text{-}C(CH_3){=}CH\text{-}\dot{C}H_2 \end{aligned} \tag{20}$$

$$\begin{aligned} &CH_2{=}C(CH_3)\text{-}CH{=}CH_2 + OH \\ &\quad \xrightarrow{(B)} CH_2{=}C(CH_3)\text{-}\dot{C}H\text{-}CH_2OH \\ &\qquad\qquad \updownarrow \\ &\qquad\quad \dot{C}H_2\text{-}C(CH_3){=}CH\text{-}CH_2OH. \end{aligned} \tag{21}$$

The ratios of the reaction pathways (20) and (21) are estimated to be 0.56 : 0.37 (Fan and Zhang, 2004). Then, O_2 can add to the either of the radical points of the two allyl-type hydroxy-isoprenyl radicals in the atmosphere (Fan and Zhang, 204; Paulot *et al*., 2009a) as shown in Fig. 3. When O_2 adds to the carbon atom adjacent to the OH-added carbon, (1, 2) and (4, 3) type hydroxy-isoprenylperoxy radicals (hydroxyl group at 1 and 4 position, and peroxy group at 2 and 3 position, respectively) are formed, from which the major products, MVK and MACR, are produced. When O_2 adds to the terminal carbon atom, (1, 4) and (4, 1) type hydroxy-isoprenylperoxy radicals are formed. For these types of radicals, two different stereochemical positions of OH and OO groups are possible. If the OH and OO groups are on the same side of the double bond, the configuration is called Z (from zusammen, the German word for "together", also called cis) while, if they are on the opposite sides of the double bond, it is called E (from entgegen for "opposite", also called trans). The $Z_{1,4}$, $E_{1,4}$, $Z_{4,1}$ and $E_{4,1}$ peroxy radicals react with NO to form corresponding oxy radicals. In Fig. 3 only $Z_{1,4}$-peroxy ($Z_{1,4}$-OO) and $Z_{4,1}$-peroxy ($Z_{4,1}$-OO) radicals pathways are shown for simplicity.

The first generation C_2 or C_3 dicarbonyl compounds, glycolaldehyde (GLCA) and methylglyoxal (MGLY), and glyoxal (GLY) and hydroxyacetone (HACT), are thought to be formed from pathways through $Z_{1,4}$- and $Z_{4,1}$-radicals as shown in Fig. 3. The ratios of the reactions (a) and (b) are 0.41 and 0.15 (total 0.56), and those of (c) and (d) are 0.23 and 0.14 (total 0.37) of the whole pathways, while the branching ratios of the $Z_{1,4}$- and $Z_{4,1}$-radicals against the $E_{1,4}$- and $E_{4,1}$-radicals are both estimated to be 0.85 : 0.15

doi:10.5047/meep.2016.00401.0001

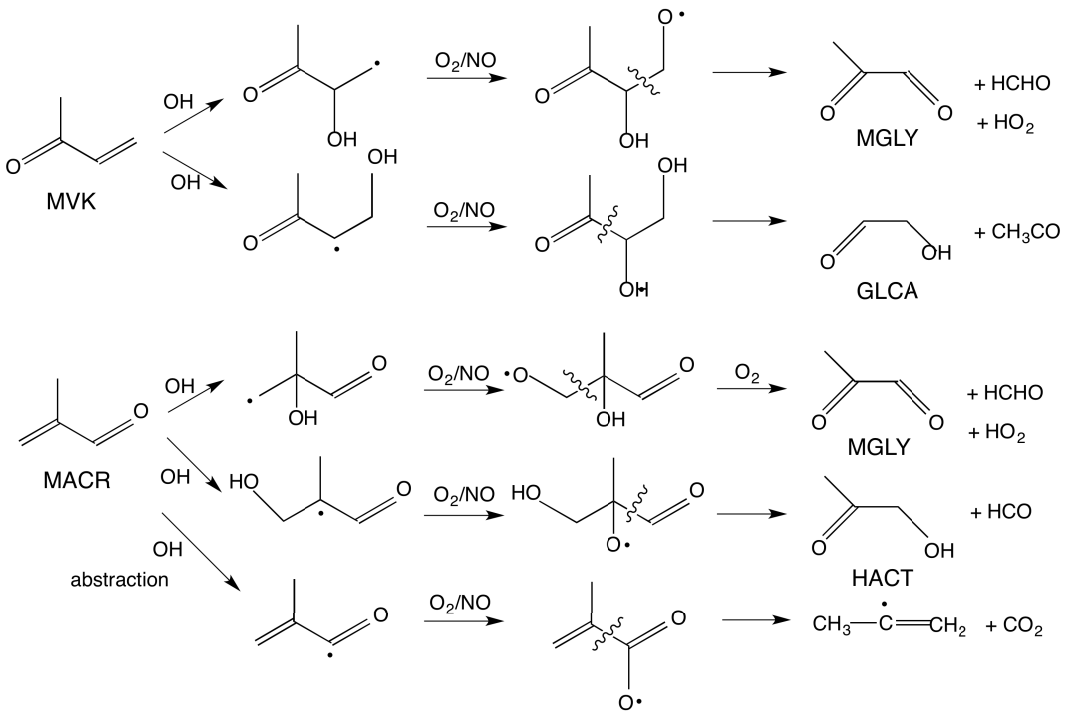

Fig. 4. Reaction mechanisms of the formation of MGLY, GLCA and HACT from the OH-initiated oxidation of MVK and MACR in the gas phase.

(Paulot *et al*., 2009a).

A peculiar fate of the $Z_{1,4}$-O and $Z_{4,1}$-O radicals would be the fast intramolecular 1, 5 H-shift of the enolic hydrogen to form alyllic-type dihydroxyl isoprenyl radicals as proposed by Dibble (2002) based on quantum chemical calculations, and shown in Reactions (22) and (23).

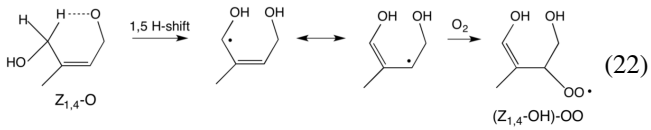

(22)

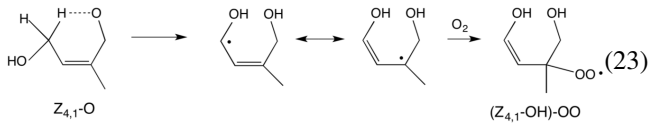

(23)

From the dihydroxyl isoprenyl radical, corresponding peroxy radicals would be formed in the atmosphere. A quantum chemical theoretical investigation by Peeters and Nguyen (2012) found that the 1, 6-H shifts of the enolic hydrogen in the ($Z_{1,4}$-OH)-OO and ($Z_{4,1}$-OH)-OO radicals have exceptionally low energy barriers such that they proceed at the rate of 10^5 to 10^6 s^{-1} at ambient temperatures to form hydroxy-hydroperoxy-ketoisoprenyl radicals. Therefore, the 1, 6-H shift reaction is considered to take precedence over the bimolecular reaction with NO to form oxy radicals even under high NO_X conditions.

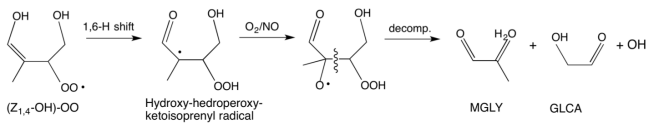

(24)

The fate of the hydroxy-hydroperoxy-ketoisoprenyl radical is the reaction with O_2 and NO to form corresponding oxy radicals as shown above, which will decompose to produce MGLY and GLCA. Similarly, ($Z_{4,1}$-OH)-OOH gives GLY and HACT as depicted in Fig. 3. In contrast to ($Z_{1,4}$-OH)-OO and ($Z_{4,1}$-OH)-OO, ($E_{1,4}$-OH)-OO and ($E_{4,1}$-OH)-OO have large barriers to the intramolecular hydrogen shift and do not proceed to form corresponding hydroxy-hydroperoxy-ketoisoprrenyl radicals according to Peeters and Nguyen (2012).

The OH-initiated secondary oxidation of MVK is also known to produce GLCA and MGLY (Tuazon and Atkinson, 1989; Paulot *et al*., 2009a), and that of MACR produces HACT and MGLY (Tuazon and Atkinson, 1990; Orlando *et al*., 1999; Paulot *et al*., 2009a). The formation mechanisms of GLCA and MGLY from MVK, and HACT and MGLY from MACR, are shown in Fig. 4 referring to previous papers (Tuazon and Atkinson, 1989; Orlando *et al*., 1999).

The reaction with MVK is initiated by OH addition to the terminal or internal carbon of the double bond. The major pathway is the addition to the terminal CH_2 accounting for about 72% (Calvert *et al*., 2011). In the case of MACR, the total reaction pathways comprise 55% by addition and 45% by abstraction of the aldehydic H-atom (Calvert *et al*., 2011). The addition of OH occurs more often at the terminal carbon of the double bond than at the internal carbon, as in the case of MVK (Tuazon and Atkinson, 1990). The abstraction of the H-atom from aldehydic carbon in MACR yields only fragmented products and does not contribute to the formation of bifunctional compounds.

The experimental yields of GLCA and MGLY from MVK are reported to be 63–67% and 24–27% (Tuazon and Atkin-

doi:10.5047/meep.2016.00401.0001

son, 1989; Paulot *et al*., 2009a; Galloway *et al*., 2011), respectively. Those of HACT and MGLY from MACR are reported to be 40–47%, and 8–<12% (Tuazon and Atkinson, 1990; Orlando *et al*., 1999; Galloway *et al*., 2011), respectively, while that of HACT is reported to be 20% (Paulot *et al*., 2009a). Galloway *et al*. (2011) summarized those yields comparing with the MCM modelling (Saunders *et al*., 2003) results.

Although it is not covered in this review, the NO_3-initiated oxidation of isoprene may result in GLY and MGLY (Fu *et al*., 2008). O_3-initiated oxidation of isoprene also forms MGLY as well as GLCA and HACT via the OH-initiated secondary oxidation reactions of the first-generation products, MVK and MACR.

Another important reaction pathway of OH-initiated isoprene oxidation reactions that is deeply relevant to SOA is the recently discovered mechanism leading to the production of isoprene epoxide (Paulot *et al*., 2009b; Surratt *et al*., 2010). Under a low concentration of NO, where the mutual reactions between HO_2 and RO_2 override the reaction with NO to form oxy radicals, the addition of OH to either of the double bonds is expected to yield hydroxy-hydroperoxides (β4-ISOPOOH and δ4-ISOPOOH) as follows (Paulot *et al*., 2009b).

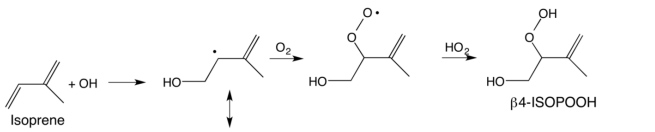

(25)

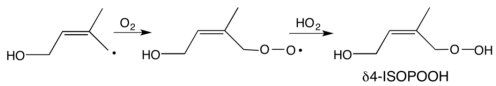

(26)

These hydroxy-hydroperoxides, β4-ISOPOOH and δ4-ISOPOOH, have been found to react further with OH to form dihydroxyepoxides, 2-methyl-2, 3-epoxy-1, 4-butanediol (β-IEPOX) and 3-methyl-3, 4-epoxy-1, 2-butandiol (δ-IEPOX) via the following mechanisms (Paulot *et al*., 2009b).

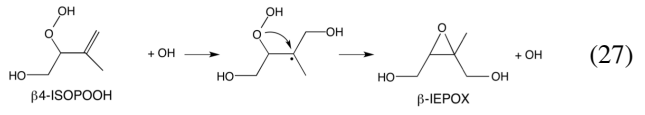

(27)

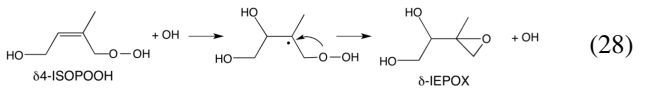

(28)

Paulot *et al*. (2009b) established the above consecutive mechanism from the kinetic analysis of the products using an isotope-labeled ^{18}OH. They further confirmed by quantum chemical calculations that ISOPOOH can be correlated to IEPOX by energetically favorable adiabatic pathways. The importance of β-IEPOX and δ-IEPOX for the formation of organosulfates in the liquid phase will be discussed in Subsection 4.2.

2.2.4 OH + toluene Early studies on the OH-initiated oxidation of toluene identified GLY and MGLY as important ring-cleavage reaction products as well as ring-retaining products of cresol (CRS) and benzaldehyde (BZA) (Shepson *et al*., 1984; Tuazon *et al*., 1984; Bandow *et al*., 1985; Gery *et al*., 1985; Dumdei *et al*., 1988). The yields of GLY and MGLY, however, varied widely in the ranges 0.04–0.39 and 0.04–0.16, respectively, including later studies (Calvert *et al*., 2002; Baltaretu *et al*., 2009). Similarly, the production of GLY from benzene, and GLY, MGLY and biacetyl (BCT) from xylenes has been reported (Calvert *et al*., 2002). These ring-ruptured products have long been thought of as primary first-generation products and formation mechanisms have been proposed, such as those compiled by Calvert *et al*. (2002).

However, a recent laboratory study on the OH-initiated oxidation of toluene by Baltaretu *et al*. (2009) using the turbulent flow system with chemical ionization mass spectrometer (CIMS) has shown that GLY and MGLY were minor primary products with upper limit yields of <4%. They identified the ring-ruptured C_7-compounds, 2-methyl-2, 4-hexadiene-1, 6-dial (MHDD), and 2, 3-epoxy-2-methyl-4-hexene-1, 6-dial (EPHD), as the major primary products, as well as previously known ring-retaining products, CRS and BZA. They suggested that secondary oxidation processes involving MHDD and EPHD are likely to be responsible for previous observations of GLY and MGLY from toluene oxidation, in addition to the first-generation production. The wide range of the yields of these compounds reported in previous studies could be ascribed to the different experimental conditions under which the contributions of the secondary reactions vary. Figure 5 shows the reaction mechanism of the OH-initiated oxidation of toluene showing the first-generation production of MGLY proposed by Baltaretu *et al*. (2009).

The absolute yields of the primary products were given as cresol (CRS) $28.1 \pm 6.1\%$, dienedial (MHDD) $23.5 \pm 8.7\%$, epoxydial (EPHD), $7.2 \pm 2.5\%$, and benzaldehyde (BZA) $4.9 \pm 1.8\%$ (Baltaretu *et al*., 2009). The formation of EPHD from toluene has been previously reported by Yu and Jeffries (1997), and Klotz *et al*. (1999), respectively. As shown in Fig. 5, the hydroxyl-cyclohexadienyl-peroxy radical (B) formed from the initially formed hydroxyl-cyclohexadienyl radical (A) transforms to hydroxy-bicyclo radical (C), and this radical reacts with O_2 and NO to give a hydroxy-bicyclo-oxy radical (G). The cyclization to form allylically stabilized five-membered bicyclo radicals (C) has been studied theoretically by ab initio calculations and is found to be exothermic by ca. 10 kcal mol^{-1} (Andino *et al*., 1996). The possible fate of the bicyclo-oxy radical (G) to form dicarbonyl compounds has also been studied theoretically (Wang *et al*., 2013).

Based on the experimental evidence, Baltaretu *et al*. (2009) proposed a reaction mechanism to produce GLY and MGLY as a secondary oxidation of the dienedial (MHDD) and epoxydial (EPHD). An example of the possible pathways to form GLY and MGLY are shown in Fig. 6 (Klotz *et al*., 1999; Baltaretu *et al*., 2009).

It should be noted that the mechanism of aromatic hydrocarbon oxidation following the initial OH addition to a benzene ring is still highly uncertain, and further investigation is necessary.

doi:10.5047/meep.2016.00401.0001

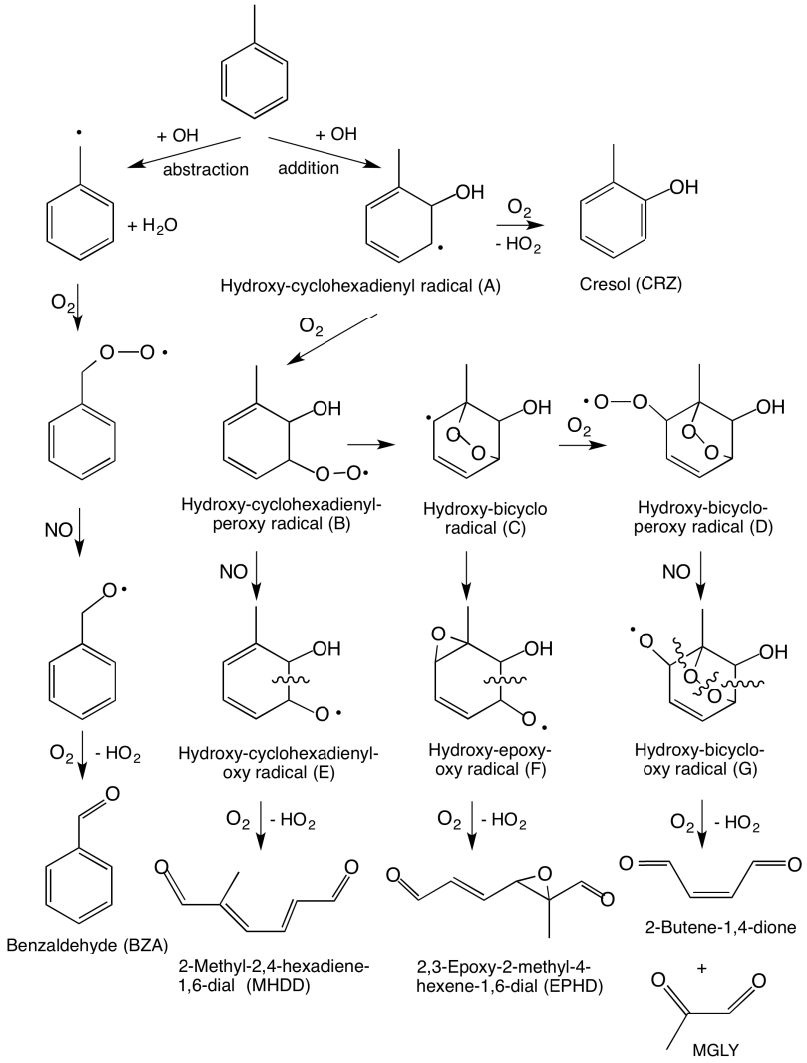

Fig. 5. Reaction mechanisms of the OH-initiated oxidation of toluene in the presence of NO_x (based on Baltaretu *et al*., 2009). The names of the radicals in the figure are for the purpose of correspondence with the text, and not the formal names.

2.2.5 OH + acetone Acetone, $CH_3C(O)CH_3$, is emitted from natural sources such as terrestrial vegetation and dissolved organic matter in the ocean, and also produced in the atmosphere by the OH-initiated oxidation of propane when the secondary hydrogen of propane is abstracted (Calvert *et al*., 2008).

$$CH_3CH_2CH_3 + OH \rightarrow CH_3CHCH_3 + H_2O \quad (29)$$

$$CH_3CHCH_3 + O_2(+M) \rightarrow CH_3CH(OO)CH_3(+M) \quad (30)$$

$$CH_3CH(OO)CH_3 + NO \rightarrow CH_3CH(O)CH_3 + NO_2 \quad (31)$$

$$CH_3CH(O)CH_3 + O_2 \rightarrow \underline{CH_3C(O)CH_3} + HO_2 \quad (32)$$

The abstraction of primary hydrogen leads to propanal as a product. The production ratio of propanal and acetone in the OH-initiated oxidation of propane is 26% and 74%, respectively, reflecting to the abstraction ratio of primary and secondary hydrogen (Kwok and Atkinson, 1995). Detailed pathways of the OH-initiated oxidation of propane has recently been studied theoretically (Rosado-Reyes and Francisco, 2007). Although it has also been reported that acetone is formed by OH and O_3 oxidation reactions of various monoterpenes (Reissell *et al*., 1999; Wisthaler *et al*., 2001), the reaction mechanisms have not been well studied and are not discussed here.

Acetone is further oxidized by OH radicals to form MGLY in the presence of NO as follows (Calvert *et al*., 2011):

$$CH_3C(O)CH_3 + OH \rightarrow CH_3C(O)CH_2 + H_2O \quad (33)$$

$$CH_3C(O)CH_2 + O_2(+M) \rightarrow CH_3C(O)CH_2OO(+M) \quad (34)$$

$$CH_3C(O)CH_2OO + NO \rightarrow CH_3C(O)CH_2O + NO_2 \quad (35)$$

$$CH_3C(O)CH_2O + O_2 \rightarrow \underline{CH_3C(O)CHO} + HO_2. \quad (36)$$

The yield of MGLY from acetone has been reported to be >85% by Talukdar *et al*. (2003) and Turpin *et al*. (2006).

2.2.6 OH + glycolaldehyde, hydroxyacetone Glycolaldehyde (GLCA) formed in the OH-initiated oxidation of ethylene (c.f. Subsection 2.2.2), and GLCA and HACT formed together with GLY and MGLY in the OH-initiated oxidation of isoprene (c.f. Subsection 2.2.3) are water-

doi:10.5047/meep.2016.00401.0001

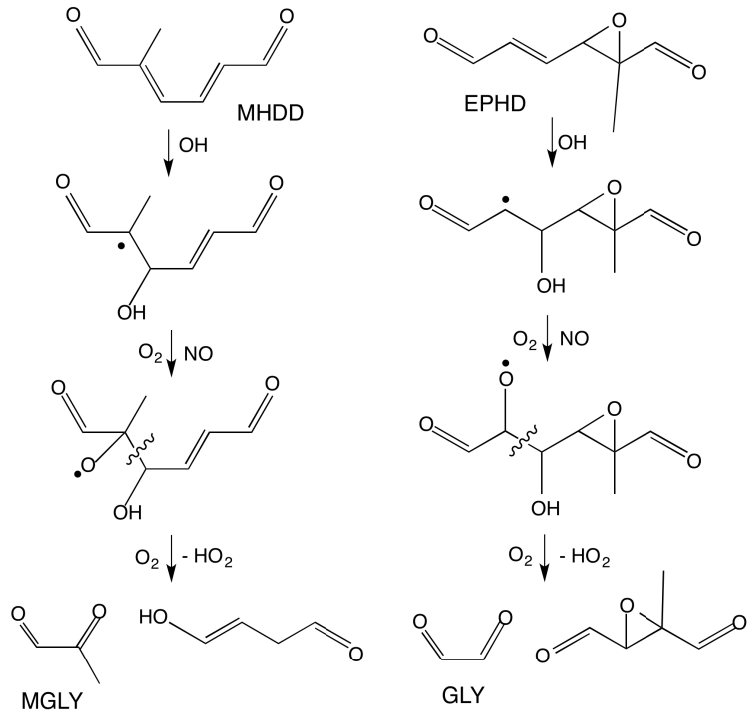

Fig. 6. Possible reaction mechanisms of the secondary formation of glyoxal and methylglyoxal from 2-methyl-2, 4-hexadien-1, 6-dial (MHDD) and 2, 3-epoxy2-methyl-4-hexene-1, 6-dial (EPHD) in the OH-initiated oxidation of toluene (Klotz *et al*., 1999; Baltaretu *et al*., 2009).

soluble (Bacher *et al*., 2001) and uptake in cloud water or an aqueous aerosol leads to the formation of SOA together with glyoxal and methylglyoxal as described in the next section. However, it should be noted that the OH-initiated gas-phase reactions of GLCA and HACT are also important dissipation processes in the atmosphere, and produce GLY and MGLY as third-generation products.

Glycolaldehyde is reactive to an OH radical and can form GLY and other products as shown below (Calvert *et al*., 2011):

$$\mathrm{HOCH_2CHO + OH \rightarrow HOCH_2\dot{C}O + H_2O} \quad (37a)$$
$$\rightarrow \mathrm{HO\dot{C}HCHO + H_2O.} \quad (37b)$$

An early study by Niki *et al*. (1987) gave a branching ratio of channels (37a) and (37b) to be 0.80 : 0.20. A more recent study by Magneron *et al*. (2005) gave 0.22 ± 0.06 for channel (37b), and a turbulent flow study with CIMS by Butkovskaya *et al*. (2006a) obtained yields for the reactions (37a) and (37b) as 0.84 and 0.16, respectively. The HOCHCHO radical formed in reaction (37b) gives GLY as follows:

$$\mathrm{HO\dot{C}HCHO + O_2 \rightarrow \underline{CHOCHO} + HO_2} \quad (38a)$$
$$\rightarrow \mathrm{HCOOH + CO + OH.} \quad (38b)$$

Butkovskaya *et al*. (2006a) obtained the fractional yields (38a) : (38b) as 0.81 : 0.19 at 296 K.

Meanwhile, the major fates of the $\mathrm{HOCH_2CO}$ radical formed in reaction (37a) are

$$\mathrm{HOCH_2\dot{C}O + O_2 \rightarrow HCHO + CO + HO_2} \quad (39a)$$
$$\rightarrow \mathrm{HCHO + CO_2 + OH} \quad (39b)$$
$$\rightarrow \mathrm{HCOOH + CO_2 + H} \quad (39c)$$

simply giving fragmentation products in the ratio of 0.58 : 0.26 : 0.15 at 296 K (Butkovskaya *et al*., 2006a).

Hydroxylacetone (HACT) is also water-soluble as glycolaldehyde and may be taken into clouds and liquid aerosols to be involved in liquid phase oxidation to form SOA. The major fate of HACT in the atmosphere other than deposition to water droplets is the oxidation initiated by OH radicals, since the recommended rate constant of the OH reaction, 4.1×10^{-12} cm^3 molecule^{-1} s^{-1}, is 22 times larger than for OH + acetone (Calvert *et al*., 2011) and photolytic decay is negligible (Orlando *et al*., 1999). The initial process of the OH-reaction is the abstraction of an H atom from the -CH_2 site and the radical formed reacts rapidly with O_2 to form MGLY:

$$\mathrm{CH_3C(O)CH_2OH + OH \rightarrow CH_3C(O)\dot{C}HOH + H_2O} \quad (40)$$
$$\mathrm{CH_3C(O)\dot{C}HOH + O_2 \rightarrow \underline{CH_3C(O)CHO} + HO_2.} \quad (41)$$

Butkovskaya *et al*. (2006b) reported a yield of MGLY of 82% at 298 K, but the yield decreased to 49% at 236 K. As well as MGLY, they observed formic and acetic acids as

doi:10.5047/meep.2016.00401.0001

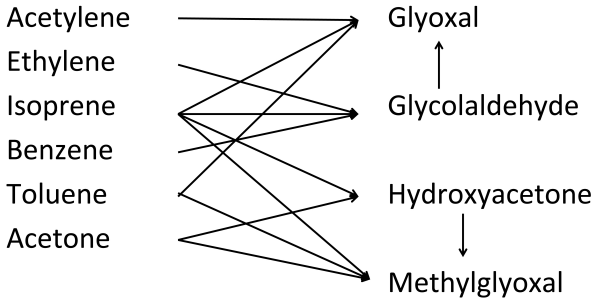

Fig. 7. Correspondence of precursors and products, which are important for the heterogeneous formation of SOA.

products, and suggested the following reaction pathways:

$$CH_3C(O)\dot{C}HOH + O_2$$
$$\rightarrow CH_2{=}C{=}O + HC(O)OH + OH \quad (42a)$$
$$\rightarrow HC(O)OH + CH_3 + CO_2 \quad (42b)$$
$$\rightarrow CH_3C(O)OH + CO + OH \quad (42c)$$
$$\rightarrow CH_3C(O)OH + CO_2 + H. \quad (42d)$$

They suggested that these reactions occur via a cyclic O_2 complex, which is favored at low temperatures over the abstraction reaction to give MGLY.

2.2.7 Summary of glyoxal and methylglyoxal formation in the gas phase Although a part of glyoxal and methylglyoxal is emitted directly from open biomass burning and biofuels as primary sources (Fu *et al*., 2008 and references therein), the greater part of them in the atmosphere are secondary products of VOC oxidation described above. Primary VOC precursors are acetylene, ethylene, isoprene, aromatics (benzene, toluene, xylenes), acetone, glycolaldehyde, hydroxyacetone and some other minor contributors as listed in Fu *et al*. (2008). Among them, acetone, glycolaldehyde and hydroxyacetone are also produced as secondary products by the oxidation of the above hydrocarbons as described previously. Figure 7 summarizes the correspondence between the precursors and the secondary carbonyl compounds, which are important as precursors of the heterogeneous formation of SOA. Table 2 cites the rate constants of the gas-phase OH radical reactions for the precursors of glyoxal and methylglyoxal.

Although a detailed discussion based on modeling studies is beyond the scope of this review, the extracted results on the global sources of GLY and MGLY calculated by Fu *et al*. (2008), using the GEOS-Chem global model coupled with the Master Chemical Mechanism (MCM v.3.1), are cited in Table 3. It can be seen that the OH-initiated oxidation of isoprene is overwhelmingly the most important source of GLY and MGLY globally, followed by that of acetylene for GLY, and acetone for MGLY. It should be noted that the contribution of acetylene and acetone as sources of GLY and MGLY, respectively, are much more important in the free troposphere due to their smaller OH rate constants given in Table 2 and subsequently longer atmospheric lifetime.

Table 2. Rate constants at 298 K for the reaction of OH radicals.

Compounds	Rate Constants (298 K) (10^{-11} cm^3 molecule^{-1} s^{-1})	Ref.
Acetylene	0.078[1)]	(a)
Ethylene	0.79[1)]	(a)
Isoprene	10	(a)
Benzene	0.12	(b)
Toluene	0.56	(b)
o-Xylene	1.4	(b)
m-Xylene	2.3	(b)
p-Xylene	1.4	(b)
Acetone	0.018	(a)
Glycolaldehyde	1.1	(a)
Hydroxyacetone	0.30	(a)

[1)] 1 atm, (a) Atkinson *et al*. (2006), (b) Atkinson and Arey (2003).

Table 3. Global sources and production of glyoxal and methyl glyoxal (Fu *et al*., 2008).

Precursor	Production (Tg a^{-1})	
	Glyoxal	Methylglyoxal
Acetylene	8.9	—
Ethylene	2.5	—
Isoprene	21	110
Benzene	0.90	—
Toluene	0.68	0.65
Xylenes	0.39	0.73
Acetone (primary)	—	10
Glycolaldehyde (primary)	0.54	—
Hydroxyacetone (primary)	—	3.6
Glyoxal (primary)	7.7	—
Methylglyoxal (primary)	—	5.0
Others	0.34	11.8
Total source	45	140

2.3 Hydration of glyoxal and methylglyoxal in aqueous solution

In the late 1990s to the early 2000s, it was suggested that cloud processing of GLY, MGLY and other carbonyl species could be a significant source of small dicarboxylic acids, and that they can be retained in the aerosol phase upon the evaporation of water droplets (Chebbi and Carlier, 1996; Buxton *et al*., 1997; Blando and Turpin, 2000; Warneck, 2003; Ervens *et al*., 2004). Since then, research on the aqueous phase chemistry of GLY and related species has been expanding to cover various aspects of SOA formation in cloud, fog and aerosol droplets. In this section, the aqueous phase reaction processes of the most fundamental cases of the formation of oxalic acids and other small dicarboxylic acid in cloud and fog conditions are discussed. The extension to the aqueous phase chemistry under conditions of higher concentration in the atmosphere will be discussed in the following sections.

Glyoxal is known to exist predominantly as a dihydrated

doi:10.5047/meep.2016.00401.0001

gem-diol $CH(OH)_2CH(OH)_2$ in an aqueous phase, as shown below (Betterton and Hoffmann, 1988; Buxton *et al*., 1997; Ervens and Volkamer, 2010; Lim *et al*., 2010):

$$CHOCHO(aq) + H_2O \rightleftarrows CHOCH(OH)_2 \quad (43)$$
$$CHOCH(OH)_2 + H_2O \rightleftarrows CH(OH)_2CH(OH)_2. \quad (44)$$

Similarly, methylglyoxal exists as monohydrated and dihydrated gem-diol in an aqueous phase:

$$CH_3COCHO(aq) + H_2O \rightleftarrows CH_3COCH(OH)_2 \quad (45)$$
$$CH_3COCH(OH)_2 + H_2O \rightleftarrows CH_3C(OH)_2CH(OH)_2. \quad (46)$$

The hydration constant, K_{hyd}, for glyoxal can be defined as:

$$K_{hyd1} = [CHOCH(OH)_2]/[CHOCHO]_{aq} \quad (47)$$
$$K_{hyd2} = [CH(OH)_2CH(OH)_2]/[CHOCH(OH)_2] \quad (48)$$
$$K_{hyd} = [CH(OH)_2CH(OH)_2]/[CHOCHO]_{aq} = K_{hyd1} \cdot K_{hyd2}. \quad (49)$$

The values of K_{hyd} are 2.2×10^5, 2.7×10^3 and 1.0×10 for GLY, MGLY and GLCA, respectively (Betterton and Hoffmann, 1988). The values of the hydration constants of each step are $K_{hyd1} = 207$ and $K_{hyd2} = 350$ for GLY (Ruiz-Montoya and Rodriguez-Mellado, 1995), so that the monohydrate concentration contributes only 0.5% and glyoxal exists mostly as dihydrated gen-diol (Ervens and Volkamer, 2010). Monohydrated and dihydrated MGLY are reported to be present at a 55 : 45 ratio, while unhydrated methylglyoxal was not detected by NMR (de Haan *et al*., 2009b).

The effective Henry's law constant in pure water, K_H^*, the intrinsic Henry's law constant, K_H, and the hydration constant are related by the following equations (Betterton and Hoffmann, 1988):

$$K_H = [CHOCHO]_{aq}/[CHOCHO]_g \quad (50)$$
$$K_H^* = ([CHOCHO]_{aq} + [(OH)_2CHCH(OH)_2])/[CHOCHO]_g. \quad (51)$$

From the above equations,

$$K_H^* = K_H(1 + K_{hyd}). \quad (52)$$

And thus $K_H^* \approx K_H K_{hyd}$ when K_{hyd} is much larger than unity. The effective Henry's law constants for GLY in pure water have been given at 298 K as 4.2×10^5 M atm^{-1} (Ip *et al*., 2009), and 3.7×10^3 and 4.1×10^4 M atm^{-1} for MGLY, and GLCA, respectively (Betterton and Hoffmann, 1988). Meanwhile, the physical solubility of glyoxal is reported to be as small as $K_H = 5.8$ M atm^{-1} (Ip *et al*., 2009). It can be seen that K_H^* for GLY and MGLY are large due to large K_{hyd}, but the large K_H^* for GLCA reflects a large intrinsic Henry's law constant owing to the hydrophilic OH-group in a molecule. Schweitzer *et al*. (1998) reported a mass accommodation coefficient of $\alpha = 0.023$ for GLY to water and an uptake coefficient $\gamma = \sim 10^{-3}$–0.02 depending on the pH and existing sulfite ion (SO_3^{2-}). Liggio *et al*. (2005b) gave γ of GLY in the range 8.0×10^{-4} to 7.3×10^{-3} with a median of $\gamma = 2.9 \times 10^{-3}$ for $(NH_4)_2SO_4$ seed aerosols at 55% relative humidity.

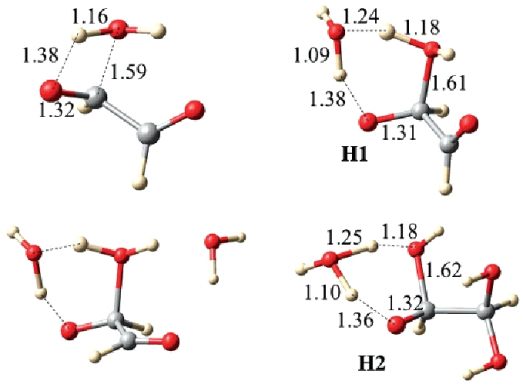

Fig. 8. The molecular structurres of the transition states for the hydration reactions of glyoxal. See the text. (Reprinted with permission from Kua, J., S. W. Hanley, and D. O. De Haan (2008), Thermodynamics and kinetics of glyoxal dimer formation: A computational study, *J. Phys. Chem. A*, *112*, 66–72. Copyright 2008 American Chemical Society.)

The hydration of GLY and the subsequent formation of a dimeric species in an aqueous solution has been studied by Kua *et al*. (2008) using ab initio quantum chemical calculations. The Gibbs free energy changes for the formation of the monohydrate and dihydrate are calculated as $\Delta_r G^\circ = -2.8$ and -4.7 kcal mol^{-1}, respectively. Figure 8 shows the transition states of the hydration reactions. If one water molecule is involved in the formation of the monohydrate, the transition state is four-centered (upper left), and when two water molecules are involved the six-centered transition state (upper right, **H1**) is realized. The transition energy via the four- and six-centered states are $\Delta^\ddagger G^\circ = 37.0$ and $\Delta^\ddagger G^\circ = 18.5$ kcal mol^{-1}, so that the latter pathway via **H1** is energetically more favourable. The lower left shows the state if three water molecules are involved to form the monohydrate. For the addition of one more water molecule to form the dihydrate via the six-centered transition state (lower right, **H2**), $\Delta^\ddagger G^\circ$ is 15.5 kcal mol^{-1} implying a preference for the formation of the dihydrate gem-diol.

Similarly, the thermodynamics and kinetics of hydration and dimerization of methylglyoxal has been calculated by Krizner *et al*. (2009). In the case of methylglyoxal, $\Delta_r G^\circ = -1.4$ and 2.7 kcal mol^{-1} for the monohydrate (diol on the carbon without methyl group) and the dihydrate, respectively, showing that the monohydrate is more favourable thermochemically, which agrees with experimental results.

2.4 Aqueous phase radical reactions of glyoxal and related species to form oxalic acid

The aqueous phase oxidation of organic molecules is thought to be predominantly initiated by an OH radical since it is known to be the most reactive among a number of radicals (Buxton *et al*., 1988; Ervens *et al*., 2003a; Monod and Doussin, 2008; Doussin and Monod, 2013). The rate constants of OH with dihydrated glyoxal is as large as 1.05×10^9 M^{-1} s^{-1} (Buxton *et al*., 1997) and the corresponding value

doi:10.5047/meep.2016.00401.0001

for monohydrated methylglyoxal is reported to be 1.1×10^9 M^{-1} s^{-1} (Ervens *et al*., 2003b) and 0.53×10^9 M^{-1} s^{-1} (Monod *et al*., 2005). As for the origin of OH radicals in atmospheric water droplets, gas-phase OH radicals are thought to be the major source (Chameides and Davis, 1982) considering the Henry's law constant of ca. 30 M atm^{-1} (Sander, 1999). In cloud droplets, OH radicals can also be formed through the photolysis of H_2O_2 with or without co-existing iron ions (Faust and Allen, 1993; Arakaki and Faust, 1998), and aqueous phase OH radical concentrations in clouds and fogs are estimated to be 10^{-14}–10^{-12} M (Jacob, 1986; Ervens *et al*., 2004; Herrmann *et al*., 2010). It has been shown that the contribution of radicals and radical anions other than OH are negligible (Ervens *et al*., 2003a).

Clear experimental evidence of the formation of oxalic acid (OXD) as a major product has been shown by Carlton *et al*. (2007) in a batch photochemical aqueous reaction of glyoxal (GLY) in the presence of H_2O_2 under UV irradiation. Formic acid appeared as a first-generation major product within the first 2 min of the experiment, and the formation of larger molecular weight compounds were detected at ∼30 min. Subsequently, Tan *et al*. (2009) observed in an online experiment (30–3000 μM) that the predominant product of the aqueous phase oxidation of GLY is OXD at a cloud-level concentration (e.g. 30 μM). They also demonstrated that the glyoxylic acid (GLXD, CHOCOOH) is a first-generation product and OXD increased rapidly as GLXD decayed in agreement with the assumption made by Warneck (2003) that GLXD is the key intermediate in the OXD formation. Figure 9 shows the time profile of GLXD and OXD in the online experiment with electrospray ionization mass spectrometry (ESI-MS) analysis. In agreement with a previous batch experiment, a large number of additional higher molecular weight ions were observed. Based on these experimental results and the proposed reaction mechanism (Lim *et al*., 2010), the formation mechanism of glyoxylic acid and formic acid as first-generation products and oxalic acid formation as a second generation product in the OH-initiated oxidation of glyoxal in the aqueous phase may be represented as shown in Fig. 10 (Lim *et al*., 2010).

Thus, the oxidation reaction is initiated by the abstraction of an H atom from a C-H bond in dihydrated glyoxal by an OH radical to form hydrated glyoxylic acid (HGLXD), and OXD is formed by a further H-atom abstraction from HGLXD by OH. The rate constants of OH with dehydrated glyoxal and hydrated glyoxylic acid have been given as 1.1×10^9 and 3.6×10^8 M^{-1} s^{-1}, respectively (Ervens *et al*., 2004). The H-atom abstracted radicals from hydrated GLY and GLXD react with O_2 rapidly. The reaction is thought to proceed through the addition of O_2 to form peroxy radicals, but, unlike the analogous peroxy radical conversions in the gas phase, the reaction with NO does not occur in the aqueous phase due to the low Henry's law constant of NO, $K_H(NO) \approx 2 \times 10^{-3}$ M atm^{-1} (Sander, 1999). It should be noted that the aqueous phase reaction of OH with OXD does not occur effectively since the H-atom abstraction from the O-H bond is 10–100 times slower than from the C-H bond (Lim *et al*., 2010), according to the estimation method of Monod *et al*. (2005) and Monod and Doussin (2008).

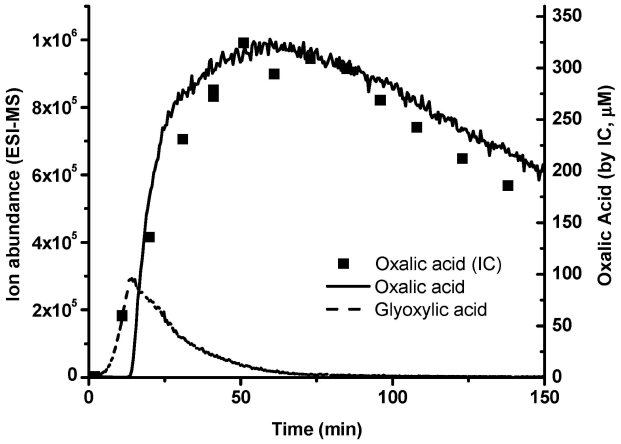

Fig. 9. Time profile of the formation of oxalic acid (OXD) and glyoxylic acid (GLXD) in the glyoxal (1 μM)+H_2O_2+UV experiment. (Reprinted with permission from Tan, Y., M. J. Perri, S. P. Seitzinger, and B. J. Turpin (2009), Effects of precursor concentration and acidic sulfate in aqueous glyoxal-OH radical oxidation and implications for secondary organic aerosol, *Environ. Sci. Technol*., *43*, 8105–8112. Copyright 2009 American Chemical Society.)

Similarly, the OH-initiated oxidation of monohydrated methylglyoxal (CH_3CO-$CH(OH)_2$) in a cloud-relevant concentration (e.g. 30 μM) gives pyruvic acid (PRVD, $CH_3COCOOH$) as the major first generation product in the aqueous OH radical oxidation reaction (Altieri *et al*., 2008; Tan *et al*., 2010; Zhao *et al*., 2012), from which acetic acid (ACD, CH_3COOH) is known to form (Carlton *et al*., 2006):

$$\underline{CH_3CO\text{-}CH(OH)_2} + OH \rightarrow CH_3CO\text{-}\dot{C}(OH)_2 + H_2O \quad (53)$$

$$CH_3CO\text{-}\dot{C}(OH)_2 + O_2 \rightarrow \underline{CH_3CO\text{-}COOH} + HO_2 \quad (54)$$

$$CH_3CO\text{-}COOH + OH + O_2 \rightarrow \underline{CH_3COOH} + CO_2 + HO_2. \quad (55)$$

Oxalic acid and glyoxylic acid have been identified as second-generation products of the oxidation reaction of MGLY in the aqueous phase, and OXD becomes the major product as the reaction proceeds (Altieri *et al*., 2006; Tan *et al*., 2010).

The OH-initiated reaction of acetic acid (ACD) has recently been studied by Tan *et al*. (2012). The major first-generation products are GLXD, and OXD is formed as the second-generation product from GLXD just as the same way as in the case of glyoxal reaction. As well as glyoxylic and oxalic acid, the formation of glycolic acid (GLCD, $HOCH_2COOH$) and formic acid (FMD) has been reported (Tan *et al*., 2012). The oxidation pathways to form GLXD, GLCD, and HCHO have been given as follows (Leitner and

doi:10.5047/meep.2016.00401.0001

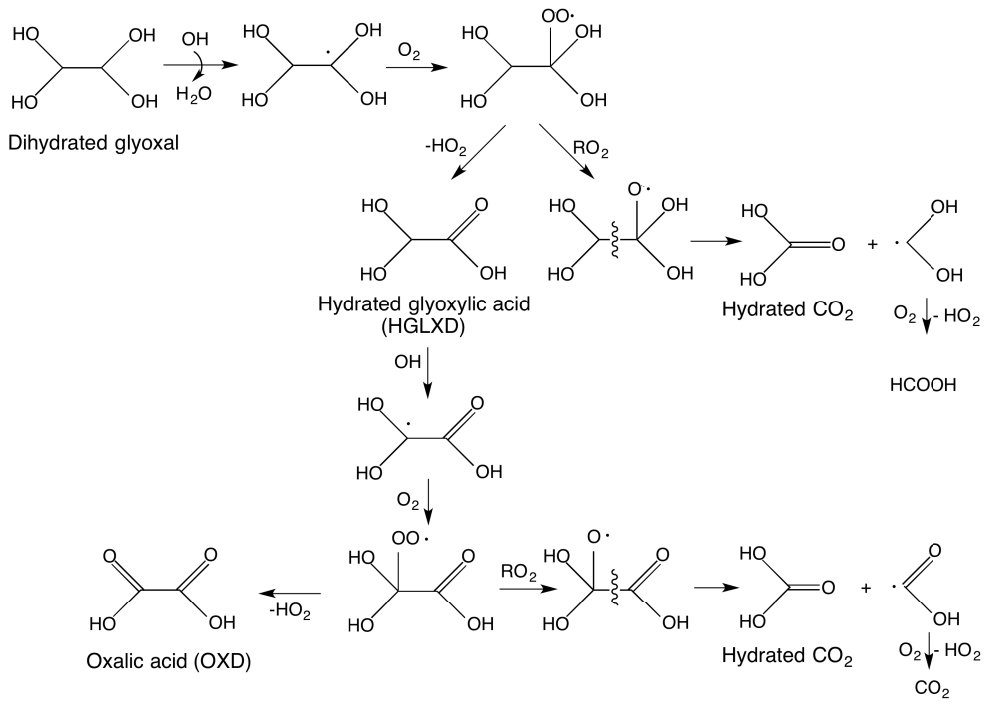

Fig. 10. Proposed mechanism of oxalic acid formation in the reaction of glyoxal dihydrate and an OH radical in the aqueous phase.

Dore, 1997; Tan *et al*., 2012):

$$\underline{CH_3COOH} + OH \rightarrow \dot{C}H_2COOH + H_2O \quad (56)$$

$$\dot{C}H_2COOH + O_2 \rightarrow \dot{O}OCH_2COOH \quad (57)$$

$$2\dot{O}OCH_2COOH \rightarrow \underline{CHO\text{-}COOH} + \underline{HOCH_2COOH} + O_2 \quad (58a)$$

$$\rightarrow 2\dot{O}CH_2\text{-}COOH + O_2 \quad (58b)$$

$$\dot{O}CH_2\text{-}COOH + O_2 \rightarrow \underline{HCHO} + CO_2 + HO_2. \quad (59)$$

The formation mechanisms of OXD from GLXD have been given before, and GLCD also forms OXD through GLXD and GLY as described below.

From glycolaldehyde (GLCA) formed in the gas phase oxidation of ethylene and isoprene, either glycolic acid (GLCD) or hydrated glyoxal is formed in the aqueous phase oxidation (Warneck, 2003; Perri *et al*., 2009), from which oxalic acid is produced through hydrated glyoxylic acid as seen in Fig. 10. The reaction pathways from GLCA to GLCD (Reaction 60–62) and GLXD (Reactions 63, 64), and to hydrated glyoxal (Reactions 65, 66) are shown as follows:

$$\underline{HOCH_2\text{-}CHO} + H_2O \rightarrow HOCH_2\text{-}CH(OH)_2 \quad (60)$$

$$HOCH_2\text{-}CH(OH)_2 + OH \rightarrow HOCH_2\text{-}\dot{C}(OH)_2 + H_2O \quad (61)$$

$$HOCH_2\text{-}\dot{C}(OH)_2 + O_2 \rightarrow \underline{HOCH_2\text{-}COOH} + HO_2 \quad (62)$$

$$HOCH_2\text{-}COOH + OH \rightarrow HO\dot{C}H\text{-}COOH + H_2O \quad (63)$$

$$HO\dot{C}H\text{-}COOH + O_2 \rightarrow \underline{CHO\text{-}COOH} + HO_2 \quad (64)$$

$$HOCH_2\text{-}CH(OH)_2 + OH \rightarrow HO\dot{C}H\text{-}CH(OH)_2 + H_2O \quad (65)$$

$$HO\dot{C}H\text{-}CH(OH)_2 + O_2 \rightarrow \underline{CHO\text{-}CH(OH)_2} + HO_2. \quad (66)$$

Hydroxyacetone (HACT) formed in the gas phase oxidation of isoprene, gives pyruvic acid (PRVD, $CH_3CO\text{-}COOH$) through hydrated methylglyoxal (Ervens *et al*., 2008). The reaction process is as follows:

$$\underline{CH_3CO\text{-}CH_2OH} + OH \rightarrow CH_3CO\text{-}\dot{C}HOH + H_2O \quad (67)$$

$$CH_3CO\text{-}\dot{C}HOH + O_2 \rightarrow CH_3CO\text{-}CHO + HO_2 \quad (68)$$

$$CH_3CO\text{-}CHO + H_2O \rightarrow \underline{CH_3CO\text{-}CH(OH)_2} \quad (69)$$

$$CH_3CO\text{-}CH(OH)_2 + OH \rightarrow CH_3CO\text{-}\dot{C}(OH)_2 + H_2O \quad (70)$$

$$CH_3CO\text{-}\dot{C}(OH)_2 + O_2 \rightarrow \underline{CH_3CO\text{-}COOH} + HO_2. \quad (71)$$

It has been shown that a cloud-relevant concentration of sulfuric acid (Tan *et al*., 2009), ammonium sulfate and nitric acid (Kirkland *et al*., 2013) have little effect on oxalic acid formation.

The aqueous medium enables the formation of glyoxal gem-diols whose functional groups are oxidized during reactions with OH, while the C-C bond structure is preserved to allow the formation of oxalic acid in cloud water being different from in the gas phase. Oxalic acid thus formed in the aqueous phase oxidation of glyoxal and other dicarbonyls in cloud and fog remains as the particle upon evaporation of water droplets.

2.5 Aqueous phase radical reactions of glyoxal and methylglyoxal to form larger diacids

In the aqueous phase the OH-initiated photooxidation of glyoxal, methylglyoxal and related species in laboratory experiments have revealed that increasing the precursor concentrations results in formation of higher carbon number (C_3-C_6) dicarboxylic acids and other multifunctional carbonyl compounds. Even higher molecular weight

doi:10.5047/meep.2016.00401.0001

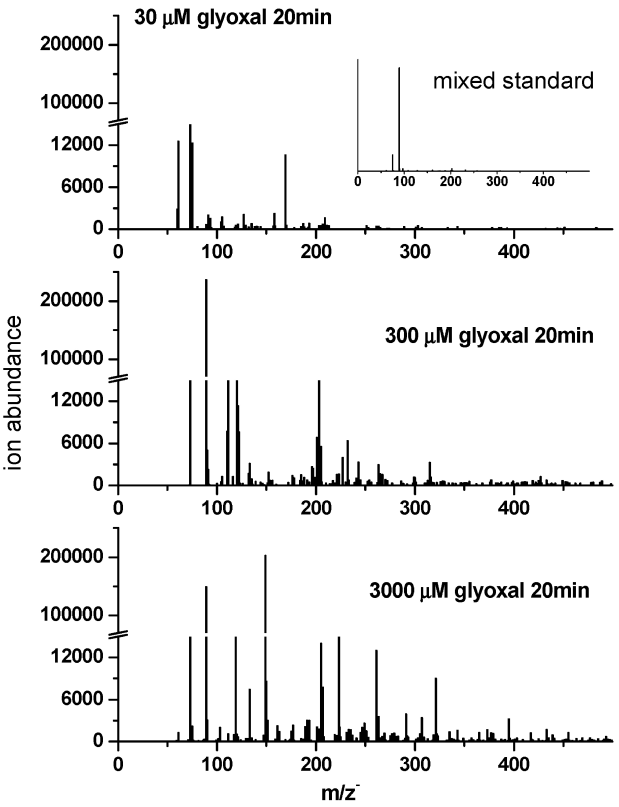

Fig. 11. ESI-MS negative ionization spectra from glyoxal + OH batch reactions. From the top to bottom: 30, 300, and 3000 μM glyoxal. (Reprinted with permission from Tan, Y., M. J. Perri, S. P. Seitzinger, and B. J. Turpin (2009), Effects of precursor concentration and acidic sulfate in aqueous glyoxal-OH radical oxidation and implications for secondary organic aerosol, *Environ. Sci. Technol.*, *43*, 8105–8112. Copyright 2009 American Chemical Society.)

"oligomers" (a molecular complex that consists of a few to several tens of monomer units) are known to form under such conditions (Hastings *et al.*, 2005; Loeffler *et al.*, 2006; Carlton *et al.*, 2007; Altieri *et al.*, 2008; Tan *et al.*, 2009; Lim *et al.*, 2010). Reaction mechanisms to form these higher carbon number dicarboxylic acids and other multifunctional carbonyl compounds are discussed in this section, and the formation of oligomers are described in the next section.

For example, according to a batch experiment by Tan *et al.* (2009), a non-linear decrease of the yield of oxalic acid was observed with an increase of the initial concentration of glyoxal, and the maximum mass yield of oxalic acid per mass of glyoxal reacted decreased from 136% in a 30-μM experiment to 94% and 38% in 300-μM and 3000-μM experiments, respectively. At a higher concentration of glyoxal (>1000 μM), the formation of tartaric acid (TTRD, HOOCCH(OH)CH(OH)COOH, molecular weight 150) was confirmed as the major first-generation product, and even higher molecular weight compounds with m/z = 200–500 also increases as major products as shown in Fig. 11 (Tan *et al.*, 2009). Acidity and the presence of ammonium, nitrate and sulfate ions have little effect on the formation of these products, which implies the pathways are dominated by radical-radical reactions (Tan *et al.*, 2010; Kirkland *et al.*, 2013). Thus, TTRD can be formed by the recombination reaction of hydrated glyoxal radicals after H-abstraction from glyoxal dihydrated gem-diol as proposed by Lim *et al.* (2010):

$$(HO)_2CHCH(OH)_2 + OH \rightarrow (HO)_2\dot{C}CH(OH)_2 + H_2O \quad (72)$$

$$(HO)_2\dot{C}CH(OH)_2 \rightarrow HOOC\dot{C}H(OH) + H_2O \quad (73)$$

$$2HOOC\dot{C}H(OH) \rightarrow HOOCCH(OH)\text{-}CH(OH)COOH. \quad (74)$$

In the case of methylglyoxal in 3000-μM experiments, oxalic acid production becomes much slower than in 30- and 300-μM experiments, and Tan *et al.* (2012) identified the compounds with a negative ion mass number, $m/z^- = 177$ by ESI-MS analysis as $C_6H_9O_6^-$, which will be discussed later in Subsection 3.2.

As for larger carbon number diacids, the formation of tartaric acid (C_4) has been explained by the radical-radical reactions in the OH-initiated aqueous phase oxidation of glyoxal. As well as the compounds, the formation of succinic acid and malonic acid (C_4 and C_3 dicarboxylic acids shown in Fig. 1, respectively) have been reported (Altieri *et al.*, 2008; Tan *et al.*, 2010). The experiments by Tan *et al.* (2010) clearly showed the formation of succinic acid to be the first-generation and malonic acid as second-generation products. While it is interesting to note that these C_3 and C_4 dicarboxylic acids are abundant in the atmospheric SOA next to oxalic acid, as seen in Fig. 2, the formation pathways for these diacids have not been well established yet. In order to explain the production of succinic and malonic acids that contain -CH_2COOH moiety in a molecule, the reaction of the CH_2COOH radical formed from the OH reaction of acetic acid may possibly be conceived as:

$$CH_3COOH + OH \rightarrow \dot{C}H_2COOH + H_2O \quad (75)$$

$$2\dot{C}H_2COOH \rightarrow HOOCCH_2CH_2COOH. \quad (76)$$

However, Tan *et al.* (2012) reported that succinic acid was not detected in the OH-initiated aqueous-phase oxidation of acetic acid, and glyoxylic and oxalic acid was formed. Instead, the formation of succinic acid has been reported in the OH-initiated oxidation of a cloud-level concentration of MGLY in the aqueous phase, although a reaction mechanism has not been proposed (Tan *et al.*, 2010).

The radical-radical reactions mentioned above have to compete with an O_2 reaction in the aqueous phase. For example, the formation of a C_4 dimer from C_2 radicals derived from glyoxal (Reaction (74)) should compete with the reaction with O_2 to form peroxy radicals. A favorable condition for the radical-radical reactions can be achieved first if the radical-radical reaction rate constants are large enough compared with the large reaction rate constant with O_2, $\sim 10^9$ M^{-1} s^{-1} (Buxton *et al.*, 1997). The rate constants of radical-radical reactions in the aqueous phase are, in general, as large as these which are diffusion controlled with suggested values of $\sim 10^9$ M^{-1} s^{-1} (Burchill and Perron, 1971; Guzmán *et*

doi:10.5047/meep.2016.00401.0001

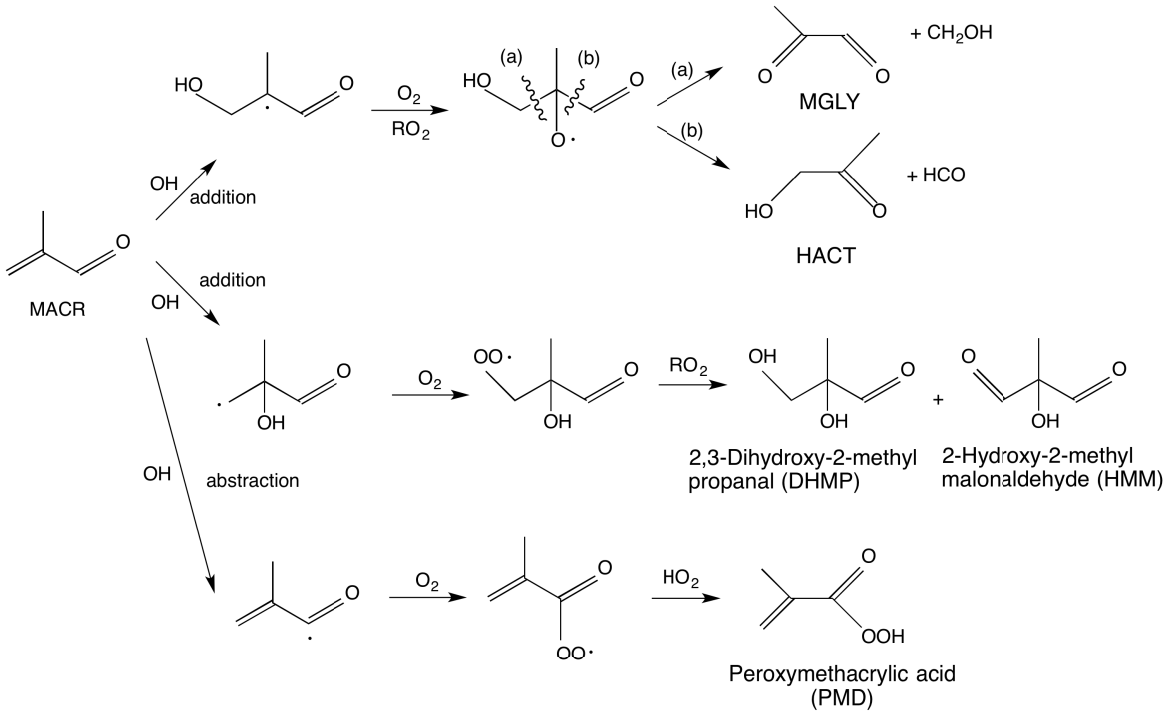

Fig. 12. Proposed mechanism of aqueous phase OH-initiated oxidation of methacrolein (MACR).

al., 2006). Second, since the concentration of the dissolved O_2 in cloud water is ∼0.3 mM (Lim *et al*., 2010), the concentration of the precursor, glyoxal or methylglyoxal should be high enough to provide a high concentration of radicals. The experimental results of Tan *et al*. (2009) that larger carboxylic compounds expected from the radical-radical reactions are significant at higher precursor concentrations of >1 mM (1000 μM), is in agreement with the above conditions with reference to the rate constants and concentrations in the aqueous phase.

Thus, relatively small carbon number diacids ubiquitously found in field aerosols as seen in Figs. 1 and 2 can partly be explained by aqueous phase radical-radical reactions in a cloud-relevant concentration of glyoxal and methylglyoxal, but this is not fully understood yet.

2.6 OH-initiated radical reactions of methylvinyl ketone and methacrolein to form multifunctional compounds

Other than glyoxal and methylglyoxal, the aqueous phase OH-initiated oxidation of MVK and MACR, the major gas phase oxidation products of isoprene, has been studied to give oxalic acid and other small acids (Liu *et al*., 2009; Zhang *et al*., 2010). Here, the discussion will be mainly considering MACR as an example, although some attention will be given in Subsection 3.2 to MVK with regard to oligomer formation in Subsection 3.2. Although MACR is expected to enter the aqueous phase in only a limited amount due to the small Henry's law constant (6.5 M atm^{-1} at 298 K) (Iraci *et al*., 1999), field observations of the characterization of organic compounds in a cloud revealed that the concentration of MACR in water exceeds its Henry's law predicted concentration by two orders of magnitude (van Pinxteren *et al*., 2005). Thus, an aqueous phase reaction of MACR could be an important source of SOA.

The OH-initiated oxidation of MACR is thought to proceed via three pathways: i) an addition on the terminal carbon of the C=C bond to form a tertiary radical; ii) an addition to the internal carbon of the C=C bond to form a primary radical; and iii) an abstraction of an aldehydic H-atom (Liu *et al*., 2009). Among the addition pathways, an addition on the terminal carbon is thought to be the most favorable, as in the case of the gas phase reactions of OH with MACR (Calvert *et al*., 2011). In either of the pathways, the formed OH-added radicals rapidly add to dissolved O_2 to form peroxy radicals. The reaction products identified with the ESI-MS/MS by Liu *et al*. (2009) include 2-hydroxy-2-methylmalonaldehyde (HMM), 2,3-dihydroxy-2-methylpropanal (DHMP), and peroxymethacrolic acid (PMD) among other C_4 compounds, in addition to more common smaller molecules such as MGLY, HACT, HCHO, etc. Zhang *et al*. (2010) also studied the aqueous phase OH-initiated oxidation of MACR, and reported the formation of high-molecular-weight compounds (HMWs) which are thought to be formed by the radical-radical reactions similar to those discussed in Subsection 2.5. The fundamental formation mechanism of the first generation products is depicted in Fig. 12 after Liu *et al*. (2009).

The major pathway of the terminal addition of OH is expected to give methylglyoxal (MGLY) and hydroxyacetone (HACT) and formaldehyde via a CH_2OH radical through C-C bond rupture in oxy radicals, which are formed by a mutual reaction between peroxy radicals. The addition of OH to the methyl-substituted internal carbon is proposed to give DHMP and HMM by the self-reaction of peroxy radicals via

doi:10.5047/meep.2016.00401.0001

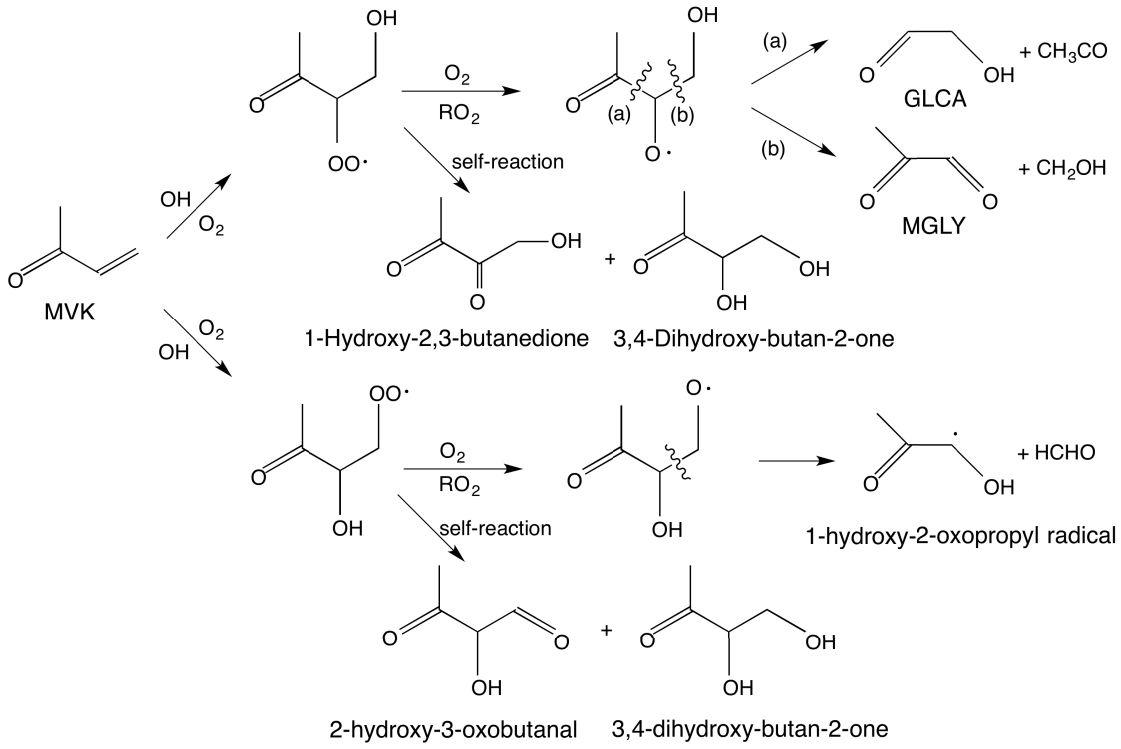

Fig. 13. Proposed mechanism of aqueous phase OH-initiated oxidation of methyl vinyl ketone (MVK).

a tetroxide structure (RCOOOOR) (Liu *et al*., 2009; Zhang *et al*., 2010). Here it has been assumed that the reaction pathways of the self-reaction of peroxide radicals in a water cage is similar to those in the gas phase:

$$2R_1R_2CHOO \rightarrow R_1R_2CHOO\text{-}OHR_1R_2$$
$$\rightarrow R_1R_2C{=}O + R_1R_2CHOH \quad (77)$$
$$\rightarrow 2R_1R_2CHO\cdot\ . \quad (78)$$

The third pathway of aldehydic H-atom abstraction would give PMD via a reaction of a MACR-peroxy radical with HO_2.

Analogous to MACR, the OH-initiated reaction of MVK proceeds through the addition to the terminal and internal carbon atoms of the double bond to form hydroxyl radicals, which are then form peroxy radicals by the addition of O_2. The self-reaction of RO_2 radicals occurs as in the case of MACR giving a tetroxide intermediate, which decomposes to give RO radicals. The proposed mechanism of aqueous phase OH-initiated oxidation of MVK is depicted in Fig. 13 after the mechanism for MACR shown in Fig. 12.

Reported products in the OH-initiated oxidation of MVK are MGLY, GLCA, formaldehyde, acetic acid, formic acid, pyruvic acid ($CH_3COCOOH$) and malonic acid ($HOOCCH_2COOH$) (Zhang *et al*., 2010). Acetic acid and pyruvic acid may be derived from the acetyl radical (CH_3CO) and the 1-hydroxy-2-oxopropyl radical ($CH_3C(O)CHOH$) shown in Fig. 13, as suggested by Zhang *et al*. (2010).

3. Formation of Oligomers in SOA

3.1 Field observation of oligomers and high molecular weight compounds

In addition to dicarboxylic acids and related species, "high molecular weight compounds" (HMWC) (MW = 200–1000) have been widely observed in ambient aerosols (Mukai and Ambe, 1986; Kalberer *et al*., 2004, 2006; Denkenberger *et al*., 2007; Krivácsy *et al*., 2008; Stone *et al*., 2009) and rainwater (Altieri *et al*., 2009a). Chemical species of HMWC include "oligomers", which means a molecular complex that consists of a few monomer units, in contrast to polymers where the number of monomer units is not limited. Among them, compounds with an MW < 300 are often assigned to dimers and trimers of carbonyl compounds (e.g. tartaric acid and 2,3-dimethyltartaric acid, as discussed in Subsection 2.5), while those with MW > 300 contain higher oligomers (Reinhardt *et al*., 2007). It should be noted that HMWC also include organic sulfur and organic nitrogen compounds that contain CHOS, CHON, and CHNOS compositions, which will be discussed in Chapter 4. Although these HMWC are also termed humic-like substances (HULIS) (Havers *et al*., 1998), their composition is, in general, different from terrestrial and marine humic acids (Graber and Rudich, 2006; Krivácsy *et al*., 2008; Altieri *et al*., 2009a).

HMWC are also measured in fog and cloud water (Herckes *et al*., 2002; Feng and Moller, 2004; Mazzoleni *et al*., 2010) suggesting that they are most probably formed in aqueous phase reactions in atmospheric particles. Figure 14 shows an example of a mass spectrum of an HMWC fraction of aerosol sampled at Budapest and Mace Head,

doi:10.5047/meep.2016.00401.0001

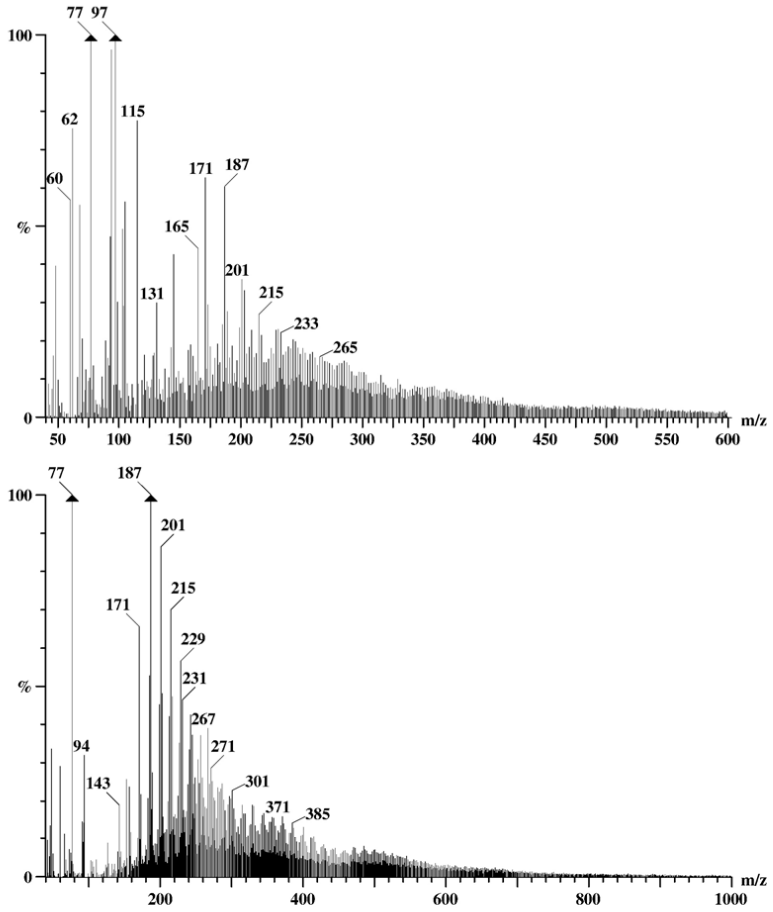

Fig. 14. Mass spectra of an HMWC fraction of (upper) Budapest and (lower) Mace Head, aerosols. (Reprinted from *Atmos. Res.*, *87*, Krivácsy, Z., G. Kiss, D. Ceburnis, G. Jennings, W. Maenhaut, I. Salma, and D. Shooter, Study of water-soluble atmospheric humic matter in urban and marine environments, 1–12, Copyright 2008, with permission from Elsevier.)

and analyzed by an electrospray ionization mass spectrometer (ESI-MS) (Krivácsy *et al*., 2008). In Fig. 14, several hundreds of compounds in a mass range of m/z 50–800 were identified. Analysis of field samples using ultrahigh-resolution Fourier Transform Ion Cyclotron Resonance Mass Spectrometry with electrospray ionization (ESI-FTICR MS) detected more than 1000 compounds in a similar mass range (Reemtsma *et al*., 2006; Wozniak *et al*., 2008; Altieri *et al*., 2009a; Mazzoleni *et al*., 2010).

Based on the chemical formula assignments, compound families of CHO, CHON, CHOS, and CHNOS were identified (Reemtsma *et al*., 2006; Mazzoleni *et al*., 2010). A major part of the compounds has been assigned to an elemental composition containing only C, H, and O (Altieri *et al*., 2009a; Mazzoleni *et al*., 2010).

Such oligomers, and organic sulfur and nitrogen compounds, may constitute a substantial fraction of unidentified constituents of organic aerosols collected in fieldwork depending on the conditions. HMWC effluent in a later stage of GC analysis might account for a substantial part of the underestimate of SOA prediction by atmospheric models compared with observations (Heald *et al*., 2005; Volkamer *et al*., 2006b). For example, the ratio of HMWC was 10–22% of the total carbon sampled at Mace Head, Ireland and Auckland and Christchurch, New Zealand (Krivácsy *et al*., 2008), and oligomer-containing particles represents 30–40% of the total detected particles sampled in Riverside, California (Denkenberger *et al*., 2007). Hallquist *et al*. (2009) and Lin *et al*. (2012) have estimated that oligomers typically contribute ca. 10%, and organosulfates may contribute an additional 10%, of the total organic aerosol mass.

3.2 Aqueous-phase radical reactions of carbonyl compounds to form oligomers

Although oxalic acid is the main product of the OH-initiated aqueous phase oxidation of glyoxal and methylglyoxal in the cloud-representative concentration range of 10–100 μM, the formation of oligomers has been found at a concentration of greater than $\sim$1 mM as mentioned in Subsection 2.4. Yields of oligomers increase with the increase of concentration of these precursors in the aqueous phase, and oligomers become major products at a high concentration range of 0.1–10 M, which is representative of an aerosol-level concentration. Figure 15 depicts model-predicted maximum mass-based yields of oxalic acid and oligomers (dimers of C_3+C_4 compounds) given by Lim *et al*. (2010) for atmospheric conditions of $[OH]_{aq}$. Thus, model

doi:10.5047/meep.2016.00401.0001

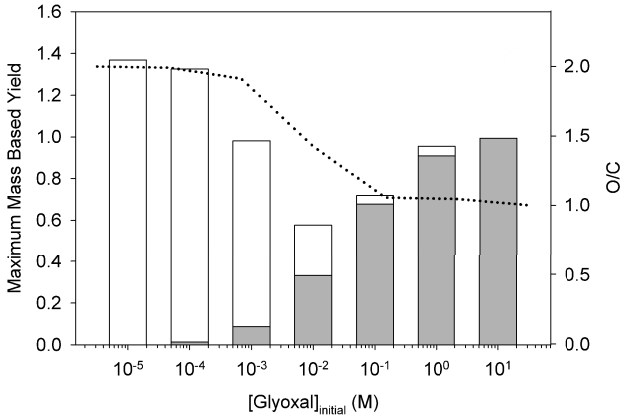

Fig. 15. Model-predicted maximum mass-based yields of oxalic acid and oligomers ($C_3 + C_4$ dimers) as a function of initial concentrations of glyoxal for an aqueous phase reaction with OH radicals (adapted from Lim *et al.*, 2010). White bar indicates oxalic acid and the grey bar oligomers, and the dotted line indicates the O/C ratio.

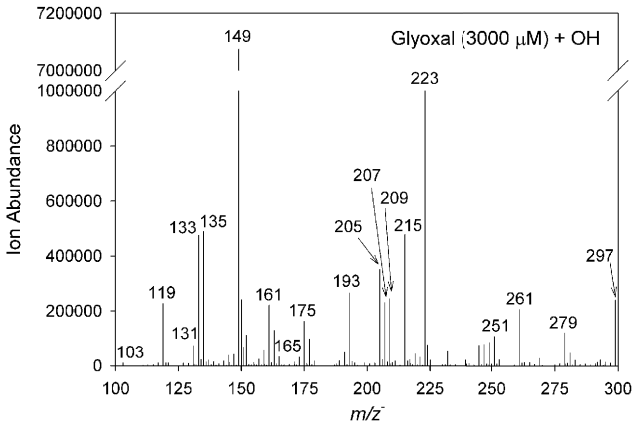

Fig. 16. FTICR-mass spectrum of the products from the reaction of glyoxal (3 mM) with OH radicals in the aqueous phase (Lim *et al.*, 2010).

predictions suggest that SOA formed in in-cloud water with 10–1000 μM of glyoxal is predominantly oxalic acid, while SOA formed in aerosol phase aqueous reactions with glyoxal over 0.1 M is predominantly oligomeric. The turnover occurs at ∼10 mM of initial glyoxal concentration (Lim *et al.*, 2010).

The chemical compositions of glyoxal oligomers have been detected in chamber experiments by using a high-resolution time-of-flight aerosol mass spectrometer (HR-ToF-AMS) or a quadrupole aerosol mass spectrometer (Q-AMS) (Kroll *et al.*, 2005; Liggio *et al.*, 2005b). Lim *et al.* (2010) reported experiments by using ESI-MS, FTICR-MS, and liquid chromatograph mass spectrometry (LC-MS). Figure 16 shows an example of FTICR mass spectrum of products formed from a 30-min reaction of glyoxal (3 mM) with OH radicals, detected in a negative ionization mode (Lim *et al.*, 2010). In general, mass peaks between 200–500 are seen in the oxidation of glyoxal. The prominent peak in Fig. 16 is $m/z^- = 149$ (MW-1), which has been assigned to tartaric acid (MW = 150). They made the important observation that the mass spectra contains a series of peaks with m/z^- difference of 74.000036 (ultra high resolution FTICR-MS provides an accurate mass number with 4–6 decimal places in general), which corresponds to the successive addition of an HOOC-CH(OH) radical ($C_2H_3O_3$, MW = 75) to the species with H-abstracted by OH. Based on this evidence, Lim *et al.* (2010) proposed that oligomerization starts, for example, from tartaric acid produced by the recombination of two ketyl radicals which are formed by H-atom abstraction followed by dehydration as shown in Reaction (73) in the previous section. The dimer then reacts with an OH radical again to form a trimer (MW = 225), tetramer (MW = 300) and so on. Another series seen in Fig. 16 starts with m/z^- 133 (possibly malic acid) to m/z^- 207 and 281 with the increases of 74.

In the case of methylglyoxal, oxidation by OH in the aqueous phase has been known to form oligomers (Altieri *et al.*, 2008). Tan *et al.* (2012) studied the products in 1 mM methylglyoxal by an analysis is using an ultra high resolution Fourier transform ion cyclotron resonance electrospray ionization mass spectrometry (ESI FT-ICR MS) in negative ion modes. They assigned parent compounds at $m/z^- = 177$ to $C_6H_9O_6^-$ and $m/z^- = 249$ to $C_9H_{13}O_8^-$, and proposed the following radical-radical reaction mechanism to explain these dimeric and trimeric compounds. Figure 17 depicts the reaction scheme given in their proposal.

The ketyl radical ($CH_3C(OH)COOH$) is assumed to be an intermediate radical to propagate the oligomerization as proposed by Guzmán *et al.* (2006). The ketyl radical is assumed to be formed by an H-atom abstraction by OH from either the monohydrated or dihydrated MGLY as shown in Fig. 17. Under the condition of relatively high concentration of MGLY, the ketyl radical reacts with monohydrated MGLY to form a $C_6H_9O_5$ radical (A) (MW = 161) as a chain propagating reaction. Further, a radical-radical reaction of the ketyl radical either by itself, or with a $C_6H_9O_5$ radical (A), forms $C_6H_{10}O_6$ (MW = 178) or $C_9H_{14}O_8$ (MW = 250), respectively, according to the scheme shown in the figure.

As well as glyoxal and methylglyoxal, MVK and MACR are known to lead to the formation of a series of oligomers (El Haddad *et al.*, 2009; Zhang *et al.*, 2010; Liu *et al.*, 2012; Renard *et al.*, 2013, 2014). Here, discussion will be presented only for MVK as a typical example. Renard *et al.* (2013) identified oligomer systems with a very regular spacing of 70.0419 Da, which corresponds to the exact mass of the precursor, MVK as shown in Fig. 18. They found that these systems extend up to 1800 Da containing 25 monomers for an initial MVK concentration of 20 mM. As in the case for OH-glyoxal reactions shown in Fig. 11, the chain length of oligomers increased with an initial MVK concentration in the range of 0.2–20 mM.

Based on observations, they proposed a chemical mechanism of OH-radical-initiated oligomerization of MVK in the aqueous phase as shown in Fig. 19. This figure shows

doi:10.5047/meep.2016.00401.0001

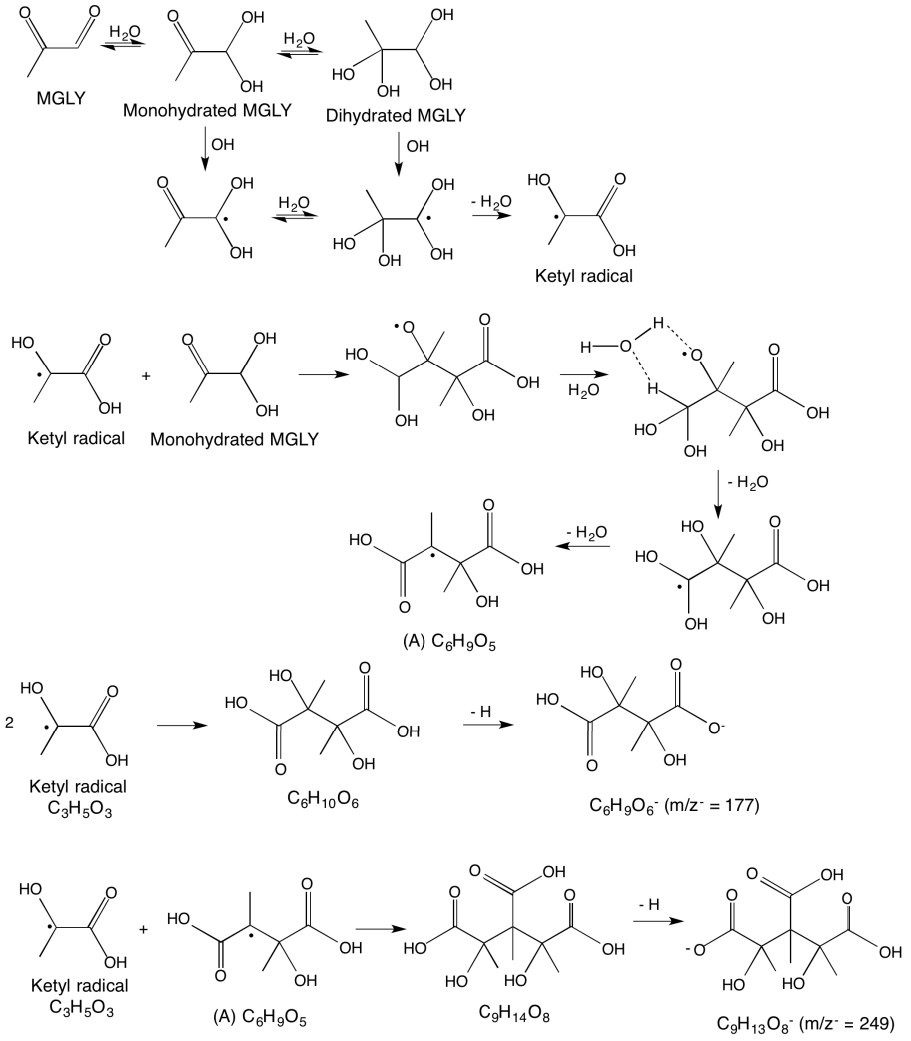

Fig. 17. Mechanism of the radical-radical reactions in the OH-initiated aqueous-phase oxidation of methylglyoxal forming oligomers (based on Tan *et al*., 2012).

that the reaction is initiated by an OH addition to the vinyl double bond of MVK to form initiator radicals HO-MVK·. Each HO-MVK· radicals adds to another MVK molecule by opening its vinyl double bond leading to another radical, HO-MVK-MVK·, which can then add to another MVK molecule in the same way. The propagation keeps on increasing the chain length leading to the formation of HO-MVK-$(MVK)_n$-MVK·. Termination occurs by a bimolecular reaction between two radicals by coupling or disproportionation. Although both α- and β-additions to a vinyl double bond are possible in each step, β-additions (addition to a terminal carbon of CH_2 moiety) are more likely since resonance with the carbonyl group gives an energetically favored pathway. Thus, the scheme of the proposed mechanism in Fig. 19 shows only radical additions on the β-carbon of MVK. Inhibition of photo-oligomerization by an increase of dissolved O_2 is in agreement with the radical chain mechanism of oligomer formation observed for the OH-initiated oligomerization of GLY and MGLY discussed before.

Oligomer formation has widely been reported in the OH or O_3 oxidation reactions of C_2H_2 (Volkamer *et al*., 2009), C_2H_4 (Sakamoto *et al*., 2013), aromatic compounds (Kalberer *et al*., 2004; Sato *et al*., 2007), isoprene (Altieri *et al*., 2006), α-pinene (Gao *et al*., 2004; Tolocka *et al*., 2004), and cycloalkenes (Gao *et al*., 2004). In addition to the OH-initiated aqueous phase radical-radical reactions discussed above, O_3-initiated gas-phase reactions and non-radical reactions in the aqueous phase are also proposed for oligomer formation in these various studies. Of these, aqueous phase non-radical reactions are mentioned below.

3.3 Aqueous-phase non-radical reactions to form oligomers

HMWC are also known to form from aldehydes and dialdehydes in the dark in the presence of seeded acid particles. Jang and Kamens (2001) observed hemiacetal/acetal formation by the use of a Fourier transform infrared (FTIR) spectrometer from glyoxal and mono-aldehydes with seeded aerosols composed of $(NH_4)_2SO_4$ acidified with H_2SO_4. These reactions were found to accelerate in the presence of an acid catalyst, and resulted in higher aerosol yields than when H_2SO_4 was not present. While the formation of dicarboxylic acids and oligomers via the OH-initiated radical-

doi:10.5047/meep.2016.00401.0001

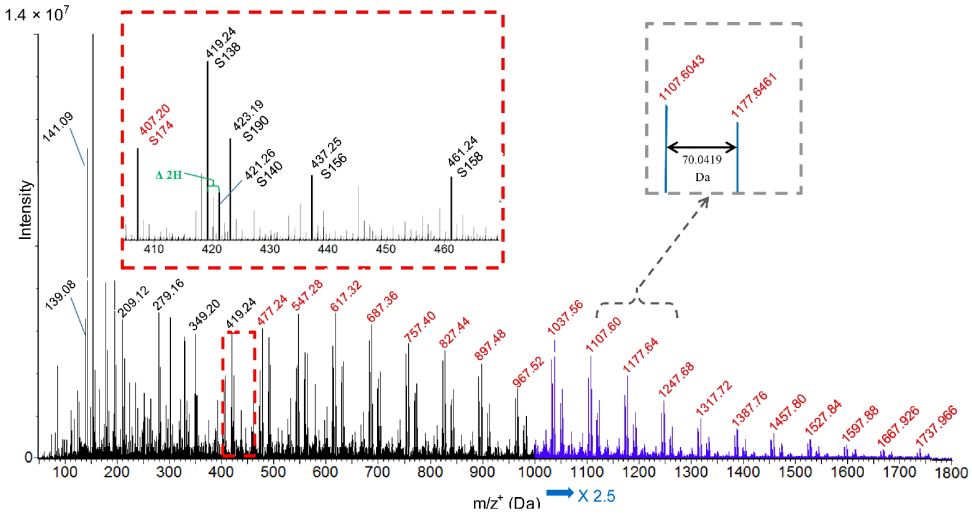

Fig. 18. Mass spectrum in the positive ion mode in the OH-initiated aqueous-phase oxidation of MVK showing a regular pattern of a mass difference of 70.0419 Da. (Renard *et al.*, 2013).

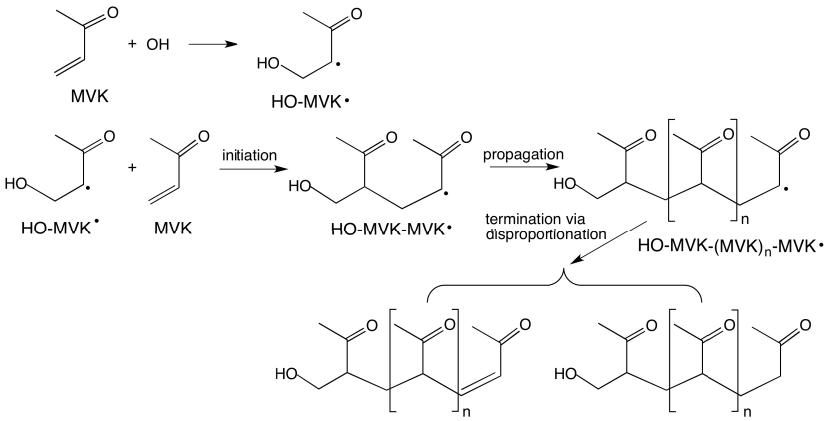

Fig. 19. Proposed reaction scheme of radical oligomerization of MVK in the aqueous phase (based on Renard *et al.*, 2013).

radical reaction in cloud-relevant concentrations are not affected much by acidity and co-existing ions (Tan *et al.*, 2009), the non-radical formation of HMWC is known to occur in acidic sulfate particles with an aerosol-relevant concentration of glyoxal (1–10 M) (Liggio *et al.*, 2005a).

A hemiacetal/acetal formation reaction is one of the well-known acid-catalyzed reactions between aldehyde/ketone with alcohol in organic chemistry. An acetal is a compound with an ether structure, R_1R_2-C(OR_3)(OR_4), and has a tetrahedral geometry. The Greek word "hemi" means half, and a hemiacetal is a compound in which one of the OR of acetal is substituted by OH. The formation of hemiacetal from aldehyde/ketone (RR′CO) with alcohol (ROH) is formally the same as the hydration of aldehyde discussed in Subsection 2.3.

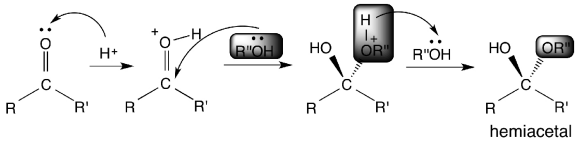

(79)

The OH group of hemiacetal is then protonated followed by dehydration to form an alkylated carbonyl compound as an intermediate. Another alcohol molecule makes a nucleophilic attack on an electron deficient carbon atom followed by deprotonation to give acetal:

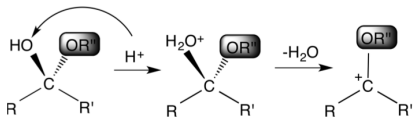

(80)

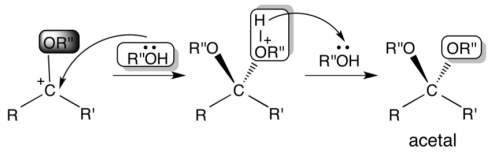

(81)

As a typical example of hemiacetal/acetal formation, the reaction mechanism is shown here for the reaction of glyoxal. When it is applied to glyoxal gem-diol, the following hemiacetal is proposed to form (Liggio *et al.*, 2005a; Loeffler *et*

doi:10.5047/meep.2016.00401.0001

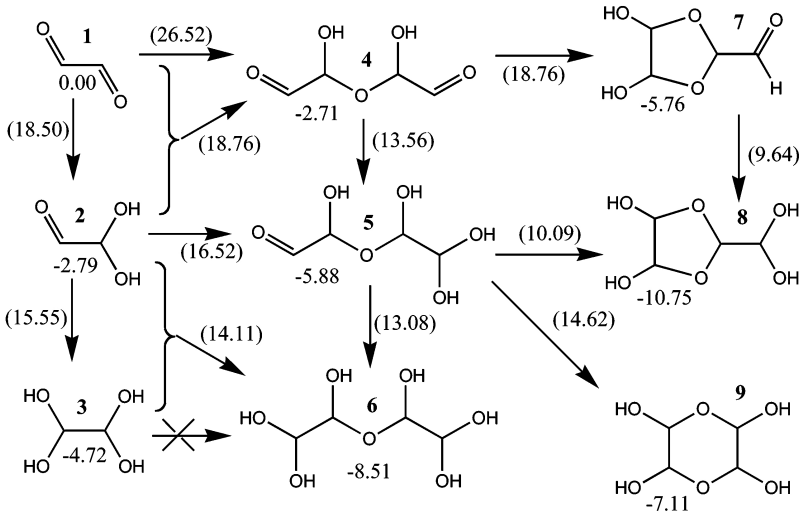

Fig. 20. Reaction pathways for monomers and dimers of glyoxal considered in the ab initio calculation. Relative Gibbs free energies and activation energies (in parentheses) are given in kcal mol^{-1} (Kua *et al*., 2008).

al., 2006):

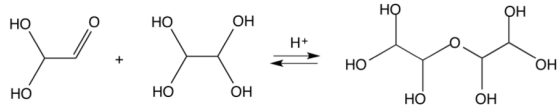

(82)

where the monohydrated and dihydrated gem-diol have been discussed in Subsection 2.3. It has been proposed that the hemiacetal formed is likely to undergo further dehydration forming a more stable five-membered ring structure, and additional dehydration can also occur resulting in the compound containing three hydrated glyoxal units:

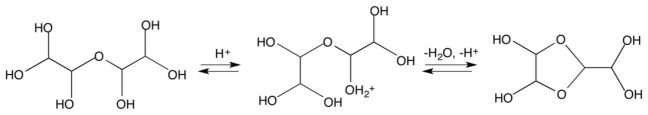

(83)

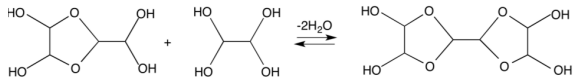

(84)

These products and the corresponding species with methyl groups are identified by the ESI mass spectrum of oligomers from glyoxal and methylglyoxal under acidic conditions of for example, pH < 3.5 (Loeffler *et al*., 2006; De Haan *et al*., 2009b; Yasmeen *et al*., 2010).

Hydration of glyoxal and the subsequent formation of a dimeric species in an aqueous solution has been studied by Kua *et al*. (2008) using ab initio quantum chemical calculations. Figure 20 shows the reaction pathways including the relative Gibbs free energies for each species (ΔG) and transition states ($\Delta^{\ddagger}G$) (in kcal mol^{-1}), referenced to glyoxal and water for monomers and dimers considered in the transformation of glyoxal in an aqueous solution.

The formation of mono- and dihydrates are thermodynamically more favorable with negative relative free energies as discussed in Subsection 2.3. According to the calculations, the dimerization of **1** to **4**, **2** to **5**, and **3** to **6** are all thermodynamically more favorable with a negative ΔG, and further ring closure is energetically favored giving dioxolane ring dimer **8** as the thermodynamic sink. The reaction pathway to form hemiacetal **6** is also energetically favored agreeing with the experimental results. Similarly, the thermodynamics and kinetics of methylglyoxal dimer formation has been calculated (Krizner *et al*., 2009). Dimer formation from methylglyoxal has also been observed experimentally (Yasmeen *et al*., 2010).

Another type of acid-catalyzed organic reaction, the aldol reaction, is also proposed to occur in the cloud and aerosol droplets (Nozière and Riemer, 2003; Zhao *et al*., 2005; Garland *et al*., 2006; Casale *et al*., 2007). The aldol reaction is a well-known reaction in organic chemistry in which a carbonyl compound with an α-hydrogen (an H atom attached to an α-carbon atom adjacent to a carbonyl carbon atom) reacts with an aldehyde or a ketone under either acidic or basic conditions to form a new C-C bond producing a β-hydroxycarbonyl compound. The acid- and base-catalyzed aldol reaction can be formulated formally as shown in Fig. 21.

Under the acid-catalytic condition, a hydrogen ion attaches to an oxygen atom of a carbonyl group to form a cation intermediate, from which a hydrogen atom of α-carbon is abstracted by an acid anion to form enol. The process is reversible and is called keto-enol tautomerism. The α-carbon of enol reacts with a protonated carbonyl carbon of another aldehyde or ketone (R′CHO in Fig. 21) by nucleophilic addition followed by the elimination of a proton of the enol to form a β-hydroxycarbonyl compound, i.e. aldol (**ald**ehyde+alcoh**ol**) adduct. Under the base-catalytic condition, an enolate ion reacts with a carbonyl carbon of another aldehyde or ketones (R′CHO) to form an enolate of aldol, from which β-hydroxycarbonyl compounds are formed, as shown in the above scheme. Here, "Base-" stands for a base

doi:10.5047/meep.2016.00401.0001

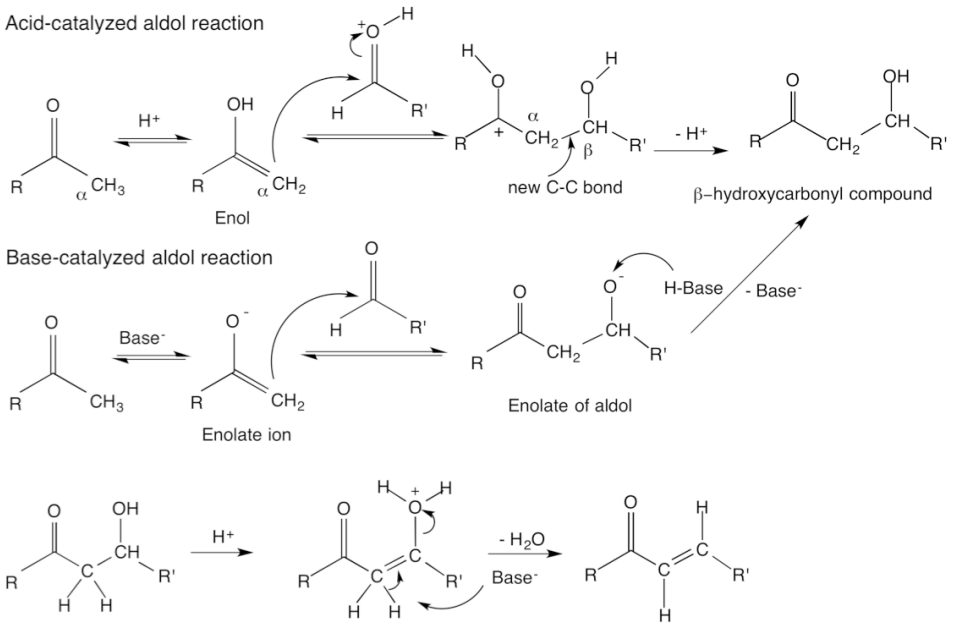

Fig. 21. Scheme of the aldol reaction via an acid- and base-catalyzed mechanism.

anion and H-Base is a species which can provide H^+ to the enolate of aldol as shown in Fig. 21.

The β-hydroxycarbonyl compounds thus formed are, in general, unstable and yield a conjugate enone, i.e. an α, β-unsaturated carbonyl compound by dehydration, as follows. This process is called aldol condensation.

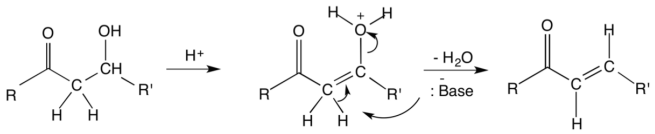

(85)

As for glyoxal and methylglyoxal, oligomers in the dark have been studied by the mass spectral identification of products. It has been reported that glyoxal predominantly forms acetal oligomers as described before, while methylglyoxal oligomers are formed by both acetal reaction and aldol condensation depending on the experimental conditions (Zhao *et al*., 2006; De Haan *et al*., 2009b; Sareen *et al*., 2010; Yasmeen *et al*., 2010).

As a typical example of aldol condensation relevant to SOA, a proposed reaction mechanism is shown here for the reaction of methylglyoxal (Yasmeen *et al*., 2010). The methyl ketone structure of methylglyoxal exists in equilibrium with the enol form in an acidic aqueous media by tautomerization:

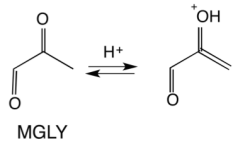

(86)

The enol form reacts with gem-hydrated methylglyoxal to form a β-hydroxy ketone, an aldol dimer of methylglyoxal according to the formulation shown in Fig. 21.

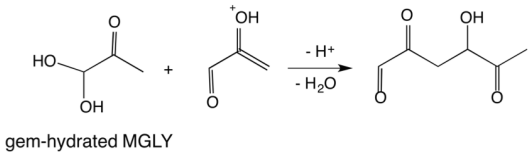

(87)

Oligomerization proceeds by the successive addition of a β-hydroxy ketone unit:

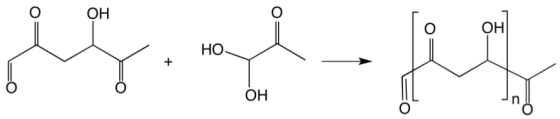

(88)

Yasmeen *et al*. (2010) reported that an aldol condensation type reaction occurs at a higher pH value than acetal formation. Such an aldol condensation reaction has also been found for methyl vinyl ketone (Nozière *et al*., 2006; Chan *et al*., 2013).

Quantum chemical calculations have given the thermochemical parameters of equilibrium constants and acetal formation reactions, and have revealed that uptake reactions of glyoxal, methylglyoxal and other aldehydes are predicted to be thermodynamically favored supporting the observations of atmospheric particle-phase reactions (Barsanti and Pankow, 2005; Tong *et al*., 2006; Krizner *et al*., 2009).

Other than hemiacetal/acetal formation and the aldol reaction, anhydride formation (Gao *et al*., 2004), and esterification reactions (Gao *et al*., 2004; Altieri *et al*., 2008), as well as imine formation (De Haan *et al*., 2009a; Galloway *et al*., 2009), and organosulfate formation (Liggio *et al*., 2005b; Surratt *et al*., 2007, 2008) have been reported. The latter two processes are discussed in the following section.

doi:10.5047/meep.2016.00401.0001

These types of reactions are expected to occur in an aerosol droplet and also when a cloud droplet evaporates, if glyoxal and methylglyoxal are remaining. However, the detailed kinetics of a wide range of non-radical liquid phase reactions has not been established and further experimental and theoretical studies are necessary to understand their role in SOA formation.

The bulk phase reactions between ammonium sulfate and glyoxal (Nozière *et al*., 2009; Shapiro *et al*., 2009) and amino acids and glyoxal (De Haan *et al*., 2009a) have been reported to give light-absorbing higher molecular weight compounds.

4. Formation of Organosulfur and Organonitrogen Compounds in SOA

4.1 Field observation of organosulfur and organonitrogen compounds

Substantial evidence has been accumulated about organic sulfur compounds in ambient aerosols (e.g. Iinuma *et al*., 2007a; Surratt *et al*., 2007; Froyd *et al*., 2010; Hatch *et al*., 2011a, b; Olson *et al*., 2011; Zhang *et al*., 2012; Liao *et al*., 2015), cloud water (Pratt *et al*., 2013) and rainwater (Altieri *et al*., 2009a). Tolocka and Turpin (2012) estimated that they could comprise as much as 5–10% of the organic mass at various sites in the US.

As for the chemical identification of organosulfur compounds, glycolic acid sulfate (GAS, $HOC(O)CH_2OSO_3^-$, $C_2H_3SO_6^-$, m/z^- 155) has been identified in ambient aerosols (Olson *et al*., 2011; Surratt *et al*., 2008), and in SOA generated by isoprene oxidation in chamber studies (Surratt *et al*., 2008; Gómez-González *et al*., 2008; Galloway *et al*., 2009; Olson *et al*., 2011). A homologue with a methyl group, lactic acid sulfate (LAS, $C_3H_5SO_6^-$, m/z^- 169), has also been identified in an ambient aerosol sample (Olson *et al*., 2011; Hettiyadura *et al*., 2015). Molecular structures of glycolic acid and lactic acid sulfate are shown in Fig. 22(a) and (b).

Another better studied ambient organosulfate is IEPOX (e.g. 2-methyl-1,2-epoxy-3,4-butanediol)-derived sulfate ($C_5H_{11}SO_7^-$, m/z^- 215) (Fig. 22(c)). IEPOX sulfate was reported to be one of the most abundant individual organic molecules in aerosols in the Southern US (Chan *et al*., 2010; Lin *et al*., 2013). The vertical profile of IEPOX sulfates was measured in the free troposphere using particle analysis by laser mass spectrometry (PALMS) during airborne campaigns (Froyd *et al*., 2010). Temporal variation has been measured by aerosol time-of flight mass spectrometry (ATOFMS) in Atlanta (Hatch *et al*., 2011a, b). Liao *et al*. (2015) measured GAS and IEPOX sulfate by PALMS in the boundary layer and free troposphere over the continental US in an aircraft campaign. IEPOX sulfate was estimated to account for 1.4% of submicron aerosol mass (or 2.2% of OA mass) on average near the ground in southeast US with lower concentration in the western US (0.2–0.4%) and at higher altitudes (<0.2%). GAS was more uniformly distributed, accounting for about 0.5% aerosol mass on average, and suggested to be more abundant globally. They also detected a number of other organosulfates, but none of them were as abundant as these two compounds.

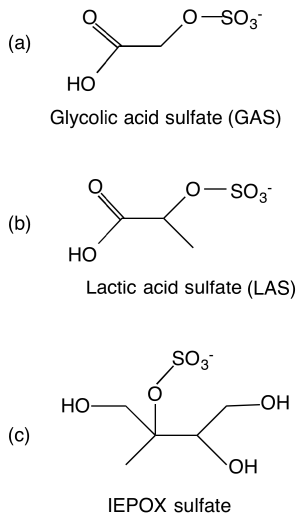

Fig. 22. Molecular structure of (a) glycolic acid sulfate (b) lactic acid sulfate, and (c) IEPOX sulfate.

Atmospheric measurements of the concentration and composition of organic nitrogen compounds are much less than those for sulfates. Zhang and Anastasio (2001) reported that fog water collected in Davis in California contained both free amino compounds (e.g. amino acids and alkyl amines) and combined amino nitrogen, the latter being more significant. Ion markers of oligomeric species, including amine and nitrates, have been reported in single-particle measurements of aged aerosol in Riverside (Denkenberger *et al*., 2007) and in fogwater in Fresno both in California (Herckes *et al*., 2007). The atomic composition of CHON and CHONS compounds in rainwater collected in New Jersey, US, were identified by ultra-high resolution electrospray ionization Fourier transform ion cyclotron resonance mass spectrometry (FT-ICR MS) by Altieri *et al*. (2009a, b). Wang *et al*. (2010) reported high molecular weight nitrogen-containing organic salts between amines and carbonyl compounds in Shanghai urban aerosols. They ascribed the no-oxygen species to amine salt (such as $R_1R_2NH\text{-}CH_2\text{-}\underset{|}{\overset{|}{C}}\text{-}C(R)=O$) formed from carboxylic compounds with amines or ammonia under acidic conditions. The compounds that contain both nitrogen and oxygen are suggested to be organonitrates such as $C_{13}H_{22}NO_3$ and $C_{12}H_{20}NO_3$. In water-soluble atmospheric organic matter in fog, molecular masses of organic nitrogen and organic nitrogen-sulfur compounds were identified by FT-ICR MS (Mazzoleni *et al*., 2010).

4.2 Aqueous-phase reactions forming organosulfates

The solubility of glyoxal in aerosol water is known to be enhanced by the presence of concentrated inorganic solutes. An effective Henry's law constant of glyoxal is dependent on the presence of specific ions and ionic strength. For example, the effective Henry's law constant, $K^*_{H,AS}$ for ammonium sulfate (AS, $(NH_4)_2SO_4$) solution is as high as 2.4×10^7 M atm^{-1} at 298 K, which is 50 times larger than for $K^*_{H,aq}$ (Ip *et al*., 2009) for pure water. Yu *et al*. (2011) found sulfate ions have a strong and specific interaction with glyoxal

doi:10.5047/meep.2016.00401.0001

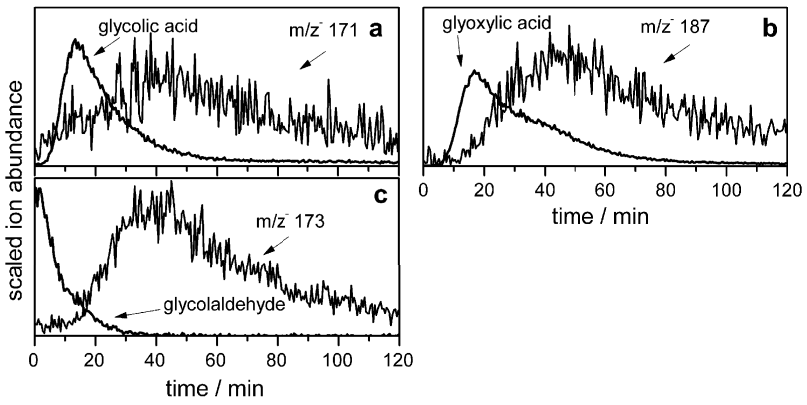

Fig. 23. Time profile of the ESI-MS data in the reaction of glycolaldehyde under irradiation in the presence of H_2SO_4. (Reprinted from *Atmos. Environ.*, *44*, Perri, M. J., Y. B. Lim, S. P. Seitzinger, and B. J. Turpin, Organosulfates from glycolaldehyde in aqueous aerosols and clouds: Laboratory studies, 2658–2664, Copyright 2010, with permission from Elsevier.)

in an aqueous solution, which shifts the hydration equilibria of glyoxal from the unhydrated carbonyl form to the hydrated form, which contributes to the observed ion-specific enhancement of the effective Henry's law constant for glyoxal in sulfur-containing solutions.

Perri *et al.* (2010) reported the identification of $HOOCCH(OH)OSO_3^-$ ($C_2H_3SO_7^-$, m/z^- 171), $HOOCC(OH)_2OSO_3^-$ ($C_2H_3SO_8^-$, m/z^- 187) and $(HO)_2CHCH(OH)OSO_3^-$ ($C_2H_5SO_7^-$, m/z^- 173) among other sulfur-containing products from the reaction of glycolaldehyde ($HOCH_2CHO$) with sulfuric acid. Those compounds have been found to form only under irradiated conditions and the time profiles of their formation are shown in Fig. 23.

From the experimental data, they concluded that the sulfates with $m/z^- = 173$, 171 and 187 are formed by reactions of H_2SO_4 with glycolaldehyde and its oxidation products, glycolic acid ($HOCH_2COOH$), and glyoxylic acid (CHOCOOH), respectively. Since they are formed only under irradiated conditions, they proposed the following radical-radical reaction for the formation of the sulfates. For example, sulfate from glycolic acid ($C_2H_3SO_7^-$, m/z^- 171) is proposed to form from a reaction between a sulfate radical and a glycolic acid radical.

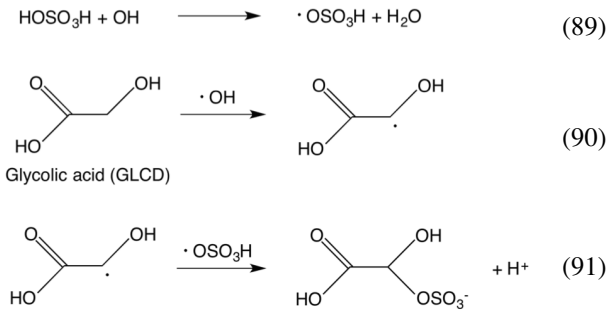

Similarly, sulfates from glyoxylic acid and glycolaldehyde can be formed from the following reactions after hydration of precursor molecules. For example, in the case of sulfate from glycolaldehyde ($C_2H_5SO_7^-$, m/z^- 173),

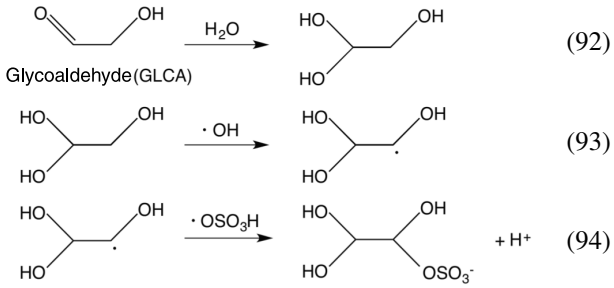

Galloway *et al.* (2009) identified glycolic acid sulfate ($HOC(O)CH_2OSO_3^-$, GAS) in the chamber studies of the glyoxal uptake into an ammonium sulfate aerosol. GAS has been observed in ambient aerosols (Surratt *et al.*, 2008; Olson *et al.*, 2011) as noted before. Although GAS may be formed from glycolic acid, glycolic acid formation from the aqueous phase reaction of glyoxal has not been reported. Meanwhile, glycolic acid is known to form from glycol aldehyde, acetic acid, and C_2H_4 as seen in Chapter 2, and glycol aldehyde is, in turn, one of the oxidation products of isoprene and MVK so that the formation of GAS is expected in the ambient aerosols. It is likely that organosulfate products exist as a neutral species ($ROSO_3H$) at a low pH, and as an ionized species ($ROSO_3^-$) at a high pH (Darer *et al.*, 2011).

An alternative formation mechanism of organosulfur compounds has been proposed. It is now established that the epoxides known to form in the oxidation of isoprene (Paulot *et al.*, 2009b) (see Subsection 2.2.3) and monoterpenes (Iinuma *et al.*, 2007a, b), react with sulfuric acid to form hydroxy sulfate esters by non-radical pathways. Epoxide ring opening and replacement by two hydroxy groups by acid-catalyzed hydrolysis is a well-known reaction (Whalen, 2005) as exemplified as follows:

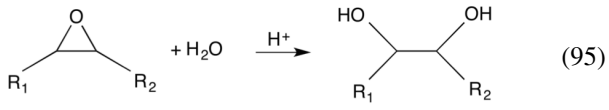

doi:10.5047/meep.2016.00401.0001

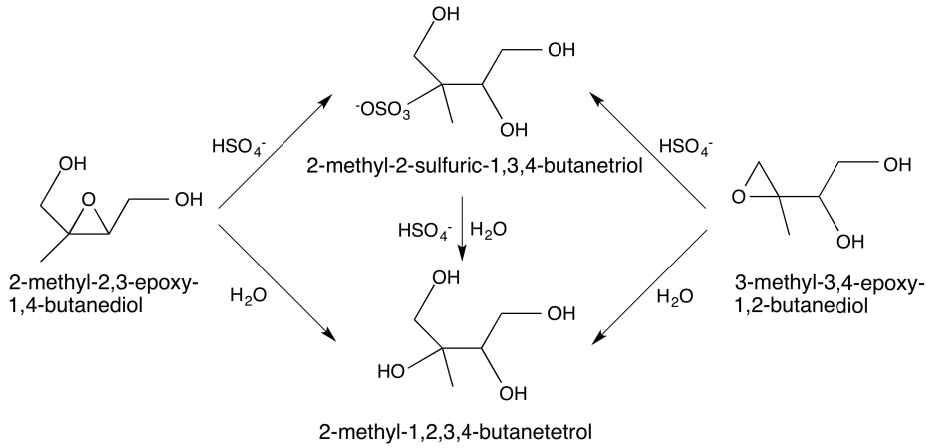

Fig. 24. Proposed reaction scheme to form organic sulfates from IEPOX (adapted from Darer *et al*., 2011).

Applying this pathway in their laboratory studies of the reaction of alcohols with sulfuric acid, Minerath and Elrod (2009) proposed an acid-catalyzed hydrolysis and hydroxy sulfate ester-forming mechanism in atmospheric aerosols:

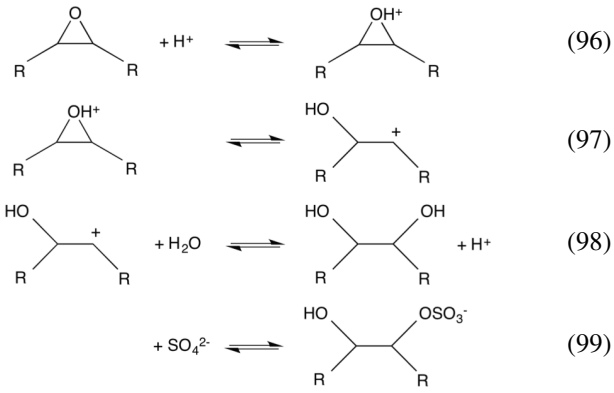

The kinetics and products of the acid-catalyzed hydrolytic ring-opening of atmospherically relevant hydroxy epoxides has been studied by Cole-Filipiak *et al*. (2010) and Eddingsaas *et al*. (2010). In the case of isoprene, the gas-phase formation of epoxides (IEPOX) has been fully characterized, as discussed in Subsection 2.2.3. The most typical IEPOX are 2-methyl-2,3-epoxy-1,4-butandiol (β-IEPOX) and 3-methyl-3,4-epoxy-1,2-butanediol (δ-IEPOX). From these epoxides the following sulfates, triol and tetrol have been found to form (Surratt *et al*., 2010; Darer *et al*., 2011) as depicted in Fig. 24.

Actually, various kinds of isoprene-derived epoxides and corresponding sulfates have been identified (Minerath and Elrod, 2009; Cole-Filipiak *et al*., 2010; Surratt *et al*., 2010; Darer *et al*., 2011). Among the organosulfate products, tertiary organosulfates are found to be easily hydrolyzed to alcohol, and primary organosulfates are more stable over a period of two months (Darer *et al*., 2011). The mechanism and ubiquity of organosulfate formation in biogenic SOA has also been proposed based on a comprehensive series of laboratory oxidations of nine monoterpenes (Surratt *et al*., 2008).

4.3 Aqueous-phase reactions to form organonitrogen compounds

Organonitrogen compounds observed in field measurements are classified into organic nitrates and other types of compounds such as imines and imidazoles. Among these, the formation mechanism of organic nitrates are quite similar to that of organic sulfates in a nucleophilic attack on epoxides. Darer *et al*. (2011) proposed a parallel pathway for a nitrate ion, as shown in Fig. 24 for sulfate formation. It appeared that a nucleophilic attack of nitrate and sulfate is kinetically competitive, and they showed that both sulfate and nitrate nucleophilic addition products were observed with similar yields (0.20 and 0.16 for sulfate and nitrate, respectively) in an experiment in which 2-methyl-2,3-epoxy-1,4-butanediol was added to a 1 M solution of both SO_4^{2-} and NO_3^-.

The tertiary nitrate ester thus formed is either hydrolyzed to 1,2,3,4-butanetetrol or reacts with sulfuric acid to form a dihydroxy nitrate sulfate ester on a time-scale of minutes (Darer *et al*., 2011).

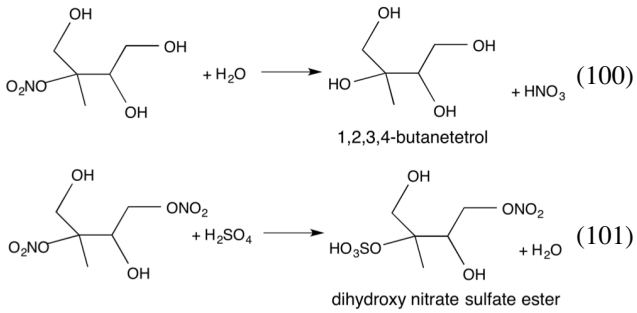

This evidence may potentially explain the fact that organosulfates are more commonly detected in ambient SOA than organonitrates.

On the other hand, the formation of imidazole and its derivatives has been observed in laboratory studies in chambers and bulk aqueous aerosol mimics (De Haan *et al*., 2009a, 2011; Galloway *et al*., 2009; Nozière *et al*., 2009; Sareen *et al*., 2010; Yu *et al*., 2011). Possible reaction products of the imidazole family in the reaction of glyoxal and ammo-

doi:10.5047/meep.2016.00401.0001

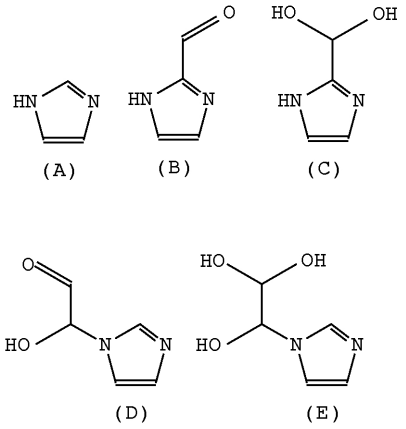

Fig. 25. Chemical structures of major products in the reaction of glyoxal and ammonium sulfate. (A) imidazole, (B) imidazole-2-carboxaldehyde, (C) hydrated imidazole-2-carboxaldehyde, (D) 1N-glyoxal substituted imidazole, (E) hydrated 1N-glyoxal substituted imidazole.

nium sulfate, suggested by Yu *et al*. (2011), are illustrated in Fig. 25. Identified major products via NMR spectroscopy as well as ESI-TOF-MS are imidazole (A), hydrated imidazole-2-carboxaldehyde (C), and hydrated 1N-glyoxal substituted imidazole (E). Imidazole-2-carboxaldehyde (B) was also identified by Galloway *et al*. (2009) based on an authentic sample. Kampf *et al*. (2012) reported identification of further substituted imidazole derivatives with reference compounds, and their implications for light-absorbing material in atmospheric aerosols. Reactions of glyoxal and methyl glyoxal with organic amines and amino acids have also been studied, and colored oligomer formation has been reported in these reactions (De Haan *et al*., 2009a, c, 2011).

Imidazole ($C_3H_4N_2$, MW 68) is a five-membered ring aromatic compound containing nitrogen atoms at the 1,3-position as depicted in Fig. 25(A). The reaction of glyoxal with ammonia to form imidazole has a long history, and the reaction of glyoxal with ammonium sulfate in a bulk solution is well studied (Galloway *et al*., 2009, and references therein). The importance of this type of reaction in the atmosphere is the formation of UV-visible-absorbing yellow-brown products, indicating a potential contribution to atmospheric "brown carbon" (De Haan *et al*., 2009a; Nozière *et al*., 2009; Shapiro *et al*., 2009). Reaction mechanisms for these products of glyoxal and methyl glyoxal with ammonium sulfate and methylamine have been proposed. For example, De Haan *et al*. (2009c) proposed a reaction scheme of imines and imine dimers as intermediates to explain the formation of imidazole derivatives and oligomers in the reaction of glyoxal with methylamine during cloud-droplet evaporation. Yu *et al*. (2011) have proposed reaction pathways for glyoxal and ammonium sulfate. Kua *et al*. (2011) studied the thermodynamics and kinetics of imidazole formation from glyoxal and methylamine in the presence and absence of formaldehyde based on quantum chemical computations. Solution phase Gibbs energy of related species relative to the neutral reactants glyoxal, water, methylamine, and formaldehyde ($\Delta_r G$ in kcal mol^{-1}), and activation energy barriers for optimized transition states were calculated. Based on a theoretical study (Kua *et al*., 2011), a scheme of the main reactions between glyoxal dihydrate and methylamine in the aqueous phase has been proposed as shown in Fig. 26.

The first step to forming an imidazole is the nucleophilic addition of CH_3NH_2 to the monohydrated glyoxal to form the intermediate **2**. Further addition of glyoxal and methylamine to **2** can lead to the oligomeric species as shown in the figure. This is thermodynamically favorable and could be one pathway toward a variety of uncharacterized oligomers observed in the mass spectrometry results (De Haan *et al*., 2009c). The dehydration of **2** forms hydroxy keto-imine **4**, from which keto-imine **5** is produced by dehydration. A quantum chemical calculation shows that the addition of CH_3NH_2 to **4** to form diimine **6** is downhill and that a diimine species **6**, **7**, **8** is a potentially important intermediate in the reaction (Kua *et al*., 2011). In the presence of formaldehyde, an acyclic conjugated keto-structure **10** formed from the addition of formaldehyde to the diimine **8** via the enol-form **9** is the thermodynamic sink. Dimethyl imidazole **12** could be formed from **10**. In the absence of formaldehyde, a hydrated intermediate **13** would be formed by the addition of monohydrated glyoxal to **8**. Under acidic conditions, the diimine acts as a nucleophile attacking the carbonyl group of glyoxal. Dehydration of **13** to a keto-intermediate **14**, followed by ring closure and further dehydration leads to imidazole carboxaldehyde **15** (Kua *et al*., 2011).

Further kinetic and theoretical studies are necessary to establish the reaction mechanisms of imidazole formation in aqueous phase aerosols.

5. Heterogeneous Reactions on Liquid and Solid Aerosol Surfaces

5.1 Chemical aging of OA in the field

It is conceivable that some of primary and secondary organic aerosols may be oxidized further in the ambient air by gas phase oxidizing species such as OH, O_3, and NO_3. Such a secondary oxidation of POA and SOA in the atmosphere is called the photochemical aging of aerosols. Recent studies suggested that the variability of chemical compositions observed in the oxygenated organic aerosols (OOA) is mainly driven by the photochemical aging (Volkamer *et al*., 2006b; Jimenez *et al*., 2009; Haddad *et al*., 2013). However, quantification of the changes in the molecular composition of organic aerosols in ambient air due to the oxidation by gas phase species is not so straightforward, since the changes in molecular composition would also be affected by newly-added species from different emission sources, regional transport and diffusion. For the analysis of atmospheric aging, individual organic compounds are commonly used as markers for sources of primary organic aerosols, such as levoglucosan for wood smoke, hopanes for motor vehicle emissions, alkenoic acids for cooking emission, etc. Although several factors are involved in the ambient aging process of organic aerosols (Rudich *et al*., 2007; Donahue *et al*., 2012), only the aspect of chemical reactions is discussed here.

doi:10.5047/meep.2016.00401.0001

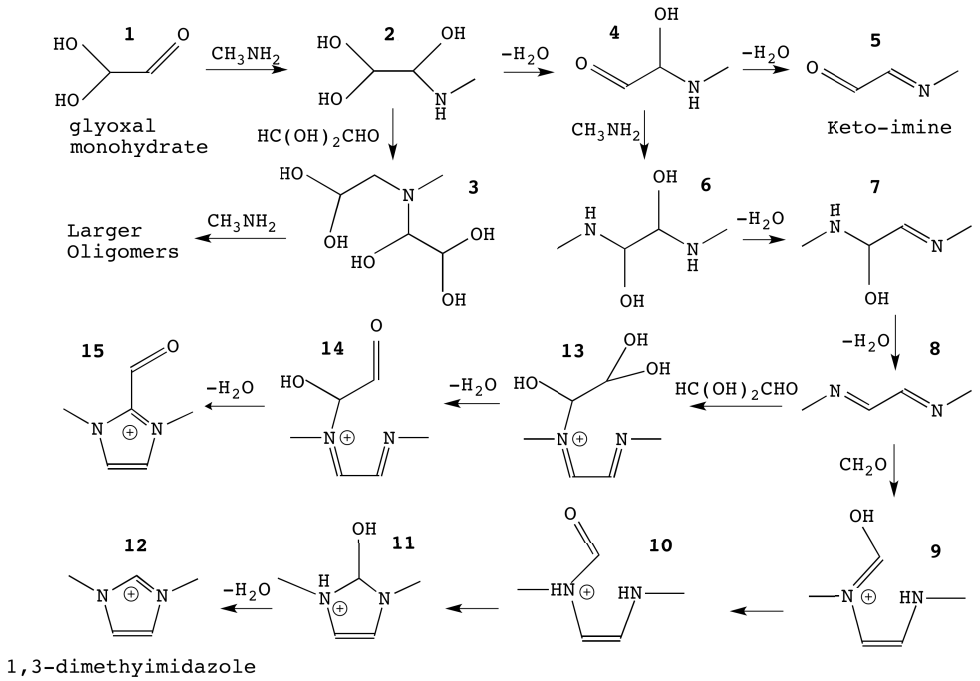

Fig. 26. Proposed reaction mechanisms of glyoxal dihydrate and methylamine in the aqueous phase (referred to Kua *et al*., 2011).

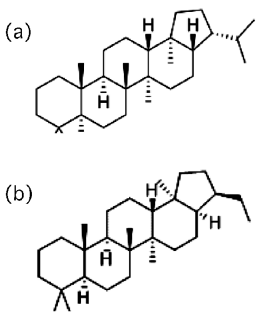

Fig. 27. Chemical structure of (a) 17α(H), 21β(H)-hopane, and (b) 17α(H), 21β(H)-29-norhopane.

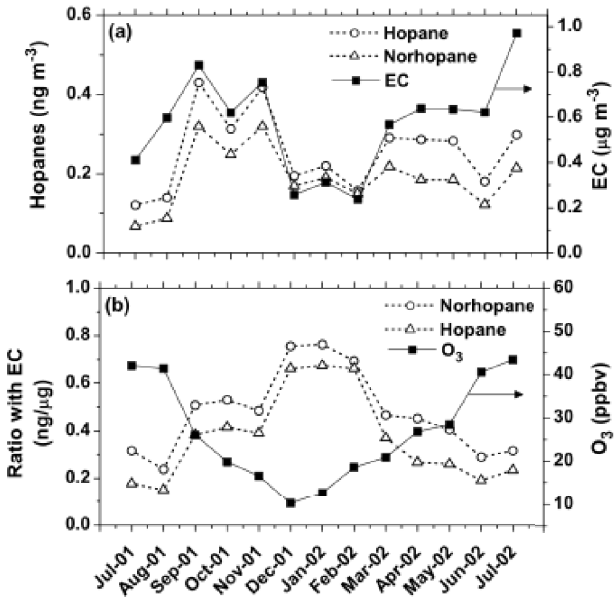

Fig. 28. Monthly average (a) hopane, norhopane and EC concentration, and (b) hopanes to EC ratios and O_3 mixing ratio measured in Pittsburgh, US from July 2001 to July 2002 (from Robinson *et al*., 2006).

Robinson *et al*. (2006) analyzed the ambient data from Pittsburg and the Southeastern United States focusing on two hopanes, 17α(H), 21β(H)-hopane and 17α(H), 21β(H)-29-norhopane. The chemical structures of these compounds are shown in Fig. 27. They demonstrated that, although hopane, norhopane, and elemental carbon (EC), concentrations show no clear seasonal patterns, the hopane- and norhopane-to-EC ratios exhibit a strong seasonal pattern, with the monthly average hopanes-to-EC ratios in winter being a factor of three higher than in summer as depicted in Fig. 28. After a careful discussion on the possible seasonal change of emission factors and other emission sources, they concluded that hopanes are significantly oxidized in the ambient atmosphere in summer most possibly by OH radicals. A more recent study (Lambe *et al*., 2009), however, has suggested that rapid gas-phase oxidation of hopanes by OH may also cause the observed seasonal pattern shown in Fig. 28, since hopanes are somewhat volatile.

Another example of the evidence of atmospheric aging of aerosols is the oxidation of unsaturated compounds by ozone. Two unsaturated acids, oleic acid (9-octadecenoic acid, $C_{18}H_{34}O_2$) and palmitoleic acid (8-hexadecenoic acid, $C_{16}H_{30}O_2$), and a saturated homologue of C_{18} acid, stearic acid (n-octadecanoic acid, $C_{18}H_{36}O_2$) as a reference species

doi:10.5047/meep.2016.00401.0001

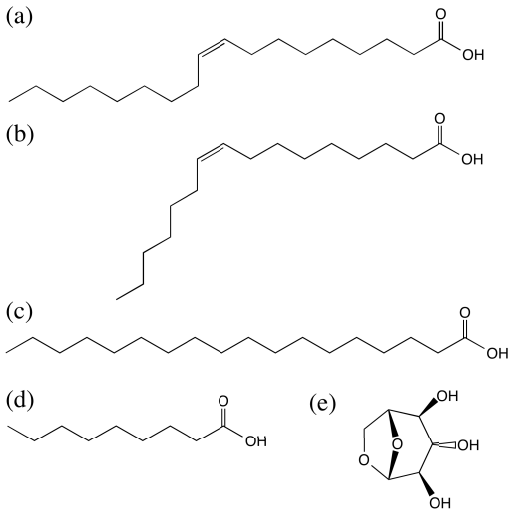

Fig. 29. Chemical structures of (a) oleic acid, (b) palmitoleic acid, (c) stearic acid (d) nonanoic acid and (e) levoglucosan.

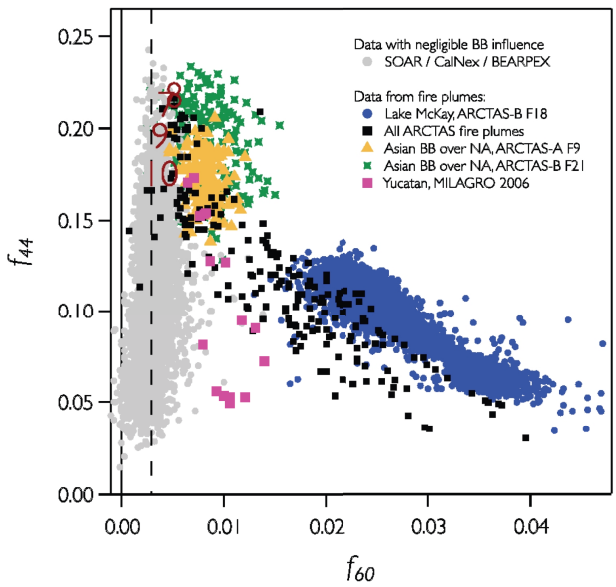

Fig. 30. Summary plot showing f_{44} vs. f_{60} for the field measurements. The nominal background value at 0.3% is shown by the vertical dashed line (adapted from Cubison *et al*., 2011).

shown in Fig. 29, were analyzed from the ambient data obtained in Pittsburg and the Southeastern United States (Robinson *et al*., 2006). The emission sources of these compounds in urban environments are cooking, motor vehicles and biomass combustion, and biogenic emission sources may also contribute (Robinson *et al*., 2006). They also showed a ratio plot of oleic and palmitoleic acid concentrations normalized by stearic acid showed a clear winter maximum and summer minimum as in the case of hopanes, and the ratio of nonanoic acid (Fig. 28(d)) which is one of the products of the oleic acid reaction with ozone, showed the opposite seasonal pattern. The strong seasonal pattern suggests an oxidation of alkenoic acids by O_3 in summer in urban air.

Levoglucosan ($C_6H_{10}O_5$ 1,6-anhydro-β-D-glucopyranose) (Fig. 29(e)) is a specific component of particles emitted through biomass burning (BB), and has recently been widely used as a molecular tracer (Lai *et al*., 2014 and references therein). However, since the specific detection of levoglucosan by an Aerosol Mass Spectrometer (AMS) is difficult, the ratio of the integrated signal at m/z 60 to the total signal in the organic component mass spectrum, f_{60}, is used as a marker of POA from biomass burning (BB-POA) to study the rate of oxidation. Also the parameter f_{44}, the ratio of m/z 44 due to acidic groups (-COOH) to the total signal is used as a tracer for aged POA (Alfarra *et al*., 2004). The chemical aging of BB-POA and the formation of photochemically oxygenated organic aerosol has been observed in field studies (DeCarlo *et al*., 2010; Ng *et al*., 2010; Cubison *et al*., 2011). Cubison *et al*. (2011) analyzed the effects of aging on organic aerosol from BB smoke in aircraft studies over the United States and Mexico. Figure 30 shows f_{44} as a function of f_{60} for the data from various samples of air containing OA, and the horizontal axis by oxidation of the levoglucosan-like species. From Fig. 30, it is suggested that the oxidation of levoglucosan-like species converts to an oxygenated aerosol represented by f_{44}. It has been revealed that the photochemical aging of OA increases f_{44} in compensation of f_{60} which is the potentially linked to levoglucosan-like oxygenates.

On a regional scale in East Asia, Mochida *et al*. (2010) observed a significant decrease of levoglucosan/OC and levoglucosan/EC ratios at Chichi-jima, a remote island in the western Pacific. The ratios showed a winter maximum and summer minimum as seen in Fig. 31, and the concentration levels of levoglucosan in winter are comparable to the estimate of the global aerosol model, whereas those in summer are significantly lower than the modeled values. The estimated ratios of levoglucosan to OC and EC in $PM_{2.5}$ over Changdao island, which is located near the source region in China, were significantly higher than those in Chichi-jima. From this evidence, they concluded the degradation of levoglucosan in the air masses that stagnated over the Pacific in summer. It should be noted that primary emissions of biomass burning aerosols are thought to be mostly semi-volatile (Grieshop *et al*., 2009; Robinson *et al*., 2007). The aging of BB-POA involves largely a gas-phase oxidation of the semi-volatile species rather than a heterogeneous process.

Polycyclic aromatic hydrocarbons (PAHs) have been known as carcinogenic and mutagenic species, and rather extensive studies on the atmospheric decay of reactive PAHs have been conducted as reviewed by Finlayson-Pitts and Pitts (2000). Figure 32 depicts chemical structures of typical PAHs mentioned here and in Subsection 5.2.5. The atmospheric lifetimes of PAHs for a gas phase reaction with an OH radical are hours to days, so that their atmospheric decay is expected in the urban and regional scale (Finlayson-Pitts and Pitts, 2000). For example, the ratios of reactive benzo[a]pyrene (BaP) to less-reactive benzo[e]pyrene (BeP)

doi:10.5047/meep.2016.00401.0001

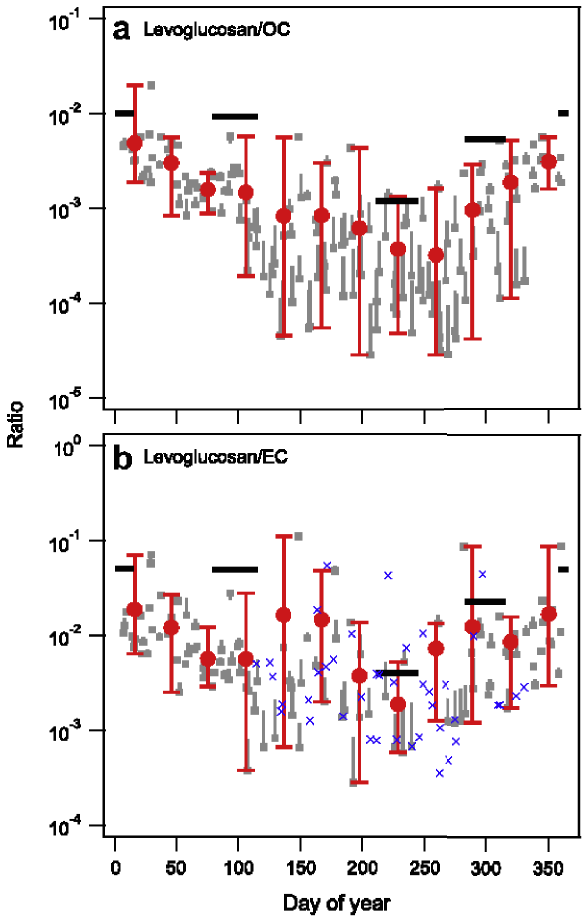

Fig. 31. Temporal variations in (a) levoglucosan/OC and (b) levoglucosan/EC. Grey dots: individual samples, red circle with ranges: monthly average, black horizontal bars: the ratio in $PM_{2.5}$ in Changdao are estimated based on Feng *et al*. (2007). (Reprinted from *Atmos. Environ.*, *44*, Mochida, M., K. Kawamura, P. Fu, and T. Takemura, Seasonal variation of levoglucosan in aerosols over the western North Pacific and its assessment as a biomass-burning tracer, 3511–3518, Copyright 2010, with permission from Elsevier.)

have been found to be higher at night and in winter than during daytime and in summer (Arey *et al*., 1987; Greenberg, 1989). The spatial and temporal distributions of primary PAH, BaP (aerosol phase), and secondary PAH, 3-nitrobiphenyl (3-NBP, vapor phase) in the Los Angeles Basin demonstrated the reactive decay of BaP and the production of 3-NBP during the transport (Fraser *et al*., 1998). Gingrich *et al*. (2001) observed the lower ratio of more reactive PAH, such as benz[a]anthracene (BaA), BaP and pyrene, to less reactive PAH, chrysene and benzo[b]fluoranthene (BbF), on aerosol films in urban versus rural locations in Toronto, Canada, and suggested that it may reflect the higher decay rate in an urban area due to a higher OH radical concentration, since the reverse trend would be expected based on emissions alone.

5.2 Heterogeneous reactions of O_3, OH, and NO_3 on liquid and solid particle surfaces

Reviews on the laboratory kinetics of secondary organic aerosols from OH- and O_3-initiated heterogeneous oxidation has been made by Kroll and Seinfeld (2008), and George and Abbatt (2010). As for the reaction mechanism, however, detailed laboratory studies are rather limited, and, here, O_3 reaction with oleic acid, OH-initiated reactions of saturated hydrocarbons (e.g. squalane), carboxylic (e.g. octanoic acid) and dicarboxylic acids (e.g. suberic acid), unsaturated hydrocarbons (e.g. squalene) and fatty acids (e.g. linoleic, linolenic acid), and O_3, OH and NO_3 reactions with PAH are discussed. Although levoglucosan has been studied in laboratory kinetics, the oxidation mechanism has not been well studied and is not included here.

5.2.1 O_3 + oleic acid Oleic acid ($C_{18}H_{34}O_2$) shown in Fig. 29(a) is a mono-unsaturated fatty acid employed as a tracer for cooking aerosols. Among heterogeneous reactions initiated by O_3 with unsaturated OA molecules, liquid-phase particles of oleic acid are the best studied system, and the corresponding reactions have been reviewed by Zahardis and Petrucci (2007).

The interest in the O_3-initiated oxidation of alkenoic molecules in aerosols from the point of view of reaction chemistry is how the heterogeneous reaction at the particle surface is different from the gas-phase and bulk liquid-phase reactions. The mechanism of ozonolysis of alkenes in the gas phase and the condensed phase has been well studied (Atkinson and Carter, 1984; Finlayson-Pitts and Pitts, 2000; Akimoto, 2016). The reaction mechanisms of oleic acid are not expected to differ significantly from those of alkenes since the double bond of oleic acid is located in the middle of the long carbon chain and is relatively isolated from the carboxylic acid group. The initial steps of the ozonolysis reaction of alkene are the addition of O_3 across the double bond of the alkene forming the primary ozonide, followed by the C-C bond break forming two possible pairs both forming aldehyde and a Criegee intermediate (CI). Thus, in the case of oleic acid, the formation of 9-oxononanoic acid (OND) and nonanal (NNA) with each corresponding CI is expected, as shown in Fig. 33 adapted from Thornberry and Abbatt (2004).

In the gas phase, the CI either decomposes to give fragmented aldehydes and carboxylic acids together with CO_2, CO, OH, etc., isomerizes to give carboxylic acid with the same carbon number, or stabilizes to further react with another atmospheric species such as SO_2, NO_2, etc. (Finlayson-Pitts and Pitts, 2000; Akimoto, 2016). In the condensed phase the CI is known to react with the counterpart aldehyde in a solvent cage to form a secondary ozonide.

The reaction products identified in the liquid phase oleic acid aerosols with O_3 are 9-oxonanoic acid (OND), azelaic acid (AZD), nonanoic acid (NND), and other larger organic molecules in the condensed phase (Katrib *et al*., 2004; Zahardis *et al*., 2005), and nonanal (NNA) as a volatile product (Moise and Rudich, 2002; Thornberry and Abbatt, 2004). Among them the major products are OND and NNA with their yield of ca. 25% each, and the yield of AZD and NND, which are expected to form by a rearrangement of each CI, is less than 10% of OND (Katrib *et al*., 2004). Expected gas-phase reaction products, octane and CO_2, formed by the decomposition of CI were not observed (Moise and

doi:10.5047/meep.2016.00401.0001

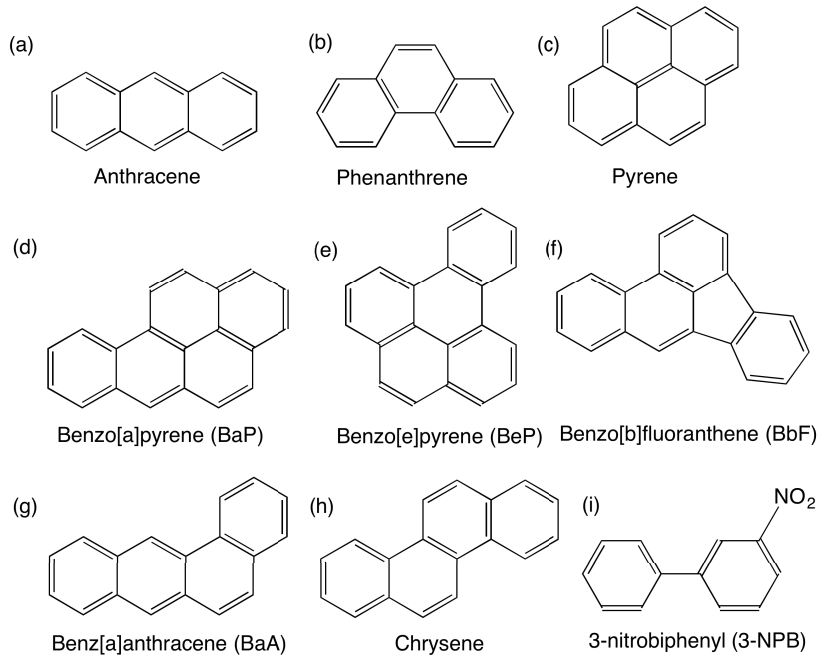

Fig. 32. Chemical structures of selected PAHs appearing in the text.

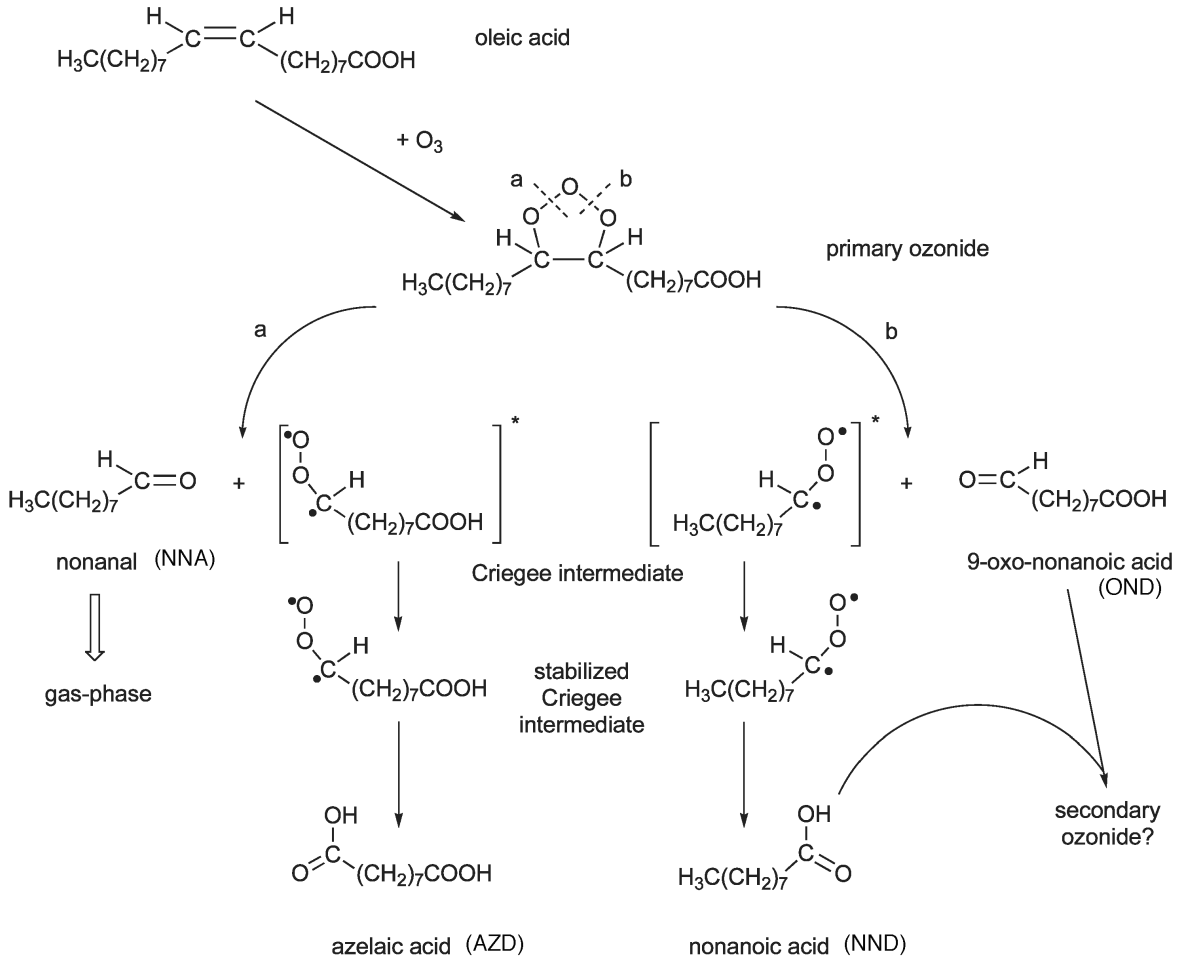

Fig. 33. Proposed scheme for the heterogeneous reaction of O_3 and oleic acid. (Adapted from Thornberry and Abbatt, 2004 with permission of the PCCP Owner Societies.)

doi:10.5047/meep.2016.00401.0001

Rudich, 2002; Thornberry and Abbatt, 2004). In addition to these smaller molecular weight C_9 compounds, Katrib *et al*. (2004) reported a large yield (35–50%) of unidentified higher molecular weight compounds. These higher molecular weight products have been identified as cyclic oxygenates, including secondary ozonides (SOZ), diperoxides (DPX), α-acyloxyalkyl hydroperoxides (AAHP), α-acyloxyalkyl hydroxyalkyl peroxides (AHP), and monoperoxide oligomers (Zahardis *et al*., 2005; Ziemann, 2005; Mochida *et al*., 2006; Reynolds *et al*., 2006).

Ozone initially adds across the double bond of oleic acid to form primary ozonide, which then decomposes to form NNA and OND and the corresponding vibrationally-excited CI (ECI) in a nearly 50 : 50 ratio, the same as in the gas phase. A part of ECI rearranges to AZD and NND, but mostly yields stabilized CI (SCI). The competitive reaction of SCI with counterpart aldehydes, self-reaction, and reaction with AZD and NND formed by rearrangement of ECI would give SOZ, DPX, and AHP, among other products. Further polymerization at the particle surface has been proposed to proceed via the addition of SCI to AHP (Zahardis *et al*., 2006). The competitive ratio may depend on experimental conditions. The reaction pathways for the O_3 initiated oxidation of methyl oleate, chosen as a surrogate of oleic acid for preventing polymerization has been proposed by Mochida *et al*. (2006), including the higher molecular compounds mentioned above.

Similar laboratory kinetic studies have been made for other liquid unsaturated fatty acids, such as linoleic acid ($C_{18}H_{32}O_2$) and linolenic acid ($C_{18}H_{30}O_2$) as well (Thornberry and Abbatt, 2004). Organic aerosol formed from the reaction of 1-tetradecene, linear alpha olefin, with O_3 in the presence of alcohols and carboxylic acids has been studied to elucidate the reactivity of stabilized Criegee intermediates (Tobias and Ziemann, 2000).

The difference in the heterogeneous reaction of O_3 at the particle surface of oleic acid from the gas-phase reaction lies in the reaction rate, rather than the reaction mechanism. The reactive uptake coefficients of O_3, γ_r, were determined to be $(8.3\pm0.2)\times10^{-4}$ and $(5.2\pm0.1)\times10^{-5}$ for liquid and frozen oleic acid, respectively, in a coated-wall flow tube (Moise and Rudich, 2002), which implies that nearly one collision in 10^3 is reactive for gas-liquid heterogeneous processes. The largest A-factors of gas-phase ozone-alkene reactions are on the order of 10^{-14} or 10^{-15} cm^3 molecule^{-1} s^{-1} (Atkinson *et al*., 2004), which is 10^{-4} to 10^{-5} times smaller than the gas-kinetic collision rate constant. Therefore, a gas-surface reaction probability of 10^{-3} implies that there is an enhancement to the rate from entropic factors. The decrease in γ_r with increasing particle size, $(7.3 \pm 1.5) \times 10^{-3}$ and $(0.99 \pm 0.09) \times 10^{-3}$ for particle radii of 0.68 and 2.45 μm, respectively, is thought to be the result from the reaction being limited by the diffusion of oleic acid within the particle (Smith *et al*., 2002), and an upper limit for the reacto-diffusive length in a liquid aerosol has been estimated to be $\sim$10 nm (Morris *et al*., 2002). In support of this idea, Vieceli *et al*. (2004) have demonstrated, in the molecular dynamics simulations, that there occurs a substantial trapping of ozone molecules at the surface of unsaturated organic molecules.

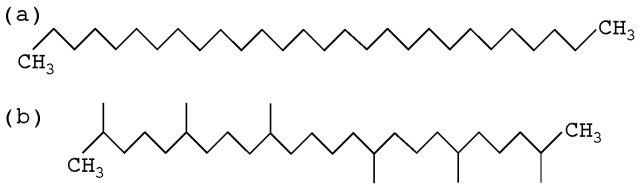

Fig. 34. Chemical structure of (a) n-octacosan ($C_{28}H_{58}$) and (b) squalane ($C_{30}H_{62}$).

As for the possibility of the enhancement of the gas-surface reaction by energetic factor, the apparent activation energy of 2–3 kJ mol^{-1} calculated from the measured temperature dependence of the uptake coefficients, is significantly smaller than that of similar gas-phase reactions (e.g. cis-2- butane, 8.1 kJ mol^{-1}) (Atkinson *et al*., 2004), suggesting a possible change in the energetics of the reaction (Thornberry and Abbatt, 2004).

5.2.2 OH + squalane, saturated hydrocarbons Heterogeneous reactions of a gas phase OH with saturated organic compounds of atmospheric interest in liquid particles have been studied typically for squalane (Ruehl *et al*., 2013; Kolesar *et al*., 2014). In order to obtain insights into the influence of the molecular structure on the chemical reaction mechanisms of OH-initiated heterogeneous oxidation of saturated hydrocarbons in submicrometer particles, Ruehl *et al*. (2013) studied n-octacosane ($C_{28}H_{58}$, a linear alkane) and squalane ($C_{30}H_{62}$, a highly-branched alkane) (Fig. 34) in a flow system in the presence of O_2 by identifying reaction products by using two-dimensional gas chromatography with electron impact ionization (EI) and vacuum ultraviolet photoionization (VUV-PI) mass spectrometry. One of the concerns for the OH-initiated heterogeneous oxidation reaction of organic compounds has been the relative importance of two pathways, termed functionalization and fragmentation. Functionalization stands for the pathway when an oxygenated functional group (e.g. carbonyl, hydroxyl, etc.) is added to a molecule leaving the carbon skeleton intact, producing a product with the same carbon number as the reactant. Alternatively, fragmentation involves C-C bond cleavage producing two oxidation products with smaller carbon numbers than the reactant. Since the fragmented products are more volatile in general, the relative importance of these processes affects the environmental impacts after the aging of aerosols.

Figure 35 compares the distributions of positional isomers of functionalization products of octacosane and squalane with the prediction of a structure-reactivity relationship (SRR) for hydrogen abstraction in the gas-phase (Kwok and Atkinson, 1995).

In the case of a linear alkane, octacosane, clear enhancement in the formation of octacosanone with the carbonyl group toward the terminus of the molecule has been revealed as shown in Fig. 35(a). A similar pattern is observed for the isomers of octacosanol as shown in Fig. 35(b), although the yield of octacosanol is smaller than that of octacosanone.

doi:10.5047/meep.2016.00401.0001

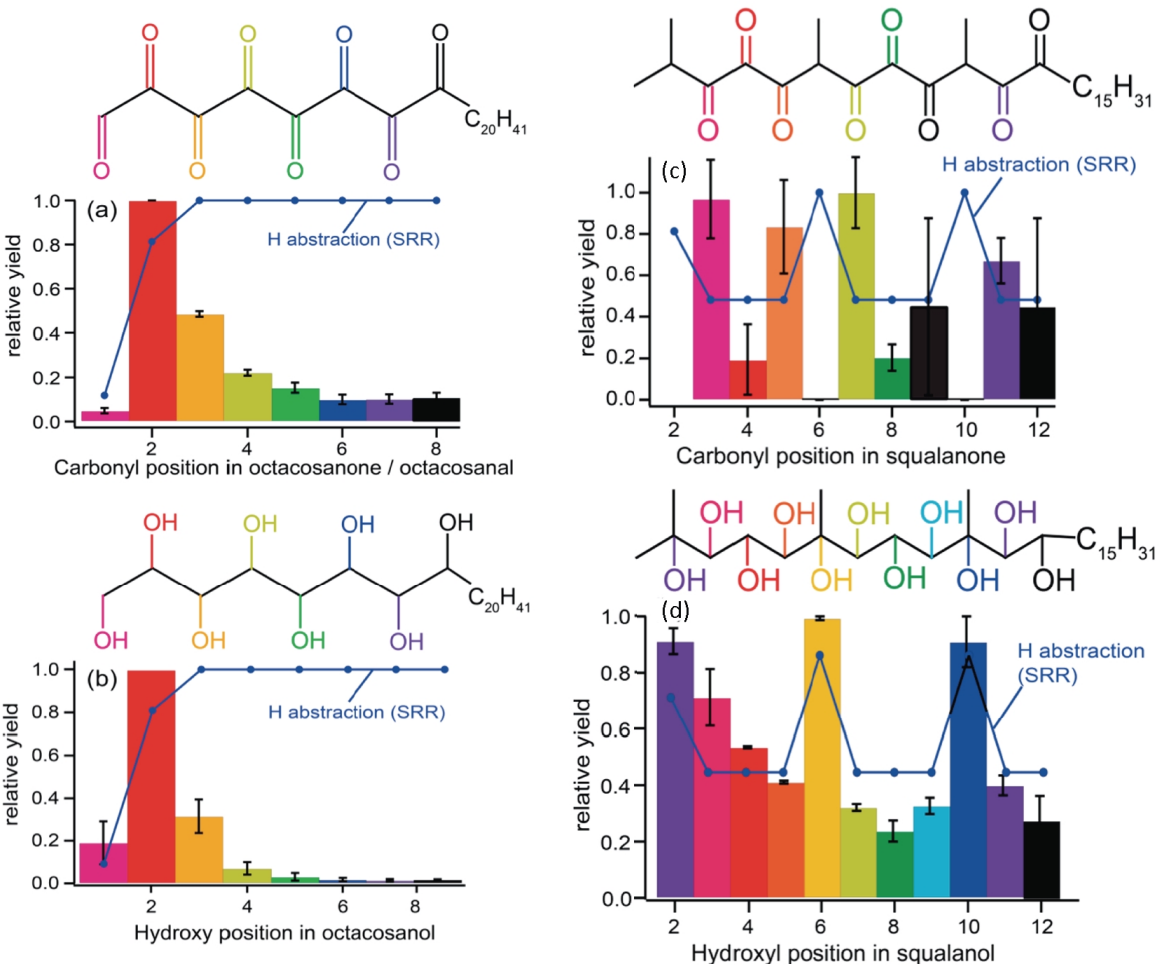

Fig. 35. Distribution of positional isomers of functionalization products from the OH-initiated surface reaction of octacosane and squalane. The lines show structure-reactivity relationship (SRR) predictions for gas-phase H-abstraction. The products are isomers of (a) octacosanone, (b) octacosanol, (c) sqalanone, and (d) sqalanol. (Adapted with permission from Ruehl, C. R., T. Nah, G. Isaacman, D. R. Worton, A. W. H. Chan, K. R. Kolesar, C. D. Cappa, A. H. Goldstein, and K. R. Wilson (2013), The influence of molecular structure and aerosol phase on the heterogeneous oxidation of normal and branched alkanes by OH, *J. Phys. Chem. A*, *117*, 3990–4000. Copyright 2013 American Chemical Society.)

This characteristic is quite different from those expected from SRR in the gas phase, which predicts a similar reactivity for all secondary carbons as shown in Fig. 35(a) and (b). The rate of hydrogen abstraction from the terminal carbon is expected to occur ten times slower than from interior carbons in the gas phase, which is consistent with the very low yield of octacosanal and n-octacosanol for the surface reaction. For squalane, a highly-branched alkane, H-atom abstraction occurs preferentially on CH_3-attached tertiary carbons, and the reaction rate for the secondary C-H is the same regardless whether it is adjacent to the CH_3-attached carbon, or one carbon apart, as shown in Fig. 35(c) according to SSR. In contrast, squalanone formation by the surface reaction occurs predominantly on the secondary carbon adjacent to the CH_3-attached carbon (α-position), followed by the secondary C-H on one carbon apart (β-position) and the abundance is the least for the tertiary C-H as seen in Fig. 35(c). Ruehl *et al*. (2013) suggested that the observed enrichment of the α- over the β-carbonyls is due to the differences in the subsequent chemistry of the peroxy or alkoxy radicals formed at these different carbon sites. Peroxy radicals formed at these α- and β-positions are converted to alkoxy radicals, which can abstract a hydrogen atom from either the same molecule (isomerization) or another molecule (chain propagation) and which then converts the alkoxy radical into a hydroxyl group. Since isomerization generally involves a six-membered ring transition state, β-alkoxy radicals have more hydrogen atoms available for abstraction than α-alkoxy radicals. Therefore, this pathway is enhanced for β-carbons, resulting in less abundant ketone formation at these sites in squalanone. In contrast to the linear alkane, the distribution of squalanol isomers is different from what is observed for squalanones. As shown in Fig. 35(d), squalanols with hydroxyl on tertiary carbon atoms are formed with the highest abundance, and the preference for α- over β-carbons for hydroxyl functionalization is much less pronounced. The most prevalent isomers with hydroxyl on a tertiary carbon can be explained by a more rapid H-atom abstraction rate as predicted by SRR.

Based on these observations and considerations, Ruehl

doi:10.5047/meep.2016.00401.0001

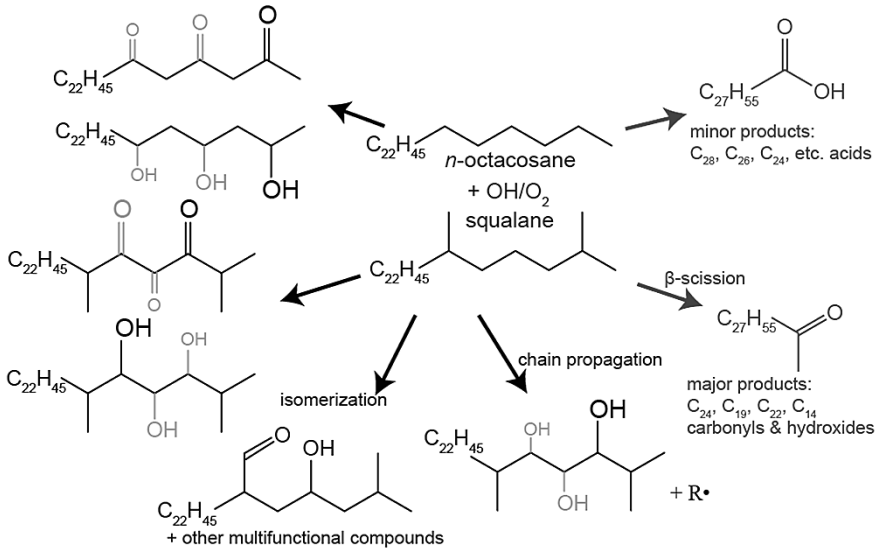

Fig. 36. Reaction pathways of the OH-initiated heterogeneous oxidation of n-octacosane and squalane liquid particles. (Adapted with permission from Ruehl, C. R., T. Nah, G. Isaacman, D. R. Worton, A. W. H. Chan, K. R. Kolesar, C. D. Cappa, A. H. Goldstein, and K. R. Wilson (2013), The influence of molecular structure and aerosol phase on the heterogeneous oxidation of normal and branched alkanes by OH, *J. Phys. Chem. A*, *117*, 3990–4000. Copyright 2013 American Chemical Society.)

et al. (2013) proposed reaction pathways of OH-initiated oxidation of n-octacosane and squalane as shown in Fig. 36.

Isaacman *et al*. (2012) studied the heterogeneous OH-initiated oxidation of motor oil particles and reported that branched isomers reacted 44±14% faster, and cyclic aliphatic compounds reacted 27±3% slower than the straight chain alkane for saturated hydrocarbons (e.g. C_{26}). The OH uptake by branched alkanes is more than the expected increase of 10% based on SRR, and the decrease by cyclic isomers is the inverse to the expected relationship. The reason for the difference in reactivity in the liquid-phase and gas-phase is so far unknown. A recent study by Kolesar *et al*. (2014) reported the uptake coefficient of OH on uncoated squalane particle to be $\gamma_{\rm eff} = 0.28 \pm 0.06$ but this increases upon coating with SOA by a factor of 2. This implies that oxidation lifetime within mixed particles would be 6–8 days, comparable to the order of typical particle atmospheric lifetime, and they suggested that heterogeneous oxidation by OH may play an important role in transforming OA.

Zhang *et al*. (2013) showed that the heterogeneous reaction of OH with cholestane ($C_{27}H_{48}$, a solid cyclic alkane with a branched aliphatic side chain) yielded insignificant ring-opening oxidation products in contrast to the case of a gas phase reaction. In gas-phase reactions, ring-opening products are predicted to form in large abundance due to the presence of highly-reactive tertiary and secondary carbons in the aliphatic ring (Atkinson, 1997).

5.2.3 OH + carboxylic, dicarboxylic acid Enami *et al*. (2014) studied the products and intermediates of the oxidation of aqueous alkenoic acids (acetic, hexanoic and octanoic acids) initiated by ∼10 ns OH(g) pulses at the air-water interface by use of a novel experimental set up of microjets coupled to electrospray mass spectrometry. OH was produced by the laser photolysis of O_3/H_2O. Figure 37 shows negative ion mass spectra of hexanoic acid (A, B) and octanoic acid (C, D) microjets exposed to OH in the presence of excess O_2(g). Under the exposure of OH radicals, peroxy radicals, R_5(-H)(COO^-)OO· at m/z 146 and R_7(-H)(COO^-)OO· m/z 174, were identified, and found to react within 50 μs to produce alcohols R(-H)(COO^-)OH and carbonyls R(-2H)(COO^-)=O.

Enami *et al*. (2015) also reported the oxidation of dicarboxylic acids, HOOC-R_n-COOH (R_n = C_2H_4, C_3H_6, C_4H_8, C_5H_{10}, and C_6H_{12}) in aqueous microjets by OH. They yield the corresponding (n − 1) species O=C(H)-R_{n-1}-COO^-/HOOC-R_{n-1}-COO^-, in addition to an array of closed-shell HOOCR_n(-H)(OOH)-COO^-, HOOC-R_n(-2H)(=O)-COO^-, HOOC-R_n(-H)(OH)-COO^-, and HOOC-R_n(-H)(OO·)-COO^- radical species. In contrast to the monocarboxylic acid case, shorter chain products, such as these assigned to OHC-R_5-COO^- and HOOC-R_5-COO^-, are formed from HOOC-R_6-COO^-. The reaction scheme shown in Fig. 38 has been proposed for the OH-initiated oxidation of suberic acid, HOOC-R_6-COOH at the air-water interface in line with the results on the reaction of aqueous monocarboxylic acids with OH.

As shown in Fig. 38 the initial reaction of the OH with aqueous (di)carboxylic acids is the H-atom abstraction followed by the formation of peroxy radicals as in the case of saturated hydrocarbons described in the previous section. The simultaneous self-reactions of the peroxyl radicals give (di)carboxylic alcohols and ketones via the Russell disproportionation (self-reaction A) and the Bennett–Summers reaction (self-reaction B), respectively. A part of the peroxy radicals forms oxy-radicals by the self-reaction C. The β-scission of the oxyradicals gives lower carbon fragments (n − 1 species), from which a lower carbon dicarboxylic acid would be formed as shown in Fig. 38. Importantly, it has

doi:10.5047/meep.2016.00401.0001

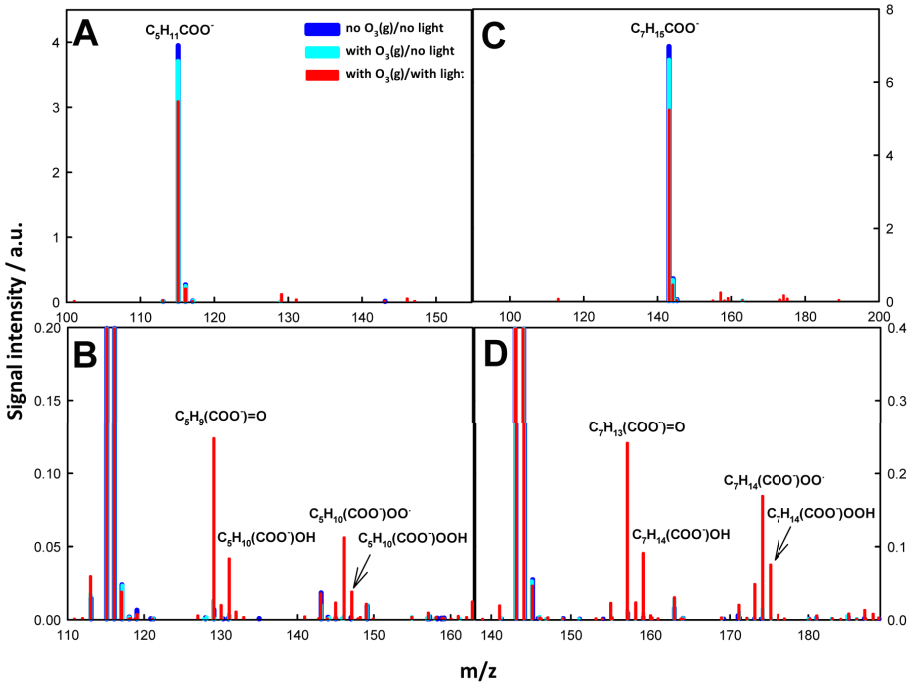

Fig. 37. Negative ion electrospray mass spectra of hexanoic acid (A, B) and octanoic acid (C, D) microjets under the condition of laser off (A, C) and on (B, D) to produce OH radicals. (Reprinted with permission from Enami, S., M. R. Hoffmann, and A. J. Colussi (2014), In situ mass spectrometric detection of interfacial intermediates in the oxidation of RCOOH(aq) by gas-phase OH-radicals, *J. Phys. Chem. A*, *118*, 4130–4137. Copyright 2014 American Chemical Society.)

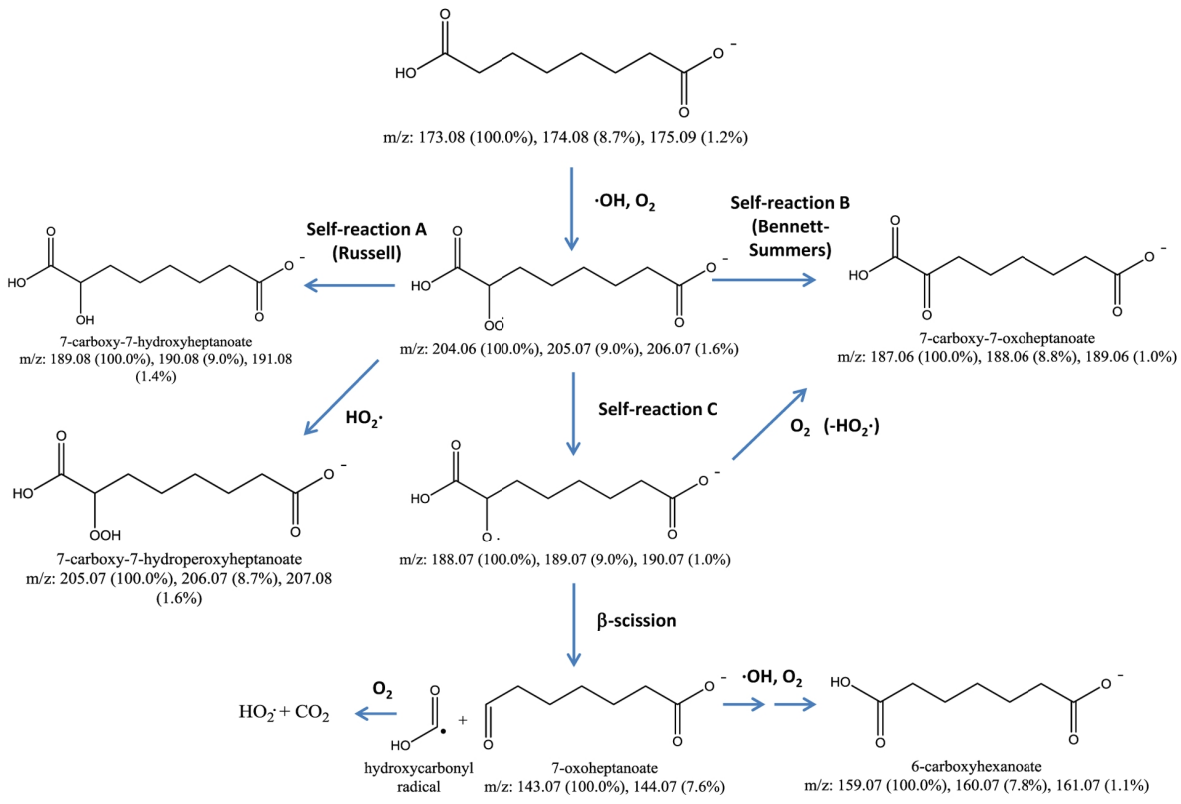

Fig. 38. Proposed mechanism of OH-initiated oxidation of suberic acid at the air-water interface. (Reprinted with permission from Enami, S., M. R. Hoffmann, and A. J. Colussi (2015), Stepwise oxidation of aqueous dicarboxylic acids by gas-phase OH radicals, *J. Phys. Chem. Lett.*, *6*, 527–534. Copyright 2015 American Chemical Society.)

doi:10.5047/meep.2016.00401.0001

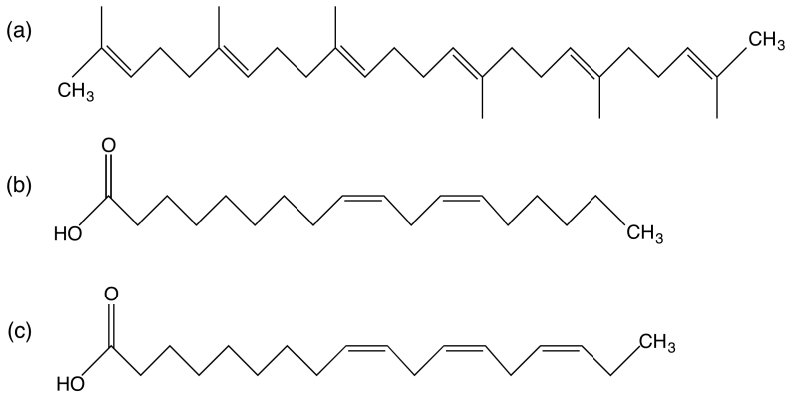

Fig. 39. Chemical structures of (a) squalene, (b) linoleic acid and (c) linolenic acid.

been found that the same products (peroxyl radicals, peroxides, carbonyls, alcohols, and n − 1 species) are observed in the case of n = 2–6 dicarboxylic acids, HOOC-R_n-COOH, but are absent for n = 0 (oxalic acid) and 1 (malonic acid) (Enami *et al*., 2015). This could be one of the reasons why oxalic and malonic acids accumulate in SOA in agreement with field observations.

The OH-initiated reactions of carboxylic (lactic, propionic, pyruvic, glycolic, glyoxylic, acetic) and dicarboxylic acid (glutaric, tartaric, succinic, malic, malonic, oxalic) in aqueous solutions have been studied by Charbouillot *et al*. (2012). They reported that the degradation of glyoxylic, tartraric, lactic, propionic and glycolic acids leads to the formation of oxalic acid, and such mechanisms leading to the accumulation of oxalic acid via the photooxidation of higher carboxylic acids could also be responsible for the relatively high concentration of oxalic acid found in cloud water and in aerosol particles.

5.2.4 OH + squalene, unsaturated fatty acids As for the OH-initiated oxidation of alkenes and unsaturated fatty acids in liquid particles, squalene ($C_{30}H_{50}$, a highly-branched olefin with six C=C double bonds, Fig. 39(a)), oleic acid ($C_{18}H_{34}O_2$) (see Fig. 29), linoleic acid (a straight-chain monocarboxylic acid with two C=C double bonds $C_{18}H_{32}O_2$, Fig. 39(b)), and linolenic acid ($C_{18}H_{30}O_2$, a straight-chain monocarboxylic acid with three C=C double bonds, Fig. 39(c)) have been studied in some detail in flow tube reactor experiments (Nah *et al*., 2013, 2014a, b). The effective uptake coefficients of squalene, oleic, linoleic and linolenic acid are found to be larger than unity, 2.92 ± 0.18 (Nah *et al*., 2014b), 1.72 ± 0.08, 3.75 ± 0.18 and 5.73 ± 0.14 (Nah *et al*., 2013), respectively, which suggests that secondary reactions take place to consume these species after the addition of OH to the C=C double bond.

For the reaction of squalene (Sqe) in the presence of O_2, the VUV mass spectra before and after the reaction are shown in Fig. 40 (Nah *et al*., 2014a). Upon exposure to OH radicals, the intensities of the squalene molecular ions (m/z 410) and the fragment ions (m/z 341) decreased, and groups of higher molecular weight products centered at m/z 426, 442, 458 shown in Fig. 40(b) inset are formed. These peaks are separated by 16 Da (amu) and shown as Sqe, SqeO, $SqeO_2$, and $SqeO_3$ denoting the number of oxygenated functional groups (alcohols and ketones). A detailed identification of these product species has been made by Nah *et al*. (2014b) who reported that the functionalization products are composed of $C_{30}H_{49}OH$, $C_{30}H_{51}OH$ and $C_{30}H_{50}(OH)_2$ isomers. In addition to these functionalization products, fragmentation products with a carbon number less than C_{30} are also formed in the reaction of OH and squalene.

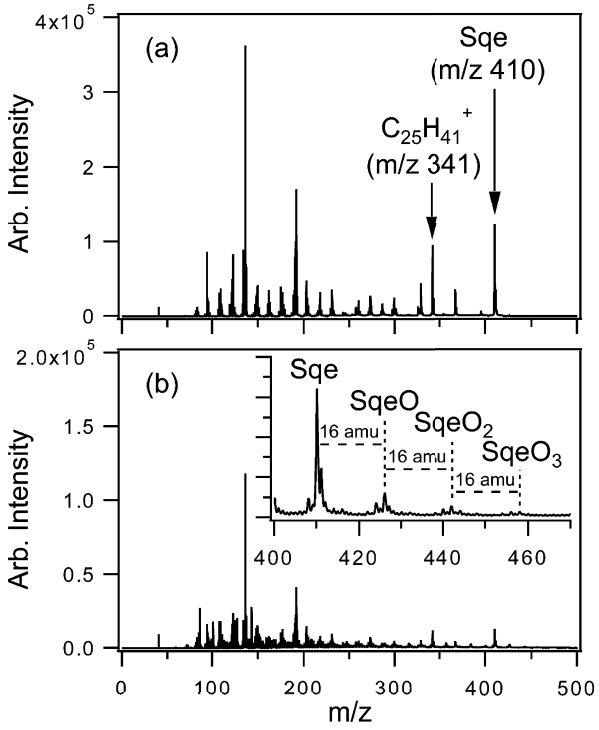

Fig. 40. VUV PI mass spectrum of squalene (Sqe) particles. (a) before, and (b) after, exposure to OH radicals at 10% [O_2]. The inset in panel (b) shows the higher molecular weight oxygenated reaction products in an expanded scale. (Reprinted with permission from Nah, T., S. H. Kessler, K. E. Daumit, J. H. Kroll, S. R. Leone, and K. R. Wilson (2014a), Influence of molecular structure and chemical functionality on the heterogeneous OH-initiated oxidation of unsaturated organic particles, *J. Phys. Chem. A*, *118*, 4106–4119. Copyright 2014 American Chemical Society.)

From the evidence, Nah *et al*. (2014b) proposed a reac-

doi:10.5047/meep.2016.00401.0001

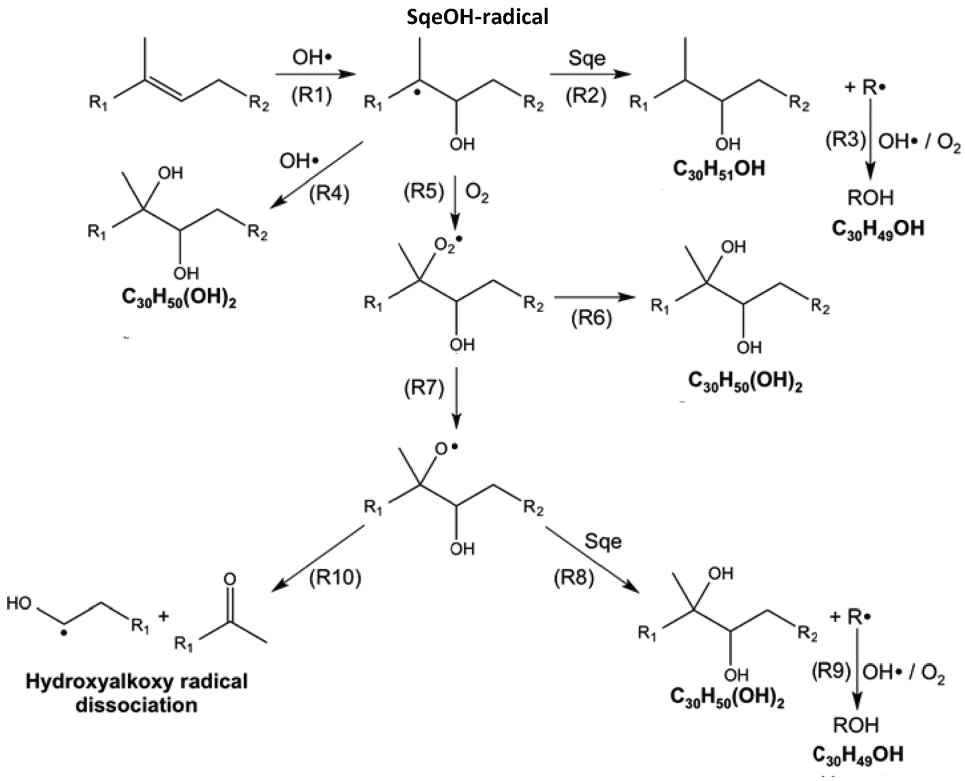

Fig. 41. Proposed reaction mechanism for the OH-initiated oxidation of liquid-particle squalene. R· represents the generic alkyl radical formed by the abstraction of an H-atom from a squalene molecule. (Adapted with permission from Nah, T., H. Zhang, D. R. Worton, C. R. Ruehl, B. B. Kirk, A. H. Goldstein, S. R. Leone, and K. R. Wilson (2014b), Isomeric product detection in the heterogeneous reaction of hydroxyl radicals with aerosol composed of branched and linear unsaturated organic molecules, *J. Phys. Chem. A*, *118*, 11555–11571. Copyright 2014 American Chemical Society.)

tion mechanism for the OH-initiated oxidation of squalene aerosol as shown in Fig. 41. The initial step (R1) is the addition of OH to the double bond of squalene to form a hydroxyalkyl radical in the same way as in the gas phase reaction. When the OH-added squalene-radical (SqeOH-radical) abstracts an H-atom from a neighboring squalene molecule (Sqe) (R2), a generic alkyl radical (R·) and a stable reaction product with an OH group ($C_{30}H_{51}OH$) result, which would explain an uptake coefficient larger than unity. Reactions (R4) and (R8) form stable products with two OH groups, and (R8) forms a second chain cycling contributing to a still larger uptake coefficient. The fragmentation products are presumed to be formed by C-C bond cleavage of an oxy radical (R10).

In the presence of 10% O_2, the total abundance of observed fragmentation products is approximately equal to the functionalization products, in contrast to the observation that ∼90% of the original squalene mass concentration can be accounted for by the functionalization products at 1% O_2.

In the case of unsaturated fatty acids, such as oleic, linoleic and linolenic acid, similar types of functionalization and fragmentation products have been identified and an analogous reaction mechanism to Fig. 41 has been proposed (Nah *et al.*, 2014a, b). It has been noted, however, that approximately 88% of the observed oxidation products are functionalization products, and approximately 12% are fragmentation products even at 10% O_2, suggesting that the formation and dissociation of secondary hydroxyalkoxy radicals are minor reaction channels for linear molecules. The larger abundance of fragmentation products at 10% O_2 for squalene can be attributed to the formation and dissociation of tertiary hydroxyalkoxy radical intermediates. Also, alcohols are formed in favor of carbonyl functional groups in the case of unsaturated compounds, suggesting that there are some key differences between heterogeneous reactions involving allylic peroxy radical intermediates and simple alkyl peroxy radicals from saturated hydrocarbons (Nah *et al.*, 2014b). The relative importance of fragmentation and functionalization pathways in the heterogeneous oxidation of organic aerosol has been of much concern since it changes the volatility of OA upon atmospheric oxidation (Kroll *et al.*, 2009). It has been revealed that the ratio is dependent on the molecular structure and experimental conditions such as the concentration of O_2.

In general, the gas-particle interface is chemically distinct from the homogeneous environment of a gaseous or condensed phase. Reaction rates and product distributions are thought to depend upon the interfacial molecular interaction, including the orientation and thermodynamics at the surface.

5.2.5 O_3, OH, NO_3 + PAH PAH and their oxidized derivatives have been of concern from the view point of carcinogenicity and mutagenicity since as early as the 1950s, so that field observations as well as laboratory studies on the processes of photooxidation, ozonolysis and NO_2 exposure

doi:10.5047/meep.2016.00401.0001

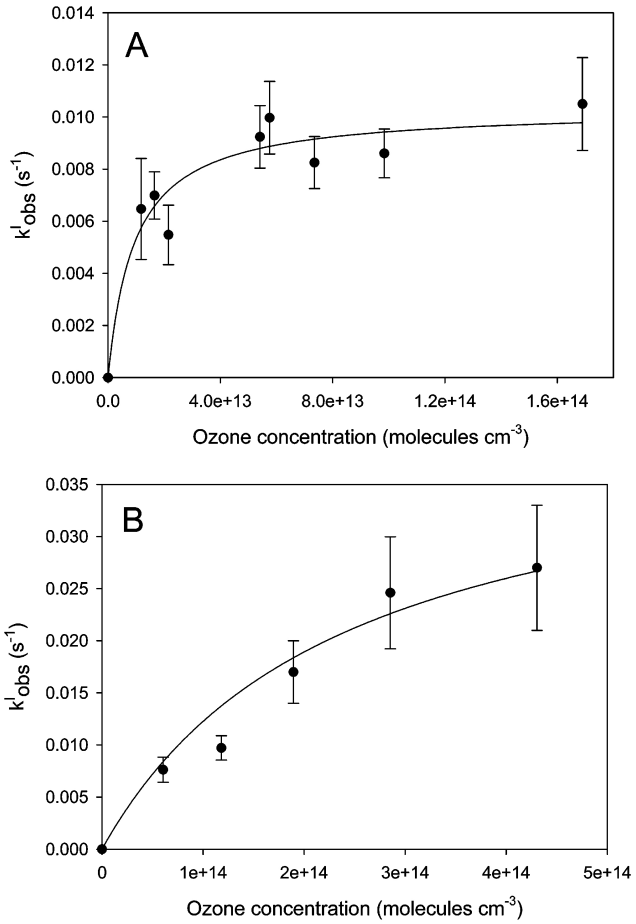

Fig. 42. Pseudo-first-order rate constants ($k^{\mathrm{I}}_{\mathrm{obs}}$) as a function of gas-phase ozone concentration for the reaction of surface bound anthracene on (A) phenyl siloxane oil aerosol and (B) azelaic acid aerosol. (Reprinted with permission from Kwamena, N.-O. A., M. G. Staikova, D. J. Donaldson, I. J. George, and J. P. D. Abbatt (2007b), Role of the aerosol substrate in the heterogeneous ozonation reactions of surface-bound PAHs, *J. Phys. Chem. A*, *111*, 11050–11058. Copyright 2007 American Chemical Society.)

of deposited PAH on a variety of substrates have a long history (Finlayson-Pitts and Pitts, 2000). It should be noted, however, that much of the oxidation of PAH in ambient air are believed to occur in the gas phase since some of PAHs are volatile and the rate constants of gas-phase reactions with OH radicals are large (Atkinson and Arey, 1994; Calvert *et al*., 2002). Recent studies, however, suggest that the heterogeneous oxidation of surface films can be an efficient reactive sink also for volatile PAHs (Kwamena *et al*., 2007a; Springmann *et al*., 2009).

Many studies have been conducted on the kinetics of heterogeneous reactions with O_3 to obtain a pseudo-first order rate coefficient ($k^{\mathrm{I}}_{\mathrm{obs}}$) at different O_3 concentrations by using flow tube reactors. It has been revealed that the plot of $k^{\mathrm{I}}_{\mathrm{obs}}$ as a function of O_3 concentration is, in general, non-linear with a shape that is consistent with the Langmuir-Hinshelwood (L-H) mechanism as exemplified in Fig. 42 for the reaction of anthracene (Kwamena *et al*., 2007b). The L-H mechanism implies that the gaseous active species adsorb to the surface molecules initially, and then the reaction proceeds via the adsorbed molecules. Justification of the L-H mechanism for the surface reaction of O_3 with benzo[a]pyrene (BaP) has been given by proposing a reactive oxygen intermediate at the interface based on experimental and theoretical considerations (Shiraiwa *et al*., 2011).

The data of the L-H plot can be fitted using the following equation (Kwamena *et al*., 2007b),

$$k^{\mathrm{I}}_{\mathrm{obs}} = \frac{k^{\mathrm{I}}_{\mathrm{max}} K_{\mathrm{O_3}} [\mathrm{O_{3(g)}}]}{1 + K_{\mathrm{O_3}} [\mathrm{O_{3(g)}}]}, \tag{102}$$

where $k^{\mathrm{I}}_{\mathrm{max}}$ is the maximum rate coefficient that would be observed at high O_3 concentrations, K_{O_3} is the gas-to-surface equilibrium constant of O_3, and $[O_3(g)]$ is the gas phase O_3 concentration. The important finding from kinetic studies on heterogeneous O_3-PAH reactions is that values of $k^{\mathrm{I}}_{\mathrm{max}}$ and K_{O_3} are very much dependent on the substrate, e.g. organic aerosols, soot, inorganic salts, SiO_2/Al_2O_3, water, etc. Table 4 summarizes the fitting parameters for the reaction of O_3 with surface adsorbed anthracene and BaP on various substrates. As seen in Table 4, $k^{\mathrm{I}}_{\mathrm{max}}$ and K_{O_3} for the reaction of anthracene and BaP can vary by a factor of 100 depending on the substrates. The theoretical interpretation for such variability has not been well elucidated yet.

In order to discuss the relative importance of heterogeneous oxidation versus gas phase reactions of atmospheric PAH, the variability of the oxidation rate on different substrates has to be taken into account. Using a model considering such parameters of air-surface reactions, Kwamena *et al*. (2007a) concluded that the heterogeneous oxidation process of PAH by O_3 is important in the urban atmosphere.

Discussions of reaction mechanisms based on the product analysis specifically for the heterogeneous reaction of PAHs, are rather scarce. Perraudin *et al*. (2007) studied the reaction of O_3 with anthracene and phenanthrene. The identified reaction products were anthraquinone and anthrone with yields of 0.42 ± 0.04 and 0.056 ± 0.005, respectively, for anthracene, and 1,1′-biphenyl-2,2′-dicarboxaldehyde (1.0 ± 0.4) for phenanthrene. Kwamena *et al*. (2006) also reported anthraquinone as a reaction product. Based on their experimental results, Perraudin *et al*. (2007) proposed a reaction mechanism for the heterogeneous reaction of particulate anthracene and phenanthrene with gaseous O_3. The proposed mechanism for the O_3-anthracene reaction is shown in Fig. 43.

The heterogeneous reaction of an NO_3 radical with PAH on an azelaic acid particle has been studied by Zhang *et al*. (2011) using a flow tube reactor. Mono-, di-, and poly-nitro compounds were identified as products from successive nitro-substitute reactions in real time with VUV-ATOFMS. A clear difference in products between heterogeneous and homogeneous reactions has been reported in the nitration reaction of pyrene by Zimmermann *et al*. (2013). They found 1-nitropyrene is formed in the surface reaction of ambient particles collected in Los Angeles in contrast to the formation of 2-nitropyrene in the gas phase nitration reaction reported by Miet *et al*. (2009).

doi:10.5047/meep.2016.00401.0001

Table 4. Comparison of fitting parameters for Eq. (102) for the reactions of surface-adsorbed anthracene and benzo[a]pyrene on various substrates (Data from Kwamena *et al*., 2006, 2007b)

PAH	Substrate	$10^3\ k^{\mathrm{I}}_{\mathrm{max}}$ (s^{-1})	K_{O_3} (10^{-15} cm^{-3})	Reference
Anthracene	azelaic acid	57 ± 9	2.2 ± 0.9	(a)
	phenylsilicoxane oil	10 ± 3	100 ± 40	(a)
	Pyrex glass	6.4 ± 1.8	2.8 ± 0.9	(b)
	1-octanol water	2.59 ± 0.14	1.96 ± 0.34	(c)
		2.55 ± 0.17	0.466 ± 0.059	(c)
	Stearic acid on water	2.26 ± 0.20	0.520 ± 0.13	(c)
	octanoic acid	1.11 ± 0.12	1.46 ± 0.62	(c)
	hexanoic acid	0.48 ± 0.07	0.85 ± 0.26	(c)
Benzo[a]pyrene	azelaic acid	48 ± 8	1.20 ± 0.04	(b)
	NaCl	32	<0.12	(b)
	fused silica	32	28	(b)
	nonactivated silica	32	9.5	(b)
	soot	15 ± 1	280 ± 20	(d)

(a) Kwamena *et al*. (2007b), (b) Kwamena *et al*. (2006), (c) Mmereki *et al*. (2004), (d) Pöschl *et al*. (2001).

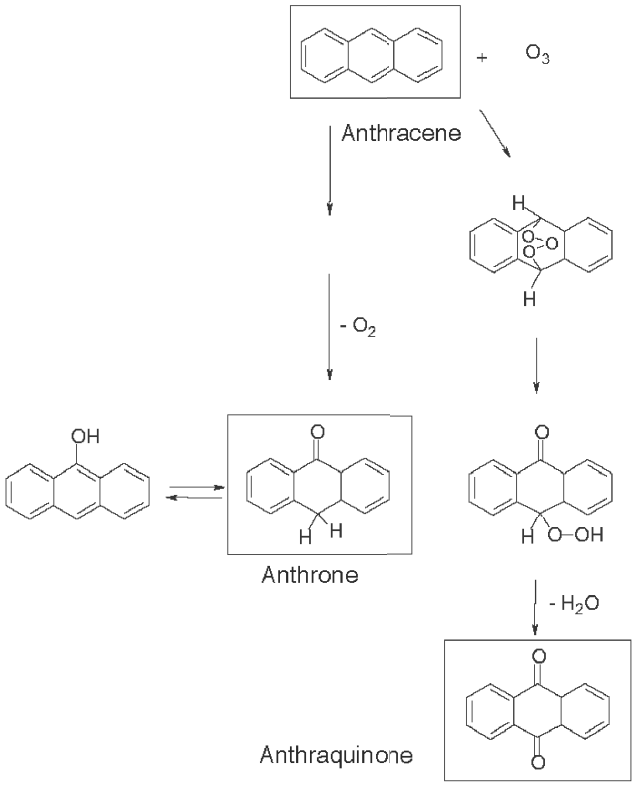

Fig. 43. Proposed mechanism for the heterogeneous reaction of particulate anthracene with gaseous ozone. (Adapted from *Atmos. Environ.*, *41*, Perraudin, E., H. Budzinski, and E. Villenave, Identification and quantification of ozonation products of anthracene and phenanthrene adsorbed on silica particles, 6005–6017, Copyright 2007, with permission from Elsevier.)

6. Concluding Remarks

Since the aim of this review has been to provide an overview of, and insight into, the major reaction processes occurring in cloud, fog and aerosol aqueous droplets, and at the air-aerosol interface related to organic aerosols, it has covered only limited types of reactions and a limited number of papers. There are many other important processes and papers that have not been discussed here. Also, this field is rapidly developing and the newest findings may not necessarily be included. I apologize to those authors whose work is not mentioned in topics discussed.

One of the foci of atmospheric chemistry has been shifting toward the study of the formation and transformation of secondary organic aerosols. I am confident that this area

doi:10.5047/meep.2016.00401.0001

will continue as an important research field in a next decade, where, for example, organic chemistry in an aqueous solution, organic and inorganic oxidative chemistry at the air-surface interface, and the interaction of water molecules at the surface of organics, are newly-evolving fundamental research fields in atmospheric science as well as reaction chemistry. Although this review has mainly discussed studies of field observations and laboratory experiments, studies on computational chemistry based on quantum chemical molecular dynamics need to be developed for understanding the basic science of SOA. This field of computational chemistry has not been well developed yet, and it is hoped that it will advance in close relation with laboratory experiments, in the same way as has been experienced historically with homogeneous gas phase reactions.

Acknowledgments. I would like to thank Professors Taro Matsuno, one of the Editors of the Monographs on Environment, Earth and Planets (MEEP), for providing me with a golden opportunity to publish my review on the heterogeneous reaction chemistry related to secondary organic aerosols (SOA). I deeply acknowledge Professor Jun Hirokawa at Hokkaido University and Dr. Kei Sato at the National Institute for Environmental Studies for their careful reading and detailed checking of the draft. The author also acknowledges the anonymous reviewers who provided valuable comments to improve the paper.

References

Akimoto, H. (2016), *Atmospheric Reaction Chemistry*, Springer, Tokyo (Japanese edition, Asakura Pub. Co., Tokyo, 2014).

Alfarra, M. R., H. Coe, J. D. Allan, K. N. Bower, H. Boudries, M. R. Canagaratna, J. L. Jimenez, J. T. Jayne, A. A. Garforth, S.-M. Li, and D. R. Worsnop (2004), Characterization of urban and rural organic particulate in the Lower Fraser Valley using two Aerodyne Aerosol Mass Spectrometers, *Atmos. Environ.*, *38*, 5745–5758.

Altieri, K., A. G. Carlton, H.-J. Lim, B. J. Turpin, and S. P. Seitzinger (2006), Evidence for oligomer formation in clouds: Reactions of isoprene oxidation products, *Environ. Sci. Technol.*, *40*, 4956–4960.

Altieri, K. E., S. P. Seitzinger, A. G. Carlton, B. J. Turpin, G. C. Klein, and A. G. Marshall (2008), Oligomers formed through in-cloud methylglyoxal reactions: Chemical composition, properties, and mechanisms investigated by ultra-high resolution FT-ICR mass spectrometry, *Atmos. Environ.*, *42*, 1476–1490.

Altieri, K. E., B. J. Turpin, and S. P. Seitzinger (2009a), Oligomers, organosulfates, and nitroxy organosulfates in rainwater identified by ultra-high resolution electrospray ionization FT-ICR mass spectrometry, *Atmos. Chem. Phys.*, *9*, 2533–2542.

Altieri, K. E., B. J. Turpin, and S. P. Seitzinger (2009b), Composition of dissolved organic nitrogen in continental precipitation investigated by ultra-high resolution FT-ICR mass spectrometry, *Environ. Sci. Technol.*, *43*, 6950–6955.

Andino, J. M., J. N. Smith, R. C. Flagan, W. A. Goddard, III, and J. H. Seinfeld (1996), Mechanism of atmospheric photooxidation of aromatics: A theoretical study, *J. Phys. Chem.*, *100*, 10967–10980.

Arakaki, T., and B. Faust (1998), Sources, sinks, and mechanism of hydroxyl radical (·OH) photoproduction and consumption in authentic acidic continental cloud waters from Whiteface Mountain, New York: The role of the Fe(r) (r = II, III) photochemical cycle, *J. Geophys. Res.*, *103*, 3487–3504.

Arey, J., B. Zielinska, R. Atkinson, and A. M. Winer (1987), Polycyclic aromatic hydrocarbon and nitroarene concentrations in ambient air during a wintertime high NO_x episode in the Los Angeles basin, *Atmos. Environ.*, *21*, 1437–1444.

Atkinson, R. (1997), Atmospheric reactions of alkoxy and β-hydroxyalkoxy radicals, *Int. J. Chem. Kinet.*, *29*, 99–111.

Atkinson, R., and J. Arey (1994), Atmospheric chemistry of gas-phase, polycyclic aromatic hydrocarbons: Formation of atmospheric mutagens, *Environmental Health Perspectives*, *102* (Suppl. 4), 117–126.

Atkinson, R., and J. Arey (2003), Atmospheric degradation of volatile organic compounds, *Chem. Rev.*, *103*, 4605–4638.

Atkinson, R., and W. L. Carter (1984), Kinetics and mechanisms of the gas-phase reactions of ozone with organic compounds under atmospheric conditions, *Chem. Rev.*, *84*, 437–470.

Atkinson, R., D. L. Baulch, R. A. Cox, J. N. Crowley, R. F. Hampson, R. G. Hynes, M. E. Jenkin, M. J. Rossi, and J. Troe (2004), Evaluated kinetic and photochemical data for atmospheric chemistry: Volume I—gas phase reactions of O_x, HO_x, NO_x, and SO_x species, *Atmos. Chem. Phys.*, *4*, 1461–1738.

Atkinson, R., D. L. Baulch, R. A. Cox, J. N. Crowley, R. F. Hampson, R. G. Hynes, M. E. Jenkin, M. J. Rossi, and J. Troe (2006), Evaluated kinetic and photochemical data for atmospheric chemistry: Volume II—gas phase reactions of organic species, *Atmos. Chem. Phys.*, *6*, 3625–4055.

Atkinson, R., D. L. Baulch, R. A. Cox, J. N. Crowley, R. F. Hampson, R. G. Hynes, M. E. Jenkin, M. J. Rossi, and J. Troe (2007), Evaluated kinetic and photochemical data for atmospheric chemistry: Volume III—gas phase reactions of inorganic halogens, *Atmos. Chem. Phys.*, *7*, 981–1191.

Atkinson, R., D. L. Baulch, R. A. Cox, J. N. Crowley, R. F. Hampson, R. G. Hynes, M. E. Jenkin, M. J. Rossi, and J. Troe, and T. J. Wallington (2008), Evaluated kinetic and photochemical data for atmospheric chemistry: Volume IV—gas phase reactions of organic halogen species, *Atmos. Chem. Phys.*, *8*, 4141–4496.

Bacher, C., G. S. Tyndall, and J. J. Orlando (2001), The atmospheric chemistry of glycolaldehyde, *J. Atmos. Chem.*, *39*, 171–189.

Baltaretu, C. O., E. I. Lichtman, A. B. Hadler, and M. J. Elrod (2009), Primary atmospheric oxidation mechanism for toluene, *J. Phys. Chem. A*, *113*, 221–230.

Bandow, H., N. Washida, and H. Akimoto (1985), Ring-cleavage reactions of aromatic hydrocarbons studies by FT-IR spectroscopy. I. Photooxidation of toluene and benzene in the NO_x-air system, *Bull. Chem. Soc. Jpn.*, *58*, 2531–2540.

Barsanti, K. C., and J. F. Pankow (2005), Thermodynamics of the formation of atmospheric organic particulate matter by accretion reactions—2. Dialdehydes, methylglyoxal, and diketones, *Atmos. Environ.*, *39*, 6597–6607.

Betterton, E. A., and M. R. Hoffmann (1988), Henry's law constants of some environmentally important aldehydes, *Environ. Sci. Technol.*, *22*, 1415–1418.

Blando, J. D., and B. J. Turpin (2000), Secondary organic aerosol formation in cloud and fog droplets: A literature evaluation of plausibility, *Atmos. Environ.*, *34*, 1623–1632.

Brasseur, G. P., and S. Solomon (2005), *Aeronomy of the Middle Atmosphere: Chemistry and Physics of the Stratosphere and Mesosphere*, 3rd edition, Springer.

Burchill, C. E., and K. M. Perron (1971), Radiation-induced rearrangement of ethylene glycol in aqueous solution, *Can. J. Chem.*, *49*, 2382–2389.

Butkovskaya, N., I. N. Pouvesle, A. Kukui, and G. Le Bras (2006a), Mechanism of the OH-initiated oxidation of glycolaldehyde over the temperature range 233–296 K, *J. Phys. Chem. A*, *110*, 13492–13499.

Butkovskaya, N. I., N. Pouvesle, A. Kukui, Y. Mu, and G. Le Bras (2006b), Mechanism of the OH-initiated oxidation of hydroxyacetone over the temperature range 236–298 K, *J. Phys. Chem. A*, *110*, 6833–6843.

Buxton, G. V., C. L. Greenstock, W. P. Helman, and A. B. Ross (1988), Critical review of rate constants for reactions of hydrated electrons, hydrogen atoms and hydroxyl radicals (·OH/·O^-) in aqueous solution, *J. Phys. Chem. Ref. Data*, *17*, 513–886.

Buxton, G. V., T. N. Malone, and G. A. Salmon (1997), Oxidation of glyoxal initiated by OH in oxygenated aqueous solution, *J. Chem. Soc., Faraday Trans.*, *93*, 2889–2891.

Calvert, J. G., R. Atkinson, J. A. Kerr, S. Madronich, G. K Moortgat, T. J. Wallington, and G. Yarwood (2000), *The Mechanisms of Atmospheric Oxidation of the Alkenes*, Oxford University Press.

Calvert, J. G., R. Atkinson, K. H. Becker, R. M. Kamens, J. H. Seinfeld, T. J. Wallington, and G. Yarwood (2002), *The Mechanisms of Atmospheric Oxidation of the Aromatic Hydrocarbons*, Oxford University Press.

Calvert, J. G., R. G. Derwent, J. J. Orlando, G. S. Tyndall, and T. J. Wallington (2008), *The Mechanisms of Atmospheric Oxidation of the Alkanes*, Oxford University Press.

Calvert, J., A. Mellouki, J. Orlando, M. J. Pilling, and T. J. Wallington (2011), *The Mechanisms of Atmospheric Oxidation of the Oxygenates*,

doi:10.5047/meep.2016.00401.0001

Oxford University Press.
Carlton, A. G., B. J. Turpin, H.-J. Lim, and K. E. Altieri (2006), Link between isoprene and secondary organic aerosol (SOA): Pyruvic acid oxidation yields low volatility organic acids in clouds, *Geophys. Res. Lett.*, *33*, L06822, doi:10.1029/2005GL025374.
Carlton, A. G., B. J. Turpin, K. E. Altieri, S. Seitzinger, A. Reff, H.-J. Lim, and B. Ervens (2007), Atmospheric oxalic acid and SOA production from glyoxal: Results of aqueous photooxidation experiments, *Atmos. Environ.*, *41*, 7588–7602.
Casale, M. T., A. R. Richman, M. J. Elrod, R. M. Garland, M. R. Beaver, and M. A. Tolbert (2007), Kinetics of acid-catalyzed aldol condensation reactions of aliphatic aldehydes, *Atmos. Environ.*, *41*, 6212–6224.
Chameides, W. L., and D. D. Davis (1982), The free radical chemistry of cloud droplets and its impact upon the composition of rain, *J. Geophys. Res.*, *87*, 4863–4877.
Chan, M. N., J. D. Surratt, M. Claeys, E. S. Edgerton, R. L. Tanner, S. L. Shaw, M. Zheng, E. M. Knipping, N. C. Eddingsaas, P. O. Wennberg, and J. H. Seinfeld (2010), Characterization and quantification of isoprene-derived epoxydiols in ambient aerosol in the southeastern United States, *Environ. Sci. Technol.*, *44*, 4590–4596.
Chan, K. M., D. D. Huang, Y. J. Li, M. N. Chan, J. H. Seinfeld, and C. K. Chan (2013), Oligomeric products and formation mechanisms from acid-catalyzed reactions of methyl vinyl ketone on acidic sulfate particles, *J. Atmos. Chem.*, *70*, 1–18.
Charbouillot, T., S. Gorini, G. Voyard, M. Parazols, M. Brigante, L. Deguillaume, A.-M. Delort, and G. Mailhot (2012), Mechanism of carboxylic acid photooxidation in atmospheric aqueous phase: Formation, fate and reactivity, *Atmos. Environ.*, *56*, 1–8.
Chebbi, A., and P. Carlier (1996), Carboxylic acids in the troposphere, occurrence, sources and sinks: A review, *Atmos. Environ.*, *30*, 4233–4249.
Cole-Filipiak, N. C., A. E. O'Connor, and M. Elrod (2010), Kinetics of the hydrolysis of atmospherically relevant isoprene-derived hydroxy epoxides, *Environ. Sci. Technol.*, *44*, 6718–6723.
Crahan, K. K., D. Hegg, D. S. Covert, and H. Jonsson (2004), An exploration of aqueous oxalic acid production in the coastal marine atmosphere, *Atmos. Environ.*, *23*, 3757–3764.
Cubison, M. J. *et al.* (2011), Effects of aging on organic aerosol from open biomass burning smoke in aircraft and laboratory studies, *Atmos. Chem. Phys.*, *11*, 12049–12064.
Darer, A. I., N. C. Cole-Filipiak, A. E. O'Connor, and M. J. Elrod (2011), Formation and stability of atmospherically relevant isoprene-derived organosulfates and organonitrates, *Environ. Sci. Technol.*, *45*, 1895–1902.
DeCarlo, P. F., I. M. Ulbrich, J. Crounse, B. de Foy, E. J. Dunlea, A. C. Aiken, D. Knapp, A. J. Weinheimer, T. Campos, P. O. Wennberg, and J. L. Jimenez (2010), Investigation of the sources and processing of organic aerosol over the Central Mexican Plateau from aircraft measurements during MILAGRO, *Atmos. Chem. Phys.*, *10*, 5257–5280.
De Haan, D. O., A. L. Corrigan, K. W. Smith, D. R. Stroik, J. J. Turley, F. E. Lee, M. A. Tolbert, L. L. Jimenez, K. E. Cordova, and G. R. Ferrell (2009a), Secondary organic aerosol-forming reactions of glyoxal with amino acids, *Environ. Sci. Technol.*, *43*, 2818–2824.
De Haan, D. O., A. L. Corrigan, M. A. Tolbert, J. L. Jimenez, S. E. Wood, and J. J. Turkey (2009b), Secondary organic aerosol formation by self-reactions of methylglyoxal and glyoxal in evaporating droplets, *Environ. Sci. Technol.*, *43*, 8184–8190.
De Haan, D. O., M. A. Tolbert, and J. L. Jimenez (2009c), Atmospheric condensed-phase reactions of glyoxal with methylamine, *Geophys. Res. Lett.*, *36*, L11819, doi:10.1029/2009GL037441.
De Haan, D. O., L. N. Hawkins, J. A. Kononenko, J. J. Turley, A. L. Corrigan, M. A. Tolbert, and J. L. Jimenez (2011), Formation of nitrogen-containing oligomers by methylglyoxal and amines in simulated evaporating cloud droplets, *Environ. Sci. Technol.*, *45*, 984–991.
Denkenberger, K. A., R. C. Moffet, J. C. Holecek, T. P. Rebotier, and K. A. Prather (2007), Real-time, single-particle measurements of oligomers in aged ambient aerosol particles, *Environ. Sci. Technol.*, *41*, 5439–5446.
Dibble, T. S. (2002), Isomerization of OH-isoprene adducts and hydroxyalkoxy isoprene radicals, *J. Phys. Chem. A*, *106*, 6643–6650.
Donahue, N. M., A. L. Robinson, E. R. Trump, I. Riipinen, and J. H. Kroll (2012), Volatility and aging of atmospheric organic aerosol, *Topics Current Chem.*, *339*, 97–143.
Doussin, J.-F., and A. Monod (2013), Structure–activity relationship for the estimation of OH-oxidation rate constants of carbonyl compounds in the aqueous phase, *Atmos. Chem. Phys.*, *13*, 11625–11641.
Dumdei, B. E., D. V. Kenny, P. B. Shepson, T. E. Kleindienst, C. M. Nero, L. T. Cupitt, and L. D. Claxton (1988), MS/MS analysis of the products of toluene photooxidation and measurement of their mutagenic activity, *Environ. Sci. Technol.*, *22*, 1493–1498.
Eddingsaas, N. C., D. G. VanderVelde, and P. O. Wennberg (2010), Kinetics and products of the acid-catalyzed ring-opening of atmospherically relevant butyl epoxy alcohols, *J. Phys. Chem. A*, *114*, 8106–8113.
El Haddad, I., Y. Liu, L. Nieto-Gligorovski, V. Michaud, B. Temime-Roussel, E. Quivet, N. Marchand, K. Sellegri, and A. Monod (2009), In-cloud processes of methacrolein under simulated conditions—Part 2: Formation of secondary organic aerosol, *Atmos. Chem. Phys.*, *9*, 5107–5117.
Enami, S., M. R. Hoffmann, and A. J. Colussi (2014), In situ mass spectrometric detection of interfacial intermediates in the oxidation of RCOOH(aq) by gas-phase OH-radicals, *J. Phys. Chem. A*, *118*, 4130–4137.
Enami, S., M. R. Hoffmann, and A. J. Colussi (2015), Stepwise oxidation of aqueous dicarboxylic acids by gas-phase OH radicals, *J. Phys. Chem. Lett.*, *6*, 527–534.
Ervens, B., and R. Volkamer (2010), Glyoxal processing by aerosol multiphase chemistry: Towards a kinetic modeling framework of secondary organic aerosol formation in aqueous particles, *Atmos. Chem. Phys.*, *10*, 8219–8244.
Ervens, B., C. George, J. E. Williams, G. V. Buxton, G. A. Salmon, M. Bydder, F. Wilkinson, F. Dentener, P. Mirabel, R. Wolke, and H. Herrmann (2003a), CAPRAM2.4 (MODAC mechanism): An extended and condensed tropospheric aqueous phase mechanism and its application, *J. Geophys. Res.*, *108*(D14), 4426, doi:10.1029/2002JD002202.
Ervens, B., S. Gligorovski, and H. Herrmann (2003b), Temperature-dependent rate constants for hydroxyl radical reactions with organic compounds in aqueous solutions, *Phys. Chem. Chem. Phys.*, *5*, 1811–1824.
Ervens, B., G. Feingold, G. J. Frost, and S. M. Kreidenweis (2004), A modeling study of aqueous production of dicarboxylic acids: 1. Chemical pathways and speciated organic mass production, *J. Geophys. Res.*, *109*, D15205, doi:10.1029/2003JD004387.
Ervens, B., A. G. Carlton, B. J. Turpin, K. E. Altieri, S. M. Kreidenweis, and G. Feingold (2008), Secondary organic aerosol yields from cloud-processing of isoprene oxidation products, *Geophys. Res. Lett.*, *35*, L02816, doi:10.1029/2007GL031828.
Ervens, B., B. J. Turpin, and R. J. Weber (2011), Secondary organic aerosol formation in cloud droplets and aqueous particles (aqSOA): a review of laboratory, field and model studies, *Atmos. Chem. Phys.*, *11*, 11069–11102.
Fan, J., and R. Zhang (2004), Atmospheric oxidation mechanism of isoprene, *Environ. Chem.*, *1*, 140–149.
Faust, B. C., and J. M. Allen (1993), Aqueous-phase photochemical formation of hydroxyl radical in authentic cloud waters and fog waters, *Environ. Sci. Technol.*, *27*, 1221–1224.
Feng, J. S., and D. Moller (2004), Characterization of water-soluble macromolecular substances in cloud water, *J. Atmos. Chem.*, *48*, 217–212.
Feng, J., Z. Guo, C. K. Chan, and M. Fang (2007), Properties of organic matter in $PM_{2.5}$ at Changdao Island, China—a rural site in the transport path of the Asian continental outflow, *Atmos. Environ.*, *41*, 1924–1935.
Finlayson-Pitts, B. J., and J. N. Pitts, Jr. (2000), *Chemistry of the Upper and Lower Atmosphere*, Academic Press.
Fraser, M. P., G. R. Cass, B. R. T. Simoneit, and R. A. Rasmussen (1998), Air quality model evaluation data for organics. 5. C_6-C_{22} nonpolar and semipolar aromatic compounds, *Environ. Sci. Technol.*, *32*, 1760–1770.
Froyd, K. D., S. M. Murphy, D. M. Murphy, J. A. de Gouw, N. C. Eddingsaas, and P. O. Wennberg (2010), Contribution of isoprene-derived organosulfates to free tropospheric aerosol mass, *Proc. Natl. Acad. Sci.*, *107*, 21360–21365.
Fu, P., K. Kawamura, K. Usukura, and K. Miura (2013), Dicarboxylic acids, ketocarboxylic acids and glyoxal in the marine aerosols collected during a round-the-world cruise, *Marine Chem.*, *148*, 22–32.
Fu, T.-M., D. J. Jacob, F. Wittrock, J. P. Burrows, M. Vrekoussis, and D. K. Henze (2008), Global budgets of atmospheric glyoxal and methylglyoxal, and implications for formation of secondary organic aerosols, *J. Geophys. Res.*, *113*, D15303, doi:10.1029/2007JD009505.
Galano, A., L. G. Ruiz-Suárez, and A. Vivier-Bunge (2008), On the mechanism of the OH initiated oxidation of acetylene in the presence of O_2 and NO_x, *Theoret. Chem. Accounts*, *121*, 219–225.

doi:10.5047/meep.2016.00401.0001

Galloway, M. M., P. S. Chhabra, A. W. H. Chan, J. D. Surratt, R. C. Flagan, J. H. Seinfeld, and F. N. Keutsch (2009), Glyoxal uptake on ammonium sulphate seed aerosol: Reaction products and reversibility of uptake under dark and irradiated conditions, *Atmos. Chem. Phys.*, *9*, 3331–3345.

Galloway, M. M., A. J. Huisman, L. D. Yee, A. W. H. Chan, C. L. Loza, J. H. Seinfeld, and F. N. Keutsch (2011), Yields of oxidized volatile organic compounds during the OH radical initiated oxidation of isoprene, methyl vinyl ketone, and methacrolein under high-NO_X conditions, *Atmos. Chem. Phys.*, *11*, 10779–10790.

Gao, S., N. L. Ng, M. Keywood, V. Varutbangkul, R. Bahreini, A. Nenes, J. W. He, K. Y. Yoo, J. L. Beauchamp, R. P. Hodyss, R. C. Flagan, and J. H. Seinfeld (2004), Particle phase acidity and oligomer formation in secondary organic aerosol, *Environ. Sci. Technol.*, *38*, 6582–6589.

Garland, R. M., M. J. Elrod, K. Kincaid, M. R. Beaver, J. L. Jimenez, and M. A. Tolbert (2006), Acid-catalyzed reactions of hexanal on sulfuric acid particles: Identification of reaction products, *Atmos. Environ.*, *40*, 6863–6878.

George, I. J., and J. P. D. Abbatt (2010), Heterogeneous oxidation of atmospheric aerosol particles by gas-phase radicals, *Nature Chem.*, *2*, 713–22.

Gery, M. W., D. L. Fox, H. E. Jeffries, L. Stockburger, and W. S. Weather (1985), A continuous stirred tank reactor investigation of the gas-phase reaction of hydroxyl radicals and toluene, *Int. J. Chem. Kinet.*, *17*, 931–955.

Gingrich, S. E., M. L. Diamond, G. A. Stern, and B. E. McCarry (2001), Atmospherically derived organic surface films along an urban-rural gradient, *Environ. Sci. Technol.*, *35*, 4031–4037.

Gómez-González, Y., J. D. Surratt, F. Cuyckens, R. Szmigielski, R. Vermeylen, M. Jaoui, M. Lewandowski, J. H. Offenberg, T. E. Kleindienst, E. O. Edney, F. Blockhuys, C. Van Alsenoy, W. Maenhaut, and M. Claeys (2008), Characterization of organosulfates from the photooxidation of isoprene and unsaturated fatty acids in ambient aerosol using liquid chromatography/(-) electrospray ionization mass spectrometry, *J. Mass. Spectrom.*, *43*, 371–382.

Graber, E. R., and Y. Rudich (2006), Atmospheric HULIS: How humic-like are they? A comprehensive and critical review, *Atmos. Chem. Phys.*, *6*, 729–753.

Greenberg, A. (1989), Phenomenological study of benzo[a]pyrene and cyclopentene[cd]pyrene decay in ambient air using winter/summer comparisons, *Atmos. Environ.*, *23*, 2797–2799.

Grieshop, A. P., J. M. Logue, N. M. Donahue, and A. L. Robinson (2009), Laboratory investigation of photochemical oxidation of organic aerosol from wood fires 1: Measurement and simulation of organic aerosol evolution, *Atmos. Chem. Phys.*, *9*, 1263–1277.

Guzmán, M. I., A. J. Colussi, and M. R. Hoffmann (2006), Photoinduced oligomerization of aqueous pyruvic acid, *J. Phys. Chem. A*, *110*, 3619–3626.

Haddad, I. E., B. D'Anna, B. Temime-Roussel, M. Nicolas, A. Boreave, O. Favez, D. Voisin, J. Sciare, C. George, J.-L. Jaffrezo, H. Wortham, and N. Marchand (2013), Towards a better understanding of the origins, chemical composition and aging of oxygenated organic aerosols: Case study of a Mediterranean industrialized environment, Marseille, *Atmos. Chem. Phys.*, *13*, 7875–7894.

Hallquist, M., J. C. Wenger, U. Baltensperger, Y. Rudich, D. Simpson, M. Claeys, J. Dommen, N. M. Donahue, C. George, A. H. Goldstein, J. F. Hamilton, H. Herrmann, T. Hoffmann, Y. Iinuma, M. Jang, M. E. Jenkin, J. L. Jimenez, A. Kiendler-Scharr, W. Maenhaut, G. McFiggans, Th. F. Mentel, A. Monod, A. S. H. Prévôt, J. H. Seinfeld, J. D. Surratt, R. Szmigielski, and J. Wildt (2009), The formation, properties and impact of secondary organic aerosol: Current and emerging issues, *Atmos. Chem. Phys.*, *9*, 5155–5236.

Hastings, W. P., C. A. Koehler, E. L. Bailey, and D. O. De Haan (2005), Secondary organic aerosol formation by glyoxal hydration and oligomer formation: Humidity effects and equilibrium shifts during analysis, *Environ. Sci. Technol.*, *39*, 8728–8735.

Hatakeyama, S., N. Washida, and H. Akimoto (1986), Rate constants and mechanisms for the reaction of OH (OD) radicals with acetylene, propyne, and 2-butyne in air at 297 ± 2 K, *J. Phys. Chem.*, *90*, 173–178.

Hatch, L. E., J. M. Creamean, A. P. Ault, J. D. Surratt, M. N. Chan, J. H. Seinfeld, E. S. Edgerton, Y. Su, and K. A. Prather (2011a), Measurements of isoprene-derived organosulfates in ambient aerosols by aerosol time-of-flight mass spectrometry—Part 1: Single particle atmospheric observations in Atlanta, *Environ. Sci. Technol.*, *45*, 5105–5111.

Hatch, L. E., J. M. Creamean, A. P. Ault, J. D. Surratt, M. N. Chan, John H. Seinfeld, E. S. Edgerton, Y. Su, and K. A. Prather (2011b), Measurements of isoprene-derived organosulfates in ambient aerosols by aerosol time-of-flight mass spectrometry—Part 2: Temporal variability and formation mechanisms, *Environ. Sci. Technol.*, *45*, 8648–8655.

Havers, N., P. Burba, J. Lambert, and D. Klockow (1998), Spectroscopic characterization of humic-like substances in airborne particulate matter, *J. Atmos. Chem.*, *29*, 45–54.

Heald, C. L., D. J. Jacob, R. J. Park, L. M. Russell, B. J. Huebert, J. H. Seinfeld, H. Liao, and R. J. Weber (2005), A large organic aerosol source in the free troposphere missing from current models, *Geophys. Res. Lett.*, *32*, L18809, doi:10.1029/2005gl023831.

Herckes, P., T. Lee, L. Trenary, G. Kang, H. Chang, and J. L. Collett, Jr. (2002), Organic matter in central California radiation fogs, *Environ. Sci. Technol.*, *36*, 4777–4782.

Herckes, P., J. A. Leenheer, and J. L. Collett, Jr. (2007), Comprehensive characterization of atmospheric organic matter in Fresno, California fog water, *Environ. Sci. Technol.*, *41*, 393–399.

Herrmann, H., D. Hoffmann, T. Schaefer, P. Bräuer, and A. Tilgner (2010), Tropospheric aqueous-phase free-radical chemistry: radical sources, spectra, reaction kinetics and prediction tools, *Chemphyschem.*, *11*, 3796–3822.

Hettiyadura, A. P. S., E. A. Stone, S. Kundu, Z. Baker, E. Geddes, K. Richards, and T. Humphry (2015), Determination of atmospheric organosulfates using HILIC chromatography with MS detection, *Atmos. Meas. Tech.*, *8*, 2347–2358.

Huang, X.-F., J. Z. Yu, L.-Y. He, and Z. Yuan (2006), Water-soluble organic carbon and oxalate in aerosols at a coastal urban site in China: Size distribution characteristics, sources, and formation mechanisms, *J. Geophys. Res.*, *111*, D22212, doi:10.1029/2006jd007408.

Iinuma, Y., C. Muller, T. Berndt, O. Boge, M. Claeys, and H. Herrmann (2007a), Evidence for the existence of organosulfates from β-pinene ozonolysis in ambient secondary organic aerosol, *Environ. Sci. Technol.*, *41*, 6678–6683.

Iinuma, Y., C. Muller, O. Boge, T. Gnauk, and H. Herrmann (2007b), The formation of organic sulfate esters in the limonene ozonolysis secondary organic aerosol (SOA) under acidic conditions, *Atmos. Environ.*, *41*, 5571–5583.

Ip, H. S. S., X. H. H. Huang, and J. Z. Yu (2009), Effective Henry's law constants of glyoxal, glyoxylic acid, and glycolic acid, *Geophys. Res. Lett.*, *36*, L01802, doi:10.1029/2008GL036212.

Iraci, L. T., B. M. Baker, G. S. Tyndall, and J. J. Orlando (1999), Measurements of the Henry's law coefficients of 2-methyl-3-buten-2-ol, methacrolein, and methyl vinyl ketone, *J. Atmos. Chem.*, *33*, 321–330.

Isaacman, G., A. W. H. Chan, T. Nah, D. R. Worton, C. R. Ruehl, K. R. Wilson, and A. H. Goldstein (2012), Heterogeneous OH oxidation of motor oil particles causes selective depletion of branched and less cyclic hydrocarbons, *Environ. Sci. Technol.*, *46*, 10632–10640.

Jacob, D. L. (1986), Chemistry of OH in remote clouds and its role in the production of formic acid and peroxymonosulfate, *J. Geophys. Res.*, *91*, 9807, doi:10.1029/JD091ID09P09807.

Jang, M., and R. M. Kamens (2001), Atmospheric secondary aerosol formation by heterogeneous reactions of aldehydes in the presence of a sulfuric acid aerosol catalyst, *Environ. Sci. Technol.*, *35*, 4758–4766.

Jimenez, J. L. *et al.* (another 63 authors) (2009), Evolution of organic aerosols in the atmosphere, *Science*, *326*, 1525–1529.

Kalberer, M., D. Paulsen, M. Sax, M. Steinbacher, M. J. Dommen, A. S. H. Prevot, R. Fisseha, E. Weingartner, V. Frankevich, R. Zenobi, and U. Baltensperger (2004), Identification of polymers as major components of atmospheric organic aerosols, *Science*, *303*, 1659–1662.

Kalberer, M., M. Sax, and V. Samburova (2006), Molecular size evolution of oligomers in organic aerosols collected in urban atmospheres and generated in a smog chamber, *Environ. Sci. Technol.*, *40*, 5917–5922.

Kampf, C. J., R. Jakob, and T. Hoffmann (2012), Identification and characterization of aging products in the glyoxal/ammonium sulfate system—Implications for light-absorbing material in atmospheric aerosols, *Atmos. Chem. Phys.*, *12*, 6323–6333.

Katrib, Y., S. T. Martin, H.-M. Hung, Y. Rudich, H. Zhang, J. G. Slowik, P. Davidovits, J. T. Jayne, and D. R. Worsnop (2004), Products and mechanisms of ozone reactions with oleic acid for aerosol particles having core-shell morphologies, *J. Phys. Chem. A*, *108*, 6686–6695.

Kawamura, K., and F. Sakaguchi (1999), Molecular distributions of water soluble dicarboxylic acids in marine aerosols over the Pacific Ocean including tropics, *J. Geophys. Res.*, *104*, 3501–3509.

doi:10.5047/meep.2016.00401.0001

Kawamura, K., H. Kasukabe, and L. A. Barrie (2010), Secondary formation of water-soluble organic acids and α-dicarbonyls and their contributions to total carbon and water-soluble organic carbon: Photochemical aging of organic aerosols in the Arctic spring, *J. Geophys. Res.*, *115*, D21306, doi:10.1029/2010JD014299.

Kerminen, V.-M., C. Ojanen, T. Pakkanen, R. Hillamo, M. Aurela, and J. Merilainen (2000), Low-molecular weight dicarboxylic acids in an urban and rural atmosphere, *J. Aerosol. Sci.*, *31*, 349–362.

Kirkland, J. R., Y. B. Lim, Y. Tan, K. E. Altieri, and B. J. Turpin (2013), Glyoxal secondary organic aerosol chemistry: Effects of dilute nitrate and ammonium and support for organic radical–radical oligomer formation, *Environ. Chem.*, *10*, 158–166.

Klotz, B., I. Barnes, and K.-H. Becker (1999), Kinetic study of the gas-phase photolysis and OH radical reaction of E, Z- and E, E-2,4-hexadienedial, *Int. J. Chem. Kinet.*, *31*, 689–697.

Kolesar, K. R., G. Buffaloe, K. R Wilson, and C. D Cappa (2014), OH-initiated heterogeneous oxidation of internally-mixed squalane and secondary organic aerosol, *Environ. Sci. Technol.*, *48*, 3196–3202.

Krivácsy, Z., G. Kiss, D. Ceburnis, G. Jennings, W. Maenhaut, I. Salma, and D. Shooter (2008), Study of water-soluble atmospheric humic matter in urban and marine environments, *Atmos. Res.*, *87*, 1–12.

Krizner, H. E., D. O. De Haan, and J. Kua (2009), Thermodynamics and kinetics of methylglyoxal dimer formation: A computational study, *J. Phys. Chem. A*, *113*, 6994–7001.

Kroll, J. H., and J. H. Seinfeld (2008), Chemistry of secondary organic aerosol: Formation and evolution of low-volatility organics in the atmosphere, *Atmos. Environ.*, *42*, 3593–3624.

Kroll, J. H., N. L. Ng, S. M. Murphy, V. Varutbangkul, R. C. Flagan, and J. H. Seinfeld (2005), Chamber studies of secondary organic aerosol growth by reactive uptake of simple carbonyl compounds, *J. Geophys. Res.*, *110*, D23207, doi:10.1029/2005JD006004.

Kroll, J. H., J. D. Smith, D. L. Che, S. H. Kessler, D. R. Worsnop, and K. R. Wilson (2009), Measurement of fragmentation and functionalization pathways in the heterogeneous oxidation of oxidized organic aerosol, *Phys. Chem. Chem. Phys.*, *11*, 8005–8014.

Kua, J., S. W. Hanley, and D. O. De Haan (2008), Thermodynamics and kinetics of glyoxal dimer formation: A computational study, *J. Phys. Chem. A*, *112*, 66–72.

Kua, J., H. E. Krizner, and D. O. De Haan (2011), Thermodynamics and kinetics of imidazole formation from glyoxal, methylamine, and formaldehyde: A computational study, *J. Phys. Chem. A*, *115*, 1667–1675.

Kwamena, N.-O. A., M. E. Earp, C. J. Young, and J. P. D. Abbatt (2006), Kinetic and product yield study of the heterogeneous gas-surface reaction of anthracene and ozone, *J. Phys. Chem. A*, *110*, 3638–3646.

Kwamena, N.-O. A., J. P. Clarke, T. F. Kahan, M. L. Diamond, and D. J. Donaldson (2007a), Assessing the importance of heterogeneous reactions of polycyclic aromatic hydrocarbons in the urban atmosphere using the Multimedia Urban Model, *Atmos. Environ.*, *41*, 37–50.

Kwamena, N.-O. A., M. G. Staikova, D. J. Donaldson, I. J. George, and J. P. D. Abbatt (2007b), Role of the aerosol substrate in the heterogeneous ozonation reactions of surface-bound PAHs, *J. Phys. Chem. A*, *111*, 11050–11058.

Kwok, E. S. C., and R. Atkinson (1995), Estimation of hydroxyl radical reaction rate constants for gas-phase organic compounds using a structure-reactivity relationship: An update, *Atmos. Environ.*, *29*, 1685–1695.

Lai, C., Y. Liu, J. Ma, Q. Ma, and H. He (2014), Degradation kinetics of levoglucosan initiated by hydroxyl radical under different environmental conditions, *Atmos. Environ.*, *91*, 32–39.

Lambe, A. T., M. A. A. Miracolo, C. J. Hennigan, A. L. Robinson, and N. M. Donahue (2009), Effective rate constants and uptake coefficients for the reactions of organic molecular markers (n-alkanes, hopanes, and steranes) in motor oil and diesel primary organic aerosols with hydroxyl radicals, *Environ. Sci. Technol.*, *43*, 8794–8800.

Leitner, N. K. V., and M. Dore (1997), Mechanism of the reaction between hydroxyl radicals and glycolic, glyoxylic, acetic and oxalic acids in aqueous solution: Consequence on hydrogen peroxide consumption in the H_2O_2/UV and O_3/H_2O_2 systems, *Water Res.*, *31*, 1383–1397.

Liao, J. *et al.* (2015), Airborne measurements of organosulfates over the continental US, *J. Geophys. Res.*, *120*, 2990–3005, doi:10.1002/2014JD022378.

Liggio, J., S.-M. Li, and R. McLaren (2005a), Heterogeneous reactions of glyoxal on particulate matter: Identification of acetals and sulfate esters, *Environ. Sci. Technol.*, *39*, 1532–1541.

Liggio, J., S. Li, and R. McLaren (2005b), Reactive uptake of glyoxal by particulate matter, *J. Geophys. Res.*, *110*, D10304, doi:10.1029/2004JD005113.

Lim, Y. B., Y. Tan, M. J. Perri, P. Seitzinger, and B. J. Turpin (2010), Aqueous chemistry and its role in secondary organic aerosol (SOA) formation, *Atmos. Chem. Phys.*, *10*, 10521–10539.

Limbeck, A., H. Puxbaum, L. Otter, and M. C. Scholes (2001), Semivolatile behavior of dicarboxylic acids and other polar organic species at a rural background site (Nylsvley, RSA), *Atmos. Environ.*, *35*, 1853–1862.

Lin, P., J. Z. Yu, G. Engling, and M. Kalberer (2012), Organosulfates in humic-like substance fraction isolated from aerosols at seven locations in East Asia: A study by Ultra-High-Resolution Mass Spectrometry, *Environ. Sci. Technol.*, *46*, 13118–13127.

Lin, Y. H., E. M. Knipping, E. S. Edgerton, S. L. Shaw, and J. D. Surratt (2013), Investigating the influences of SO_2 and NH_3 levels on isoprene-derived secondary organic aerosol formation using conditional sampling approaches, *Atmos. Chem. Phys.*, *13*, 8457–8470.

Liu, Y., I. El Haddad, M. Scarfogliero, L. Nieto-Gligorovski, B. Temime-Roussel, E. Quivet, N. Marchand, B. Picquet-Varrault, and A. Monod (2009), In-cloud processes of methacrolein under simulated conditions—Part 1: Aqueous phase photooxidation, *Atmos. Chem. Phys.*, *9*, 5093–5105.

Liu, Y., F. Siekmann, P. Renard, A. El Zein, G. Salque, I. El Haddad, B. Temime-Roussel, D. Voisin, R. Thissen, and A. Monod (2012), Oligomer and SOA formation through aqueous phase photooxidation of methacrolein and methyl vinyl ketone, *Atmos. Environ.*, *49*, 123–129.

Liu, Y. J., I. Herdlinger-Blatt, K. A. McKinney, and S. T. Martin (2013), Production of methyl vinyl ketone and methacrolein via the hydroperoxyl pathway of isoprene oxidation, *Atmos. Chem. Phys.*, *13*, 5715–5730.

Loeffler, K. W., C. A. Koehler, N. M. Paul, and D. O. De Haan (2006), Oligomer formation in evaporating aqueous glyoxal and methyl glyoxal solutions, *Environ. Sci. Technol.*, *40*, 6318–6323.

Magneron, I., A. Mellouki, G. Le Bras, G. K. Moortgat, A. Horowitz, and K. Wirtz (2005), Photolysis and OH-initiated oxidation of glycolaldehyde under atmospheric conditions, *J. Phys. Chem. A*, *109*, 4552–4561.

Mazzoleni, L. R., B. M. Ehrmann, X. Shen, A. G. Marshall, and J. L. Collett (2010), Water-soluble atmospheric organic matter in fog: Exact masses and chemical formula identification by ultrahigh-resolution Fourier transform ion cyclotron resonance mass spectrometry, *Environ. Sci. Technol.*, *44*, 3690–3697.

Miet, K., K. Le Menach, P.-M. Flaud, H. Budzinski, and E. Villenave (2009), Heterogeneous reactivity of pyrene and 1-nitropyrene with NO 2: Kinetics, product yields and mechanism, *Atmos. Environ.*, *43*, 837–843.

Minerath, E. C., and M. J. Elrod (2009), Assessing the potential for diol and hydroxy sulfate ester formation from the reaction of epoxides in tropospheric aerosols, *Environ. Sci. Technol.*, *43*, 1386–1392.

Mkoma, S. L., and K. Kawamura (2013), Molecular composition of dicarboxylic acids, ketocarboxylic acids, dicarbonyls and fatty acids in atmospheric aerosols from Tanzania, East Africa during wet and dry seasons, *Atmos. Chem. Phys.*, *13*, 2235–2251.

Mmereki, B. T., D. J. Donaldson, J. B. Gilman, T. L. Eliason, and V. Vaida (2004), Kinetics and products of the reaction of gas-phase ozone with anthracene adsorbed at the air-aqueous interface, *Atmos. Environ.*, *38*, 6091–6103.

Mochida, M., Y. Katrib, J. T. Jayne, D. R. Worsnop, and S. T. Martin (2006), The relative importance of competing pathways for the formation of high-molecular-weight peroxides in the ozonolysis of organic aerosol particles, *Atmos. Chem. Phys.*, *6*, 4851–4866.

Mochida, M., K. Kawamura, P. Fu, and T. Takemura (2010), Seasonal variation of levoglucosan in aerosols over the western North Pacific and its assessment as a biomass-burning tracer, *Atmos. Environ.*, *44*, 3511–3518.

Moise, T., and Y. Rudich (2002), Reactive uptake of ozone by aerosol-associated unsaturated fatty acids: Kinetics, mechanism, and products, *J. Phys. Chem. A*, *106*, 6469–6476.

Monod, A., and J. F. Doussin (2008), Structure-activity relationship for the estimation of OH-oxidation rate constants of aliphatic organic compounds in the aqueous phase: Alkanes, alcohols, organic acids and bases, *Atmos. Environ.*, *42*, 7611–7622.

Monod, A., L. Poulain, S. Grubert, D. Voisin, and H. Wortham (2005), Kinetics of OH-initiated oxidation of oxygenated organic compounds in the aqueous phase: New rate constants, structure-activity relationships and atmospheric implications, *Atmos. Environ.*, *39*, 7667–7688.

Morris, J. W., P. Davidovits, J. T. Jayne, J. L. Jimenez, Q. Shi, C. E. Kolb,

doi:10.5047/meep.2016.00401.0001

D. R. Worsnop, W. S. Barney, and G. Cass (2002), Kinetics of submicron oleic acid aerosols with ozone: A novel mass spectrometric technique, *Geophys. Res. Lett.*, *29*, 71/71–71/74.

Mazzoleni, L. R., B. M. Ehrmann, X. Shen, A. G. Marshall, and J. L. Collett, Jr. (2010), Water-soluble atmospheric organic matter in fog: Exact masses and chemical formula identification by ultrahigh-resolution Fourier transform ion cyclotron resonance mass spectrometry, *Environ. Sci. Technol.*, *44*, 3690–3697.

Mukai, H., and Y. Ambe (1986), Characterization of a humic acid-like brown substance in airborne particulate matter and tentative identification of its origin, *Atmos. Environ.*, *20*, 813–819.

Nah, T., S. H. Kessler, K. E. Daumit, J. H. Kroll, S. R. Leone, and K. R. Wilson (2013), OH-initiated oxidation of sub-micron unsaturated fatty acid particles, *Phys. Chem. Chem. Phys.*, *15*, 18649–18663.

Nah, T., S. H. Kessler, K. E. Daumit, J. H. Kroll, S. R. Leone, and K. R. Wilson (2014a), Influence of molecular structure and chemical functionality on the heterogeneous OH-initiated oxidation of unsaturated organic particles, *J. Phys. Chem. A*, *118*, 4106–4119.

Nah, T., H. Zhang, D. R. Worton, C. R. Ruehl, B. B. Kirk, A. H. Goldstein, S. R. Leone, and K. R. Wilson (2014b), Isomeric product detection in the heterogeneous reaction of hydroxyl radicals with aerosol composed of branched and linear unsaturated organic molecules, *J. Phys. Chem. A*, *118*, 11555–11571.

Ng, N. L. *et al.* (2010), Organic aerosol components observed in Northern Hemispheric datasets from Aerosol Mass Spectrometry, *Atmos. Chem. Phys.*, *10*, 4625–4641.

Niki, H., P. D. Maker, C. M. Savage, and L. P. Breitenbach (1981), An FTIR study of mechanisms for the HO radical initiated oxidation of C_2H_4 in the presence of NO: Detection of glycolaldehyde, *Chem. Phys. Lett.*, *80*, 499–503.

Niki, H., P. D. Maker, C. M. Savage, and M. D. Hurley (1987), Fourier transform infrared study of the kinetics and mechanisms for the chlorine-atom- and hydroxyl-radical-initiated oxidation of glycolaldehyde, *J. Phys. Chem.*, *91*, 2174–2178.

Nozière, B., and D. D. Riemer (2003), The chemical processing of gas-phase carbonyl compounds by sulfuric acid aerosols: 2,4-pentanedione, *Atmos. Environ.*, *37*, 841–851.

Nozière, B., D. Voisin, C. A. Longfellow, H. Friedli, B. E. Henry, and D. R. Hanson (2006), The uptake of methyl vinyl ketone, methacrolein, and 2-methyl-3-butene-2-ol onto sulfuric acid solutions, *J. Phys. Chem. A*, *110*, 2387–2395.

Nozière, B., P. Dziedzic, and A. Córdova (2009), Products and kinetics of the liquid-phase reaction of glyoxal catalyzed by ammonium ions (NH_4^+), *J. Phys. Chem. A*, *113*, 231–237.

Olson, C. N., M. M. Galloway, G. Yu, C. J. Hedman, M. R. Lockett, T. Yoon, E. A. Stone, L. M. Smith, and F. N. Keutsch (2011), Hydroxycarboxylic acid-derived organosulfates: Synthesis, stability, and quantification in ambient aerosol, *Environ. Sci. Technol.*, *45*, 6468–6474.

Orlando, J. J., G. S. Tyndall, and S. E. Paulson (1999), Mechanism of the OH-initiated oxidation of methacrolein, *Geophys. Res. Lett.*, *26*, 2191–2194.

Paulot, F., J. D. Crounse, H. G. Kjaergaard, J. H. Kroll, J. H. Seinfeld, and P. O. Wennberg (2009a), Isoprene photooxidation: New insights into the production of acids and organic nitrates, *Atmos. Chem. Phys.*, *9*, 1479–1501.

Paulot, F., J. D. Crounse, H. G. Kjaergaard, A. Kürten, J. M. St. Clair, J. H. Seinfeld, and P. O. Wennberg (2009b), Unexpected epoxide formation in the gas-phase photooxidation of isoprene, *Science*, *325*, 730–733.

Peeters, J., and T. L. Nguyen (2012), Unusually fast 1,6-H shifts of enolic hydrogens in peroxy radicals: Formation of the first-generation C_2 and C_3 carbonyls in the oxidation of isoprene, *J. Phys. Chem.*, *116*, 6134–6141.

Perraudin, E., H. Budzinski, and E. Villenave (2007), Identification and quantification of ozonation products of anthracene and phenanthrene adsorbed on silica particles, *Atmos. Environ.*, *41*, 6005–6017.

Perri, M. J., S. Seitzinger, and B. J. Turpin (2009), Secondary organic aerosol production from aqueous photooxidation of glycolaldehyde: Laboratory experiments, *Atmos. Environ.*, *43*, 1487–1497.

Perri, M. J., Y. B. Lim, S. P. Seitzinger, and B. J. Turpin (2010), Organosulfates from glycolaldehyde in aqueous aerosols and clouds: Laboratory studies, *Atmos. Environ.*, *44*, 2658–2664.

Pöschl, U., T. Letzel, C. Schauer, and R. Niessner (2001), Interaction of ozone and water vapor with spark discharge soot aerosol particles coated with benzo[a]pyrene: O_3 and H_2O adsorption, benzo[a]pyrene degradation, and atmospheric implications, *J. Phys. Chem. A*, *105*, 4029–4041.

Pratt, K. A., M. N. Fiddler, P. B. Shepson, A. G. Carlton, and J. D. Surratt (2013), Organosulfates in cloud water above the Ozarks' isoprene source region, *Atmos. Environ.*, *77*, 231–238.

Ravishankara, A. R., Y. Rudich, and J. A. Pyle (2015), Role of chemistry in Earth's climate, *Chem. Rev.*, *115*, 3679–3681.

Reemtsma, T., A. These, P. Venkatachari, X. Y. Xia, P. K. Hopke, A. Springer, and M. Linscheid (2006), Identification of fulvic acids and sulfated and nitrated analogues in atmospheric aerosol by electrospray ionization Fourier transform ion cyclotron resonance mass spectrometry, *Anal. Chem.*, *78*, 8299–8304.

Reinhardt, A., C. Emmenegger, B. Gerrits, C. Panse, J. Dommen, U. Baltensperger, R. Zenobi, and M. Kalberer (2007), Ultrahigh mass resolution and accurate mass measurements as a tool to characterize oligomers in secondary organic aerosols, *Anal. Chem.*, *79*, 4074–4082.

Reissell, A., C. Harry, S. M. Aschmann, R. Atkinson, and J. Arey (1999), Formation of acetone from the OH radical- and O_3-initiated reactions of a series of monoterpenes, *J. Geophys. Res.*, *104*, 13869–13879.

Renard, P., F. Siekmann, A. Gandolfo, J. Socorro, G. Salque, S. Ravier, E. Quivet, J.-L. Clément, M. Traikia, A.-M. Delort, D. Voisin, V. Vuitton, R. Thissen, and A. Monod (2013), Radical mechanisms of methyl vinyl ketone oligomerization through aqueous phase OH-oxidation: On the paradoxical role of dissolved molecular oxygen, *Atmos. Chem. Phys.*, *13*, 6473–6491.

Renard, P., A. E. R. Harris, R. J. Rapf, S. Ravier, C. Demelas, B. Coulomb, E. Quivet, V. Vaida, and A. Monod (2014), Aqueous phase oligomerization of methyl vinyl ketone by atmospheric radical reactions, *J. Phys. Chem. C*, *118*, 29421–29430.

Reynolds, J. C., D. J. Last, M. McGillen, A. Nijs, A. B. Horn, C. Percival, L. J. Carpenter, and A. C. Lewis (2006), Structural analysis of oligomeric molecules formed from the reaction products of oleic acid ozonolysis, *Environ. Sci. Technol.*, *40*, 6674–6681.

Rinaldi, M., S. Decesari, C. Carbone, E. Finessi, S. Fuzzi, D. Ceburnis, C. D. O'Dowd, J. Sciare, J. P. Burrows, M. Vrekoussis, B. Ervens, K. Tsigaridis, and M. C. Facchini (2011), Evidence of a natural marine source of oxalic acid and a possible link to glyoxal, *J. Geophys. Res.*, *116*, D16204, doi:10.1029/2011JD015659.

Robinson, A. L., N. M. Donahue, and W. F. Rogge (2006), Photochemical oxidation and changes in molecular composition of organic aerosol in the regional context, *J. Geophys. Res.*, *111*, D03302, doi:10.1029/2005JD006265.

Robinson, A. L., N. M. Donahue, M. K. Shrivastava, E. A. Weitkamp, A. M. Sage, A. P. Grieshop, T. E. Lane, J. R. Pierce, and S. N. Pandis (2007), Rethinking organic aerosols: Semivolatile emissions and photochemical aging, *Science*, *315*, 1259–1262.

Rosado-Reyes, C. M., and J. S. Francisco (2007), Atmospheric oxidation pathways of propane and its by-products: Acetone, acetaldehyde, and propionaldehyde, *J. Geophys. Res.*, *112*, D14310, doi:10.1029/2006JD007566.

Rudich, Y., N. M. Donahue, and T. F. Mentel (2007), Aging of organic aerosol: Bridging the gap between laboratory and field studies, *Annu. Rev. Phys. Chem.*, *58*, 321–352.

Ruehl, C. R., T. Nah, G. Isaacman, D. R. Worton, A. W. H. Chan, K. R. Kolesar, C. D. Cappa, A. H. Goldstein, and K. R. Wilson (2013), The influence of molecular structure and aerosol phase on the heterogeneous oxidation of normal and branched alkanes by OH, *J. Phys. Chem. A*, *117*, 3990–4000.

Ruiz-Montoya, M., and J. M. Rodriguez-Mellado (1995), Hydration constants of carbonyl and dicarbonyl compounds comparison between electrochemcial and no electrochemical techniques, *Portugaliae Electrochim. Acta*, *13*, 299–303.

Sakamoto, Y., S. Inomata, and J. Hirokawa (2013), Oligomerization reaction of the Criegee intermediate leads to secondary organic aerosol formation in ethylene ozonolysis, *J. Phys. Chem. A*, *117*, 12912–12921.

Sander, R. (1999), Compilation of Henry's law constants for inorganic and organic species of potential importance in environmental chemistry (version 3), Max-Planck Inst. of Chem., Mainz, Germany. (Available at http://www.mpch-mainz.mpg.de/˜sander/res/henry.html)

Sander, S. P., R. Baker, D. M. Golden, M. J. Kurylo, P. H. Wine, J. P. D. Abatt, J. B. Burkholder, C. E. Kolb, G. K. Moortgat, R. E. Huie, and V. L. Orkin (2011), Chemical Kinetics and Photochemical Data for Use in Atmospheric Studies, Evaluation Number 17, JPL Publication 10-6, Pasadena, California. (Available at http://jpldataeval.jpl.nasa.gov/)

doi:10.5047/meep.2016.00401.0001

Sareen, N., A. N. Schwier, E. L. Shapiro, D. Mitroo, and V. F. McNeill (2010), Secondary organic material formed by methylglyoxal in aqueous aerosol mimics, *Atmos. Chem. Phys.*, *10*, 997–1016.

Sato, K., S. Hatakeyama, and T. Imamura (2007), Secondary organic aerosol formation during the photooxidation of toluene: NO_x dependence of chemical composition, *J. Phys. Chem. A*, *111*, 9796–9808.

Saunders, S. M., M. E. Jenkin, R. G. Derwent, and M. J. Pilling (2003), Protocol for the development of the Master Chemical Mechanism, MCM v3 (Part A): Tropospheric degradation of nonaromatic volatile organic compounds, *Atmos. Chem. Phys.*, *3*, 161–180.

Schweitzer, F., L. Magi, P. Mirabel, and C. George (1998), Uptake rate measurements of methane-sulfonic acid and glyoxal by aqueous droplets, *J. Phys. Chem. A*, *102*, 593–600.

Seinfeld, J. H., and S. N. Pandis (2006), *Atmospheric Chemistry and Physics: Air Pollution to Climate Change*, 2nd ed., John Wiley and Sons.

Sempéré, R., and K. Kawamura (2003), Trans-hemispheric contribution of C_2-C_{10}, α, ω-dicarboxylic acids, and related polar compounds to water-soluble organic carbon in the western Pacific aerosols in relation to photochemical oxidation reactions, *Global Biogeochem. Cycles*, *17*(2), 1069, doi:10.1029/2002GB001980.

Shapiro, E. L., J. Szprengiel, N. Sareen, C. N. Jen, M. R. Giordano, and V. F. McNeill (2009), Light-absorbing secondary organic material formed by glyoxal in aqueous aerosol mimics, *Atmos. Chem. Phys.*, *9*, 2289–2300.

Shepson, P. B., E. O. Edney, and E. W. Corse (1984), Ring fragmentation reactions in the photooxidations of toluene and o-xylene, *J. Phys. Chem.*, *88*, 4122–4126.

Shiraiwa, M., Y. Sosedova, A. Rouvière, H. Yang, Y. Zhang, J. P. D. Abbatt, M. Ammann, and U. Pöschl (2011), The role of long-lived reactive oxygen intermediates in the reaction of ozone with aerosol particles, *Nature Chem.*, *3*, 291–295.

Smith, G. D., E. Woods, III, C. L. DeForest, T. Baer, and R. E. Miller (2002), Reactive uptake of ozone by oleic acid aerosol particles: Application of single-particle mass spectrometry to heterogeneous reaction kinetics, *J. Phys. Chem. A*, *106*, 8085–8095.

Sorooshian, A., F. J. Brechtel, B. Ervens, G. Feingold, V. Varutbangkul, R. Bahreini, S. Murphy, J. S. Holloway, E. L. Atlas, K. Anlauf, G. Buzorius, H. Jonsson, R. C. Flagan, and J. H. Seinfeld (2006), Oxalic acid in clear and cloudy atmospheres: Analysis of data from International Consortium for Atmospheric Research on Transport and Transformation 2004, *J. Geophys. Res.*, *111*, D23S45, doi:10.1029/2005JD006880.

Springmann, M., D. A. Knopf, and N. Riemer (2009), Detailed heterogeneous chemistry in an urban plume box model: Reversible co-adsorption of O_3, NO_2, and H_2O on soot coated with benzo[a]pyrene, *Atmos. Chem. Phys.*, *9*, 7461–7479.

Stone, E. A., C. J. Hedmana, R. J. Sheesley, M. M. Shafera, and J. J. Schauera (2009), Investigating the chemical nature of humic-like substances (HULIS) in North American atmospheric aerosols by liquid chromatography tandem mass spectrometry, *Atmos. Environ.*, *43*, 4205–4213.

Surratt, J. D., J. H. Kroll, T. E. Kleindienst, E. O. Edney, M. Claeys, A. Sorooshian, N. L. Ng, J. H. Offenberg, M. Lewandowski, M. Jaoui, R. C. Flagan, and J. H. Seinfeld (2007), Evidence for organosulfates in secondary organic aerosol, *Environ. Sci. Technol.*, *41*, 517–527.

Surratt, J. D., Y. Gómez-González, A. W. H. Chan, R. Vermeylen, M. Shahgholi, T. E. Kleindienst, E. O. Edney, J. H. Offenberg, M. Lewandowski, M. Jaoui, W. Maenhaut, M. Claeys, R. C. Flagan, and J. H. Seinfeld (2008), Organosulfate formation in biogenic secondary organic aerosol, *J. Phys. Chem. A*, *112*, 8345–8378.

Surratt, J. D., A. W. H. Chan, N. C. Eddingsaas, M. N. Chan, C. L. Loza, A. J. Kwan, S. P. Hersey, R. C. Flagan, P. O. Wennberg, and J. H. Seinfeld (2010), Reactive intermediates revealed in secondary organic aerosol formation from isoprene, *Proc. Nat. Acad. Sci.*, *107*, 6640–6645.

Talukdar, R. K., T. Gierczak, D. C. McCabe, and A. R. Ravishankara (2003), Reaction of hydroxyl radical with acetone. 2. Products and reaction mechanism, *J. Phys. Chem. A*, *107*, 5021–5032.

Tan, Y., M. J. Perri, S. P. Seitzinger, and B. J. Turpin (2009), Effects of precursor concentration and acidic sulfate in aqueous glyoxal-OH radical oxidation and implications for secondary organic aerosol, *Environ. Sci. Technol.*, *43*, 8105–8112.

Tan, Y., A. G. Carlton, S. P. Seitzinger, and B. Turpin (2010), SOA from methylglyoxal in clouds and wet aerosols: Measurement and prediction of key products, *Atmos. Environ.*, *44*, 5218–5226.

Tan, Y., Y. B. Lim, K. E. Altieri, S. P. Seitzinger, and B. J. Turpin (2012), Mechanisms leading to oligomers and SOA through aqueous photooxidation: Insights from OH radical oxidation of acetic acid and methylglyoxal, *Atmos. Chem. Phys.*, *12*, 801–813.

Thornberry, T., and J. P. D. Abbatt (2004), Heterogeneous reaction of ozone with liquid unsaturated fatty acids: Detailed kinetics and gas-phase product studies, *Phys. Chem. Chem. Phys.*, *6*, 84–93.

Tobias, H. J., and P. J. Ziemann (2000), Thermal desorption mass spectrometric analysis of organic aerosol formed from reactions of 1-tetradecene and O_3 in the presence of alcohols and carboxylic acids, *Environ. Sci. Technol.*, *34*, 2105–2115.

Tolocka, M. P., and B. Turpin (2012), Contribution of organosulfur compounds to organic aerosol mass, *Environ. Sci. Technol.*, *46*, 7978–7983.

Tolocka, M. P., M. Jang, J. M. Ginter, F. J. Cox, R. M. Kamens, and M. V. Johnston (2004), Formation of oligomers in secondary organic aerosol, *Environ. Sci. Technol.*, *38*, 1428–1434.

Tong, C., M. Blanco, W. A. Goddard, III, and J. Seinfeld (2006), Secondary organic aerosol formation by heterogeneous reactions of aldehydes and ketones: A quantum mechanical study, *Environ. Sci. Technol.*, *40*, 2333–2338.

Tuazon, E. C., and R. Atkinson (1989), A product study of the gas-phase reaction of methyl vinyl ketone with the OH radical in the presence of NO_x, *Int. J. Chem. Kinet.*, *21*, 1141–1152.

Tuazon, E. C., and R. Atkinson (1990), A product study of the gas-phase reaction of methacrolein with the OH radical in the presence of NO_x, *Int. J. Chem. Kinet.*, *22*, 591–602.

Tuazon, E. C., R. Atkinson, H. MacLeod, H. W. Biermann, A. M. Winer, W. P. L. Carter, and J. N. Pitts (1984), Yields of glyoxal and methylglyoxal from the nitrogen oxide (NO_x)-air photooxidations of toluene and m- and p-xylene, *Environ. Sci. Technol.*, *18*, 981–984.

Turekian, V. C., S. A. Macko, and W. C. Keene (2003), Concentrations, isotopic compositions, and sources of size-resolved, particulate organic carbon and oxalate in near-surface marine air at Bermuda during spring, *J. Geophys. Res.*, *108*(D5), 4157, doi:10.1029/2002JD002053.

Turpin, E., A. Thomas, C. Fittschen, P. Devolder, and J. C. Galloo (2006), Acetone-h_6 or -d_6 + OH reaction products: Evidence for heterogeneous formation of acetic acid in a simulation chamber, *Environ. Sci. Technol.*, *40*, 5956–5961.

van Pinxteren, D., A. Plewka, D. Hofmann, K. Müller, H. Kramberger, B. Svrcina, K. Bächmann, W. Jaeschke, S. Mertes, J. L. Collett, Jr., and H. Herrmann (2005), Schmücke hill cap cloud and valley stations aerosol characterization during FEBUKO (II): Organic compounds, *Atmos. Environ.*, *39*, 4305–4320.

Vieceli, J., O. L. Ma, and D. J. Tobias (2004), Uptake and collision dynamics of gas phase ozone at unsaturated organic interfaces, *J. Phys. Chem. A*, *108*, 5806–5814.

Volkamer, R., I. Barnes, U. Platt, L. T. Molina, and M. J. Molina (2006a), Remote sensing of glyoxal by differential optical absorption spectroscopy (DOAS): Advancements in simulation chamber and field experiments, in *Environmental Simulation Chambers: Application to Atmospheric Chemical Processes*, edited by I. Barnes and J. Rudinski, Springer.

Volkamer, R., J. L. Jimenex, F. San Martini, K. Dzepina, Q. Zhang, D. Salcedo, L. T. Molina, D. R. Worsnop, and M. L. Molina (2006b), Secondary organic aerosol formation from anthropogenic air pollution: Rapid and higher than expected, *Geophys. Res. Lett.*, *33*, L17811, doi:10.1029/2006GL026899.

Volkamer, R., P. J. Ziemann, and M. J. Molina (2009), Secondary organic aerosol formation from acetylene (C_2H_2): Seed effect on SOA yields due to organic photochemistry in the aerosol aqueous phase, *Atmos. Chem. Phys.*, *9*, 1907–1928.

Wang, G., K. Kawamura, C. Cheng, J. Li, J. Cao, R. Zhang, T. Zhang, D. Liu, and Z. Zhao (2012), Molecular distribution and stable carbon isotopic composition of dicarboxylic acids, ketocarboxylic acids, and α-dicarbonyls in size-resolved atmospheric particles from Xi'an city, China, *Environ. Sci. Technol.*, *46*, 4783–4791.

Wang, L. M., R. R. Wu, and C. Xu (2013), Atmospheric oxidation mechanism of benzene. Fates of alkoxy radical intermediates and revised mechanism, *J. Phys. Chem. A*, *117*, 14163–14168.

Wang, X. F., S. Gao, X. Yang, H. Chen, J. M. Chen, G. S. Zhuang, J. D. Surratt, M. N. Chang, and J. H. Seinfeld (2010), Evidence for high molecular weight nitrogen-containing organic salts in urban aerosols, *Environ. Sci. Technol.*, *44*, 4441–4446.

Warneck, P. (2003), In-cloud chemistry opens pathway to the formation of oxalic acid in the marine atmosphere, *Atmos. Environ.*, *37*, 2423–2427.

Whalen, D. L. (2005), Mechanisms of hydrolysis and rearrangements of

doi:10.5047/meep.2016.00401.0001

epoxides, *Adv. Phys. Org. Chem.*, *40*, 247–298.

Wisthaler, A., N. R. Jensen, R. Winterhalter, W. Lindinger, and J. Hjorth (2001), Measurements of acetone and other gas phase product yields from the OH-initiated oxidation of terpenes by proton-transfer-reaction mass spectrometry (PTR-MS), *Atmos. Environ.*, *35*, 6181–6191.

Wozniak, A. S., J. E. Bauer, R. L. Sleighter, R. M. Dickhut, and P. G. Hatcher (2008), Technical note: Molecular characterization of aerosol-derived water soluble organic carbon using ultrahigh resolution electrospray ionization Fourier transform ion cyclotron resonance mass spectrometry, *Atmos. Chem. Phys.*, *8*, 5099–5111.

Yao, X., M. Fang, and C. K. Chan (2002), Size distributions and formation of dicarboxylic acids in atmospheric particles, *Atmos. Environ.*, *36*, 2099–2107.

Yasmeen, F., N. Sauret, J.-F. Gal, P.-C. Maria, L. Massi, W. Maenhaut, and M. Claeys (2010), Characterization of oligomers from methylglyoxal under dark conditions: A pathway to produce secondary organic aerosol through cloud processing during nighttime, *Atmos. Chem. Phys.*, *10*, 3803–3812.

Yeung, L. Y., M. J. Pennino, A. M. Miller, and M. J. Elrod (2005), Kinetics and mechanistic studies of the atmospheric oxidation of alkynes, *J. Phys. Chem. A*, *109*, 1879–1889.

Yu, G., A. R. Bayer, M. M. Galloway, K. J. Korshavn, C. G. Fry, and F. N. Keutsch (2011), Glyoxal in aqueous ammonium sulfate solutions: Products, kinetics and hydration effects, *Environ. Sci. Technol.*, *45*, 6336–6342.

Yu, J. Z., and H. E. Jeffries (1997), Atmospheric photooxidation of alkylbenzenes—II. Evidence of formation of epoxide intermediates, *Atmos. Environ.*, *31*, 2281–2287.

Yu, J. Z., X.-F. Huang, J.-H. Xu, and M. Hu (2005), When aerosol sulfate goes up, so does oxalate: Implication for the formation mechanisms of oxalate, *Environ. Sci. Technol.*, *39*, 128–133.

Zahardis, J., and G. A. Petrucci (2007), The oleic acid-ozone heterogeneous reaction system: Products, kinetics, secondary chemistry, and atmospheric implications of a model system—a review, *Atmos. Chem. Phys.*, *7*, 1237–1274.

Zahardis, J., B. W. LaFranchi, and G. A. Petrucci (2005), Photoelectron resonance capture ionization-aerosol mass spectrometry of the ozonolysis products of oleic acid particles: Direct measure of higher molecular weight oxygenates, *J. Geophys. Res.*, *110*, D08307, doi:10.1029/2004JD005336.

Zahardis, J., B. W. LaFranchi, and G. A. Petrucci (2006), Direct observation of polymerization in the oleic acid-ozone heterogeneous reaction system by photoelectron resonance capture ionization aerosol mass spectrometry, *Atmos. Environ.*, *40*, 1661–1670.

Zhang, H., D. R. Worton, M. Lewandowski, J. Ortega, C. L. Rubitschun, J.-H. Park, K. Kristensen, P. Campuzano-Jost, D. A. Day, J. L. Jimenez, M. Jaoui, J. H. Offenberg, T. E. Kleindienst, J. Gilman, W. C. Kuster, J. de Gouw, C. Park, G. W. Schade, A. A. Frossard, L. Russell, L. Kaser, W. Jud, A. Hansel, L. Cappellin, T. Karl, M. Glasius, A. Guenther, A. H. Goldstein, J. H. Seinfeld, A. Gold, R. M. Kamens, and J. D. Surratt (2012), Organosulfates as tracers for secondary organic aerosol (SOA) formation from 2-methyl-3-buten-2-ol (MBO) in the atmosphere, *Environ. Sci. Technol.*, *46*, 9437–9446.

Zhang, H., C. R. Ruehl, A. W. H. Chan, T. Nah, D. R. Worton, G. Isaacman, A. H. Goldstein, and K. R. Wilson (2013), OH-initiated heterogeneous oxidation of cholestane: A model system for understanding the photochemical aging of cyclic alkane aerosols, *J. Phys. Chem. A*, *117*, 12449–12458.

Zhang, Q., and C. Anastasio (2001), Chemistry of fog waters in California's Central Valley—Part 3: Concentrations and speciation of organic and inorganic nitrogen, *Atmos. Environ.*, *35*, 5629–5643.

Zhang, X., Z. M. Chen, and Y. Zhao (2010), Laboratory simulation for the aqueous OH-oxidation of methyl vinyl ketone and methacrolein: Significance to the in-cloud SOA production, *Atmos. Chem. Phys.*, *10*, 9551–9561.

Zhang, Y., B. Yang, J. Gan, C. Liu, X. Shu, and J. Shu (2011), Nitration of particle-associated PAHs and their derivatives (nitro-, oxy-, and hydroxy-PAHs) with NO_3 radicals, *Atmos. Environ.*, *45*, 2515–2521.

Zhao, J., N. P. Levitt, and R. Zhang (2005), Heterogeneous chemistry of octanal and 2, 4-hexadienal with sulfuric acid, *Geophys. Res. Lett.*, *32*, L09802, doi:10.1029/2004GL022200.

Zhao, J., N. P. Levitt, R. Zhang, and J. Chen (2006), Heterogeneous reactions of methylglyoxal in acidic media: Implications for secondary organic aerosol formation, *Environ. Sci. Technol.*, *40*, 7682–7687.

Zhao, R., A. K. Y. Lee, and J. P. D. Abbatt (2012), Investigation of aqueous-phase photooxidation of glyoxal and methylglyoxal by aerosol chemical ionization mass spectrometry: Observation of hydroxyhydroperoxide formation, *J. Phys. Chem. A*, *116*, 6253–6263.

Ziemann, P. J. (2005), Aerosol products, mechanisms, and kinetics of heterogeneous reactions of ozone with oleic acid in pure and mixed particles, *Faraday Discuss.*, *130*, 469–490.

Zimmermann, K., N. Jariyasopit, S. L. M. Simonich, S. Tao, R. Atkinson, and J. Arey (2013), Formation of nitro-PAHs from the heterogeneous reaction of ambient particle-bound PAHs with N_2O_5/NO_3/NO_2, *Environ. Sci. Technol.*, *47*, 8434–8442.

doi:10.5047/meep.2016.00401.0001